Wideband spectrum sensing using sub-Nyquist sampling

S Aziz

23185600

Dissertation submitted in fulfilment of the requirements for the degree *Magister in Computer and Electronic Engineering* at the Potchefstroom Campus of the North-West University

Supervisor: Prof ASJ Helberg

May 2014

It all starts here ™

NORTH-WEST UNIVERSITY
YUNIBESITI YA BOKONE-BOPHIRIMA
NOORDWES-UNIVERSITEIT ®

Declaration

I, ***Shanu Aziz*** hereby declare that this dissertation entitled "***Wideband spectrum sensing using sub-Nyquist sampling***", which I herewith submit to the NorthWest University in partial fulfilment of the requirements for the ***Master of Engineering*** degree, is my own original work and has not already been submitted to any other university or institution for examination.

S. Aziz

Student number: 23185600

Signed on the ***23***rd day of ***October 2013*** at ***Potchefstroom***.

Acknowledgements

"This dissertation is dedicated to my loving parents and my sweet heart."

I am expressing my thankfulness towards **THE ALMIGHTY GOD** without whose blessings and mercifulness nothing could have happened.

I am indebted to my supervisor ***Prof A. S. J. Helberg*** for his valuable support and guidance throughout the journey of this research whose technical advices and encouragement has always helped me in finding a way out from all the major difficulties at various stages

Thank you to my loving husband, ***Sunir Hassan*** without whose help, support and encouragement, all my efforts would have gone in vain.

I am grateful to my parents ***Abdul Aziz*** and ***Sajitha Aziz*** who have always supported, encouraged and believed in me, in all my endeavours without whose care and affection I would not have achieved anything in my life.

I must acknowledge and express my affection towards my sister ***Sumia*** and brother in law ***Binoy*** for their prayers and understanding that kept me going.

I am thankful to everyone in the Telenet Research Group especially *Sune*, *Joubert* , *Leenta* and *Melvyn* for all their whole hearted encouragements.

I am thankful to all my colleagues who were with me throughout my life in the campus, especially *Heila*, *Melanie*, *Christian*, *Hanno* and *Zuann* during the past two years

I also express my sincere gratitude to ***THRIP*** for their financial support to conduct this research.

Last but not least, my heartfelt thankfulness to all my friends, family members and well-wishers who contributed directly or indirectly to successfully materialise this dissertation.

Abstract

Spectrum sensing is the process of identifying the frequencies of a spectrum in which Signals Of Interest (SOI) are present. In case of continuous time signals present in a wideband spectrum, the information rate is seen to be much less than that suggested by its bandwidth and are therefore known as sparse signals. A review of the literature in [1] and [2] indicates that two of the many techniques used in wideband spectrum sensing of sparse signals are the Wideband Compressive Radio Receiver (WCRR) for multitoned signals and the mixed analog digital system for multiband signals. In both of these techniques even though the signals are sampled at sub-Nyquist rates using Compressive Sampling (CS), the recovery algorithms used by them are different from that of CS. In WCRR, a simple correlation function is used for the detection of carrier frequencies and in a mixed analog digital system, a simple digital algorithm is used for the identification of frequency support. Through a literature survey, we could identify that a VHSIC hardware descriptive ModelSim simulation model for wideband spectrum sensing of multitoned and multiband signals using sub Nyquist sampling does not exist. If a ModelSim simulation model can be developed using VHDL codes, it can be easily adapted for FPGA implementation leading to the development of a realistic hardware prototype for use in Cognitive Radio (CR) communication systems.

The research work reported through this dissertation deals with the implementation of simulation models of WCRR and mixed analog digital system in ModelSim by making use of VHDL coding. Algorithms corresponding to different blocks contained in the conceptual design of these models have been formulated prior to the coding phase. After the coding phase, analyses of the models are performed using test parameter choices to ensure that they meet the design requirements. Different parametric choices are then assigned for the parametric study and a sufficient number of iterations of these simulations were carried out to verify and validate these models.

Keywords: *sub-Nyquist Sampling, Support Recovery, Carrier Detection*

Contents

List of Figures **xii**

List of Tables **xv**

List of Acronyms **xvii**

1 Introduction **1**

1.1 Background 1

1.1.1 Cognitive Radios and Spectrum Sensing 1

1.1.2 Spectrum Sensing 4

1.2 Problem Statement 5

1.3 Issues to be Addressed 5

1.4 Research Methodology 6

1.5 Modelling Process 7

1.6 Dissertation Overview 9

1.6.1 Literature Review 9

1.6.2 Wideband Compressive Radio Receiver 10

1.6.3 Verification and Validation of WCRR 10

1.6.4 Modulated Wideband Converter 10

1.6.5 Verification and Validation of Modulated Wideband Converter (MWC) . . . 10
1.6.6 Conclusion . . . 11

2 Literature Review **12**

2.1 Introduction . . . 12
2.2 Nyquist Sampling . . . 13
2.3 Classic sub-Nyquist Methods . . . 13
2.3.1 Demodulation . . . 14
2.3.2 Undersampling Analog to Digital Converter (ADC) . . . 14
2.3.3 Periodic Non-uniform Sampling (PNS) . . . 15
2.4 Union of subspaces . . . 15
2.4.1 MWC . . . 16
2.4.2 Random Demodulator . . . 17
2.5 Classic sub-Nyquist Sampling Vs Union of Subspaces . . . 17
2.6 Compressive Sampling . . . 18
2.7 CS Based Wideband Spectrum Sensing . . . 19
2.7.1 Compressive Sensing Basics . . . 19
2.7.2 CS Recovery Algorithms . . . 22
2.8 ModelSim . . . 24
2.8.1 Basic Simulation Flow . . . 24
2.8.2 Project Flow . . . 26
2.8.3 Multiple Library Flow . . . 27
2.8.4 Debugging Tools . . . 28
2.9 Summary . . . 28

3 Wideband Compressive Radio Receiver **29**

3.1 Introduction . . . 29
3.2 Generic Wideband Receiver . . . 30
3.3 Wideband Compressive Radio Receiver . . . 31
3.3.1 Multitone Signal . . . 31
3.3.2 Random Demodulator . . . 32
3.3.3 Carrier Detection . . . 33
3.4 Prototype Architecture . . . 34
3.4.1 System Parameters . . . 34
3.4.2 Generation of Multitoned Signal . . . 35
3.4.3 Pseudo-random Chipping Sequence Generator . . . 36
3.4.4 Mixing . . . 40
3.4.5 Integration . . . 40
3.4.6 Generation of Φ . . . 42
3.4.7 Frequency Set . . . 44
3.4.8 Correlation for Carrier Detection . . . 46
3.5 Summary . . . 49

4 Verification and Validation of WCRR **50**

4.1 Introduction . . . 50
4.2 Verification: WCRR Simulation Model . . . 51
4.2.1 Parameter Choices . . . 51
4.2.2 Testing: Input Model Generation . . . 52
4.2.3 Testing: Pseudo Random Sequence Generation . . . 52
4.2.4 Testing: Generation of Mixed Signal . . . 53
4.2.5 Testing: Simulation Model for Integration . . . 53
4.2.6 Testing: Generation of Φ . . . 54

4.2.7 Testing: Frequency Set Generation . . . 54
4.2.8 Testing: Carrier Detection . . . 55
4.3 Model Verification: WCRR Simulation Model . . . 55
4.4 Operational Validation of WCRR . . . 57
4.4.1 Parameter Choices for the numerical investigation of WCRR . . . 57
4.4.2 Frequency Correlation for a f_{nyq} of 1 GHz . . . 58
4.4.3 Frequency Correlation for a f_{nyq} of 2 GHz . . . 59
4.4.4 Frequency Correlation for a f_{nyq} of 2.4 GHz . . . 60
4.4.5 Percentage Variation of Successful Detection with Decimation Factor . . . 62
4.5 Verification of Successful Carrier Detection . . . 63
4.6 Validation of Successful Carrier Detection . . . 64
4.7 Summary . . . 65

5 Modulated Wideband Converter **67**

5.1 Introduction . . . 67
5.2 Mixed Analog Digital System . . . 68
5.3 Multiband Signal Model . . . 69
5.4 Modulated Wideband Converter . . . 70
5.5 Continuous To Finite Block . . . 73
5.6 Prototype Architecture . . . 74
5.6.1 System Parameters . . . 74
5.6.2 Signal Representation . . . 75
5.6.3 Mixing . . . 79
5.6.4 Analog low-pass filtering and actual sampling . . . 80
5.6.5 Continuous To Finite (CTF) . . . 84

5.7 Summary 88

6 Verification and Validation of Modulated Wideband Converter 89

6.1 Introduction 89

6.2 Verification: Mixed Analog Digital System Simulation Model 90

6.2.1 Parameter Choices 90

6.2.2 Testing: Input Signal Generation 91

6.2.3 Testing: Pseudo Random Sequence Generation 92

6.2.4 Testing: Generation of Original Support 92

6.2.5 Testing: Mixing Algorithm 92

6.2.6 Testing: Signal Filtering and Sampling 94

6.2.7 Testing: CTF Block 95

6.3 Model Verification: Mixed Analog Digital System Simulation Model . . 97

6.4 Operational Validation of Mixed Analog Digital System 98

6.4.1 Parameter Choices for the numerical investigation of Mixed Analog Digital System 99

6.4.2 Variation of minimum Number of Channels required with respect to Signal-to-Noise Ratio (SNR) 100

6.4.3 Variation of minimum Number of Channels required with respect to Nyquist Frequency 102

6.4.4 Percentage Variation of Successful Recovery with Number of Channels 104

6.5 Verification of Successful Support Recovery 117

6.6 Validation of Successful Support Recovery 119

6.7 Summary 121

7 Conclusion 122

7.1 Introduction 122

7.2 Summary of Work . . . 123
7.3 Problem Statement . . . 123
7.4 Issues to be Addressed . . . 123
7.5 Suggested Solutions . . . 124
7.5.1 WCRR model for Multitoned Signals . . . 124
7.5.2 MWC model for Multiband Signals . . . 124
7.5.3 Testing the Models . . . 125
7.5.4 Execution of simulation . . . 125
7.5.5 Validation of Implementation . . . 126
7.5.6 Summary of Results . . . 127
7.6 Future Work . . . 128
7.6.1 Extending the Parametric Study . . . 128
7.6.2 FPGA Implementation of Simulations . . . 128
7.6.3 Implementation in CR communication . . . 129
7.7 Publications from this Research . . . 129
7.7.1 SATNAC 2011 . . . 129
7.7.2 ICICT 2012 . . . 130
7.7.3 SATNAC 2012 . . . 130
7.8 Achievements . . . 130
7.9 Summary . . . 130

Bibliography **132**

Appendices

A Conference Contributions from Dissertation **137**

List of Figures

1.1 Research Methodology 6

1.2 Modelling Process 8

2.1 Basic Simulation Flow 25

2.2 Project Flow 26

2.3 Multiple Library Flow 27

3.1 Generic Wideband Receiver 30

3.2 Random Demodulator 32

3.3 Flow diagram for generation of multitoned signals 37

3.4 Flow diagram for Pseudo-random Chipping Sequence 39

3.5 Flow diagram for mixing 41

3.6 Flow diagram for integration 43

3.7 Flow diagram for Generating Φ 45

3.8 Flow diagram for correlating frequency 47

3.9 Flow diagram for carrier detection 48

4.1 Frequency Correlation Graph for Test Data 56

4.2 Frequency Correlation Graph for f_{nyq} = 1GHz 58

4.3 Frequency Correlation Graph for f_{nyq} = 2GHz 60

4.4 Frequency Correlation Graph for f_{nyq} = 2.4GHz 61

4.5 Successful Carrier Detection Vs Decimation Factor for f_{nyq} = 2.4GHz . . 62

4.6 Percentage of Successful Carrier Detection 64

5.1 Mixed Analog Digital System 69

5.2 Typical Spectrum Support of $x(t) \epsilon \mathcal{M}$ 70

5.3 Modulated Wideband Converter 71

5.4 Continuous To Finite Block 73

5.5 Flow diagram for the generation of original support 77

5.6 Flow diagram for Mixing 81

5.7 Flow diagram for LPF 82

5.8 Flow diagram for OMP algorithm in CTF 86

6.1 Minimum Number of Channels for Fully Successful Recovery Vs SNR for N = 2 101

6.2 Minimum Number of Channels for Fully Successful Recovery Vs. SNR for N = 4 101

6.3 Minimum Number of Channels for Full Successful Recovery Vs. Nyquist Frequency for N = 2 103

6.4 Minimum Number of Channels for Full Successful Recovery Vs. Nyquist Frequency for N = 4 103

6.5 Successful Support Recovery Vs. Number of Channels for N=4, NoiseFree105

6.6 Successful Support Recovery Vs. Number of Channels for N=2, Noise Free 106

6.7 Successful Support Recovery Vs. Number of Channels for N=4, SNR=25dB107

6.8 Successful Support Recovery Vs. Number of Channels for N=2, SNR=25dB108

6.9 Successful Support Recovery Vs. Number of Channels for N=4, SNR=10dB109

6.10 Successful Support Recovery Vs. Number of Channels for N=2, SNR=10dB111

6.11 Successful Support Recovery Vs. Number of Channels for N=2, $f_{nyq} = 1GHz$ 113

6.12 Successful Support Recovery Vs. Number of Channels for N=2, $f_{nyq} = 2GHz$ 113

6.13 Successful Support Recovery Vs. Number of Channels for N=2, $f_{nyq} = 2.4GHz$ 114

6.14 Successful Support Recovery Vs. Number of Channels for N=4, $f_{nyq} = 1GHz$ 115

6.15 Successful Support Recovery Vs. Number of Channels for N=4, $f_{nyq} = 2GHz$ 115

6.16 Successful Support Recovery Vs. Number of Channels for N=4, $f_{nyq} = 2.4GHz$ 116

6.17 Probability for the occurrence of False Positives for N = 4 120

6.18 Probability for the occurrence of False Positives for N = 2 120

List of Tables

1.1 Spectrum Sensing Approaches for Cognitive Radio. 3

2.1 Sub Nyquist Strategies (Spectrally Sparse) 18

3.1 System Parameters for WCRR. 35

4.1 Parameter Choices for Verification of Simulation 52

4.2 Parameter Choices 57

4.3 Successful Carrier Detection for f_{nyq} = 1 GHz 63

4.4 Successful Carrier Detection for f_{nyq} = 2 GHz 63

4.5 Successful Carrier Detection for f_{nyq} = 2.4 GHz 64

5.1 System Parameters for MWC. 75

6.1 Parameter Choices for Verification of Simulation 91

6.2 Verification of Support Recovery for Test Data 98

6.3 Parameter Choices 99

6.4 Minimum Number of Channels for 100% Support Recovery when N=2 . 100

6.5 Minimum Number of Channels for 100% Support Recovery when N=4 . 102

6.6 Percentage of Successful Support Recovery at Noise Free for N=4 105

6.7 Percentage of Successful Support Recovery at Noise Free for N=2 106

6.8 Percentage of Successful Support Recovery at SNR=25dB for N=4 107
6.9 Percentage of Successful Support Recovery at SNR=25dB for N=2 109
6.10 Percentage of Successful Support Recovery at SNR=10dB for N=4 110
6.11 Percentage of Successful Support Recovery at SNR=10dB for N=2 111
6.12 Verification of Successful Support Recovery for f_{nyq}=1 GHz 118
6.13 Verification of Successful Support Recovery for f_{nyq}=2 GHz 118
6.14 Verification of Successful Support Recovery for f_{nyq}=2.4 GHz 119

List of Acronyms

WCRR Wideband Compressive Radio Receiver

ADC Analog to Digital Converter

MWC Modulated Wideband Converter

CTF Continuous To Finite

SOI Signals Of Interest

SNR Signal-to-Noise Ratio

CS Compressive Sampling

CR Cognitive Radio

DTFT Discrete Time Fourier Transform

LPF Low Pass Filter

OMP Orthogonal Matching Pursuit

VHDL VHSIC Hardware Description Language

VHSIC Very High Speed Integrated Circuits

FPGA Field-Programmable Gate Arrays

FCC Federal Communications Commission

DSA Dynamic Spectrum Access

CR Cognitive Radio

DSP Digital Signal Processor

PNS Periodic Non-uniform Sampling

Chapter 1

Introduction

This chapter starts with a brief background on the problem addressed by this work, followed by the problem statement and issues to be addressed. The methodology and modelling process used in this research are then discussed and in the last section an overview of the dissertation is presented.

1.1 Background

1.1.1 Cognitive Radios and Spectrum Sensing

Frequency bands used by present day communication systems such as television, radio and mobile carriers are allocated in a predetermined manner making it necessary for every legacy user to operate in a particular range of frequencies reserved for them by the government agency or an authorised regulator. This permanent way of band allocation is leading to heavy spectrum congestion and is becoming impractical due to the limitation in available fixed frequency bands. On the contrary, in [3] it is given that many of the studies conducted by agencies like Federal Communica-

tions Commission (FCC) regarding the spectrum utilization indicates that most of the time, the allocated spectrum are left underutilized in a given geographical area and time, as the concurrent transmissions by legacy users are very less. Dynamic Spectrum Access (DSA) [4] can be used to access these underutilized spectrum in radio communication system. DSA defined in IEEE 1900.1 states that it is a technique by which a radio system dynamically adapts to select operating spectrum to use available spectrum holes with limited spectrum usage rights [4]. Cognitive Radio (CR) system included in DSA may be utilized to control dynamic spectrum access.

According to FCC, " Cognitive radio is a radio or system that senses its operational electromagnetic environment and can dynamically and autonomously adjust its radio operating parameters to modify system operation, such as maximize throughput, mitigate interference, facilitate interoperability and access secondary markets " [5]. As per the terminology used in CR, 'primary users' are assigned with access rights for a specific part of the spectrum and are protected from any interference. On the other hand a 'secondary user' has to identify and use those parts of the spectrum that are not utilized by any of the primary users at a given time. One of the methods used is spectrum sensing technique that takes place whenever the CR searches for available transmission holes. After a certain frequency band is chosen, the CR continuously monitors the spectrum in order to detect any change in the activity of the primary users. Once a primary user becomes active, the CR must choose another working band, or tailor its transmission to reduce in-band power. Quick and efficient spectrum sensing is evidently [3] an essential component of CR functionality. Opportunity based utilization of unused frequency regions by CRs is based on the current trend of increasing interests in spectrum sensing and its capability to take real time cognitive decisions by making use of minimum hardware and software resources. This is becoming very crucial in a commercial environment. Therefore enabling widespread use of CRs calls for innovative spectrum sensing techniques. Various present-day spectrum sensing approaches for CR such as parametric approaches and generic approaches are given in Table 1.1 [3].

While parametric approaches depend on a specific structure of the input signal, generic methods on the contrary, do not depend on this. Parametric approaches can be com-

Table 1.1: Spectrum Sensing Approaches for Cognitive Radio.

Approach	Analog Front-end	ADC/ DSP rate	Shared with CR reception
	Parametric		
Analog pilot detection / matched-filtering	Scanning	N/A	No
Digital pilot detection / matched-filtering	No	Nyquist	Yes
Cyclostationary feature extraction	No	Nyquist	Yes
Waveform-based sensing	No	Nyquist	Yes
Radio identification	No	Nyquist	Yes
	Generic		
Analog energy detection	scanning	N/A	No
Digital energy detection	No	Nyquist	Yes
Multi taper spectrum estimation	No	Nyquist	Yes
Filter bank spectrum sensing	No	Nyquist	Yes
Wideband spectrum sensing using sub-Nyquist sampling	Fixed	sub-Nyquist	Yes

pared to matched filtering that requires the exact transmission shape of the primary user. There are parametric approaches as mentioned in [5, 6] that acquire required knowledge from preambles, midambles, synchronisation bits, cyclostationarity, modulation format etc. On the other hand generic methods avoid any assumptions based on the underlying signal content and the wideband spectrum sensing using sub-Nyquist sampling presented in [3] belonging to the generic family of methods requires only fixed hardware and can have shared acquisition resources. One of the major points about wideband spectrum sensing using sub-Nyquist sampling illustrated in [3] is that it can very well operate in sub-Nyquist Analog to Digital Converter (ADC) and Digital Signal Processor (DSP) rates.

1.1.2 Spectrum Sensing

The term wideband refers to a wide range of frequencies in a spectrum while spectrum sensing is the identification process of frequency support of a given input signal that essentially includes the spectrum intervals in which the signal power exceeds the noise floor [3]. In [3], it is mentioned that the previously existing spectrum sensing methods can be categorised as having either fully hardware dependent or fully software dependent solutions. While hardware dependent analog methods require independent tuning circuits for imitating the scanning mechanism used in the laboratory, software dependent solutions are derived based on the assumption that the input is sampled at a rate obtained using the Nyquist - Shannon sampling theorem [7]. Even though this theorem suggests that the Nyquist frequency, f_{nyq} should be calculated as twice the highest frequency component in the band of interest, f_{max}, it is noted that a practically viable rate may be even higher than this. Also because of this higher rate, premium ADC and DSP devices that can accommodate high-rate streaming data must be included [3]. A sub-Nyquist sampling system will significantly reduce the hardware requirements of the sensing system.

In [1], sub-Nyquist sampling techniques are presented as a classic sub-Nyquist strategies and union of subspaces approach. The classic sub-Nyquist method includes demodulation, an undersampling ADC and periodic nonuniform sampling whereas the union of subspaces approach includes random demodulator and Modulated Wideband Converter (MWC) techniques. The Wideband Compressive Radio Receiver (WCRR) [8] which uses random demodulator architecture and MWC system [9] can be used for identifying the carrier frequencies and frequency support when the input signals are multitoned signals [10] and multiband signals [11] respectively. The carrier frequency is the nominal frequency of radio signals with digital modulation and the frequency support is defined as the position index of a particular interval at which a band is present when the wideband spectrum of a multiband signal is divided into a number of equi-spaced intervals [11].

Through our literature study we could identify that a Very High Speed Integrated

Circuits (VHSIC) hardware descriptive ModelSim simulation model for wideband spectrum sensing of multitoned and multiband signals using sub Nyquist sampling does not exist. If these systems can be implemented in a VHSIC Hardware Description Language (VHDL), it can be used to model digital and mixed signal systems for implementation in Field-Programmable Gate Arrays (FPGA) and integrated circuits which are used in electronic design automation. Such an implementation would reduce the bandwidth requirements of the Compressive Sampling (CS) system, making spectrum sensing less expensive and more agile.

1.2 Problem Statement

The aim of this research is to develop a VHSIC hardware descriptive ModelSim simulation model for wideband spectrum sensing of multitoned and multiband signals using sub Nyquist sampling.

1.3 Issues to be Addressed

We have the following issues to be addressed for the research:

- Identification of sub Nyquist sampling systems for sparse wideband analog signals;
- Development of a ModelSim simulation model for detection of carrier frequency of multitoned signals from sub-Nyquist samples;
- Development of a ModelSim simulation model for blind determination of the support of multiband signals from sub-Nyquist samples where both the sampling and the reconstruction stages do not require knowledge of the spectral support.

1.4 Research Methodology

The research methodology used in this work is based on the methods used in the engineering field. A block diagram showing different processes involved in research methodology is shown in Figure 1.1 [12].

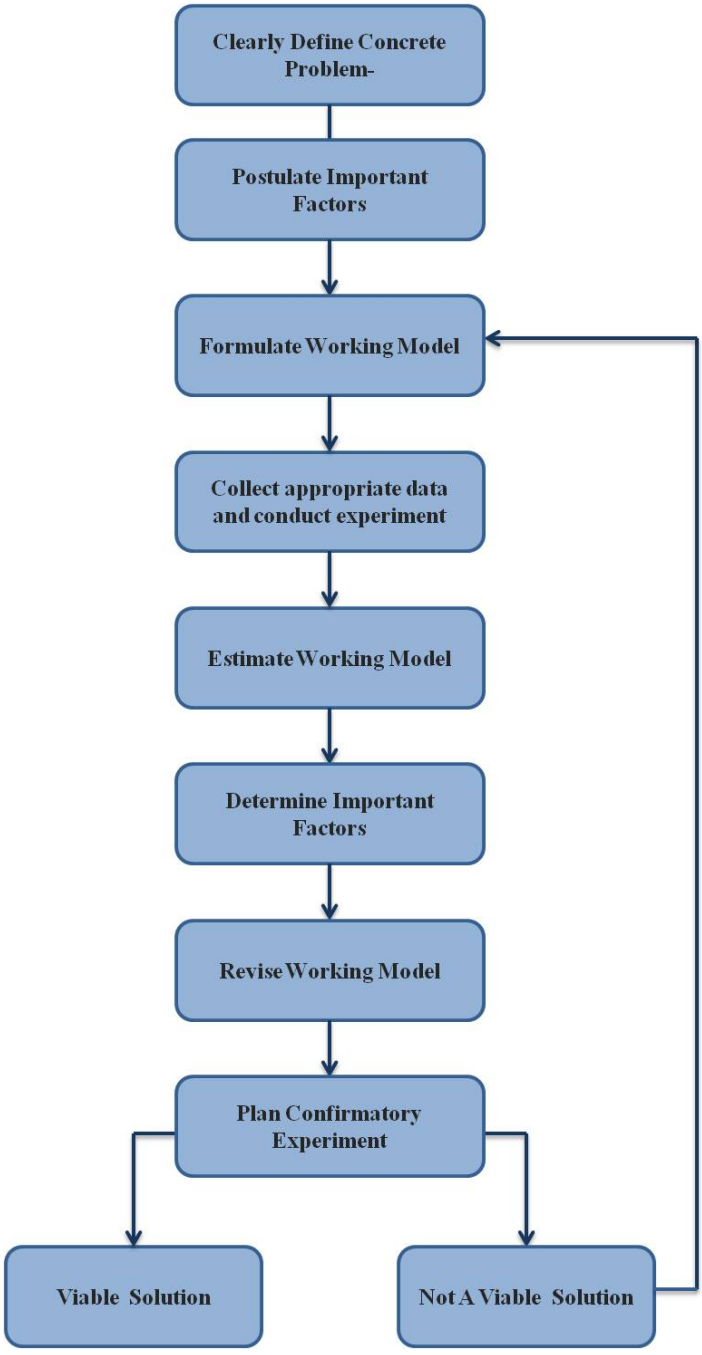

Figure 1.1: Research Methodology

The foremost process indicated in the block diagram is to clearly and correctly define the problem to be researched. This has been done in the present research in Section 1.2 of this chapter. Important factors to be considered are mentioned in Section 1.3. A literature review has been conducted and reported in Chapter 2 to collect appropriate data and determine important factors relevant to the problem stated above. As per the third process in Figure 1.1, working models of the solution have been formulated using the modelling process explained in Section 1.5 and reported in Chapters 3 and 5. The suitability of the working models have been examined and appropriate data have been collected and sufficient analysis has been carried out to validate and verify the solutions in Chapters 4 and 6 before concluding this research in Chapter 7 with a viable solution as suggested by the later processes in the given figure.

1.5 Modelling Process

A method which is used for the complete assessment and evaluation of computer based simulation models starting from the model development process is discussed in [13]. As this thesis deals with the development of simulation models, the verification and validation is done using this paradigm. Figure 1.2 adapted from [13] represents how verification and validation map onto the modelling process.

Definitions of each terminologies used in the Modelling Process as given in [13] are given here:

- Problem Entity is the proposed idea, situation or phenomena to be modelled.
- Conceptual Model is the mathematical/logical/verbal representation of the problem entity developed for a particular study.
- Conceptual Model Validation is defined as determining that the theories and assumptions underlying the conceptual model are correct and that the model representation of the problem entity is reasonable for the intended purpose of the model.

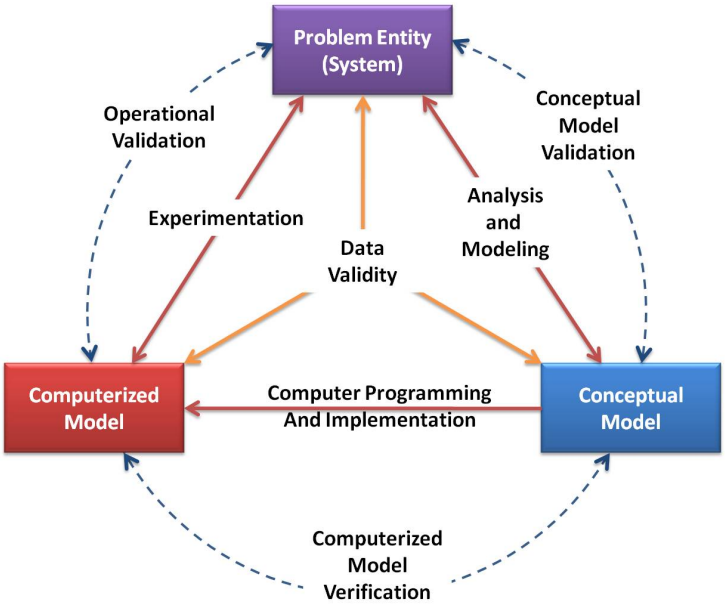

Figure 1.2: Modelling Process

- Computerized Model is the conceptual model implemented on a computer.
- Computerized Model Verification is defined as assuring that the computer programming and implementation of the conceptual model is correct.
- Operational Validation is defined as determining that the model's output behaviour has sufficient accuracy for the model's intended purpose over the domain of the model's intended applicability.
- Data Validity is defined as ensuring that the data necessary for model building, model evaluation and testing and conducting the model experiments to solve the problem are adequate and correct.

This iterative modelling process which is used for the development of a valid simulation model includes the development of a conceptual model followed by its validation. Once the model becomes valid, the computerized model is developed. This model is then verified for assuring that the computer programming of the conceptual model is correct. Operational validation is done when the computerized model verification is completed and has given satisfactory results.

The problem entity considered in our modelling process is given in Section 1.2. In order to develop conceptual model detailed in the form of algorithms and flow diagrams in Chapters 3 and 5, the technique we used is the data validation process given in [14]. For validation technique, the data collected from the literature, is used for building the model as well as to check whether the behaviour of the model is similar to that of the system. The VHDL code which serves as the computerised model for implementing the simulation model in ModelSim is discussed along with the conceptual model. A numerical investigation of different blocks of algorithms of the conceptual model has been conducted using test parameter choices to verify the correctness of the functioning of the simulation model. This is done so as to verify that the programming and implementation of the conceptual model is correct in Chapters 4 and 6. As the models we considered consist of different sub blocks, the method which we use for computerised model verification is the bottom-up strategy. Bottom-up testing is defined in [14] as a method of testing the sub models first and then the overall model. Then the operational validation is done for further assessment and validation of the models using parameter variability - sensitivity analysis. This technique described in [14] determines the effect upon the model's behaviour and its output by changing the values of the input and internal parameters of a model. Data validity is done by summarising the results of our system in Chapter 7.

1.6 Dissertation Overview

Overview of this dissertation is given as follows:

1.6.1 Literature Review

The literature study presented in Chapter 2 provides an overview of the different aspects of the problem to be investigated through this research. These topics have been identified as sub-Nyquist sampling techniques, compressive sampling, CS based wide-

band spectrum sensing and its recovery algorithms. An attempt to throw some light onto the conceptual overview of the simulation tool ModelSim that is used for the simulation of design models has also been presented in this chapter.

1.6.2 Wideband Compressive Radio Receiver

Development of a simulation model for WCRR [8] has been done using ModelSim by formulating required algorithms and has been reported in Chapter 3.

1.6.3 Verification and Validation of WCRR

Chapter 4 describes the verification and validation of the WCRR model developed for the simulation by conducting a numerical investigation using test parameter choices. Also the results generated using the simulation models by assuming actual parameter choices are presented. It also deals with the statistical analysis for validating the results obtained.

1.6.4 Modulated Wideband Converter

A simulation model of mixed analog digital system [9] is developed using ModelSim and is described in chapter 5. The system consists of mainly three blocks namely the multiband signal model, MWC and Continuous To Finite (CTF) block.

1.6.5 Verification and Validation of MWC

Chapter 6 describes the verification and validation of the MWC developed for the simulation using test parameter choices. This chapter also presents the results generated by assuming actual parameter choices and a statistical analysis for validating the results.

1.6.6 Conclusion

The dissertation is concluded in Chapter 7 by giving a summary of the work that has been carried out during this research. Contributions in conferences and scope of future work in this area are also listed in this chapter.

Chapter 2

Literature Review

A literature survey on the topics of sub-Nyquist sampling techniques, compressive sampling and its various recovery algorithms is presented in this chapter. This is followed by a brief conceptual overview of the simulation tool ModelSim used in this research.

2.1 Introduction

The research focused on this dissertation deals with wideband spectrum sensing based on a system that uses a fixed hardware with ADCs and DSPs having low rates. In this chapter, a literature survey is conducted on the topics of traditional sub- Nyquist sampling and their comparison as well as compressive sensing and recovery for wideband signals. The former part of this chapter explains Nyquist sampling while the latter discusses a review on the fundamentals of compressive sensing and those of the recovery algorithms based on compressive sensing. Prior to arriving at a conclusion and summarising the chapter, a brief description highlighting the major aspects of the simulation environment ModelSim, a tool that can accept VHDL and Verilog commands as specific instructions, is also provided.

2.2 Nyquist Sampling

The amount of information in a signal was characterised mathematically for the first time by Shannon in 1948 [7] and has led to the foundation of a new field in science called Information Theory. The Shannon sampling theorem has in effect made a positive impact on the information theory when it suggested that a discrete sequence of samples can replace a continuous band limited signal without the loss of any required information. This theorem also specifies the lowest rate known as the Nyquist rate of such samples to be acquired for successful reproduction of the original continuous signal [15]. The original statement of Shannon's sampling theorem is reproduced here as follows [7]:

*"If a function f(t) contains no frequencies higher than **B** cycles per second it is completely determined by giving its ordinates at a series of points spaced (1/2**B**) seconds apart".*

However there are cases in which sampling at this higher rate may not be feasible or may prove to be totally inefficient due to hardware or software limitations. Also sampling at this higher rate leads to the need of ADCs which are very expensive [16]. These limitations can be overcome by a method which effectively samples at sub-Nyquist rates. In this literature survey we give an overview of various classic sub-Nyquist methods and union of subspaces.

2.3 Classic sub-Nyquist Methods

The classic sampling techniques assume a multiband signal with known frequency support and reduces the sampling rate below Nyquist. Some of these techniques are described in the following subsections.

2.3.1 Demodulation

Demodulation is the most common technique used for reducing the Nyquist sampling rate. In [17] the purpose of the receivers is given as to recover the desired signal from a wide spectrum of transmitting sources for efficient use of the radio spectrum, thereby making it available for more users. The direct conversion receiver also known as I/Q demodulation, zero I/F receiver or homodyne receiver is a common and useful RF signal processing receiver [18]. This demodulator consists of two demodulator circuits for the conversion of RF input signal directly to baseband signal. This conversion is obtained by splitting the input signal and then multiplying with a carrier frequency of a band of interest having a 90° phase shift. Then the outputs undergoes lowpass filtering so as to remove the high-frequency mixing products. This provides baseband signals that are then sampled and converted to digital values using low rate ADC devices which can then be demodulated using an angle or phase measurement algorithm.

2.3.2 Undersampling ADC

Aliasing is a phenomenon which destroys the ability to recover the signal when the sampling rate is less than the Nyquist rate. Undersampling exploits this aliasing phenomenon to enable the ADC to sample the signal using a rate that intentionally aliases the modulated carrier into the operating range of the ADC. In undersampling, the ADC is done directly to the input signal without any preprocessing. When uniform sampling of a bandpass signal is done, the samples are indistinguishable from the samples of a low-frequency alias of the high-frequency signal. Such sampling is also termed as direct bandpass sampling, super-Nyquist sampling, harmonic sampling, IF sampling, and direct IF-to-digital conversion [19].

The conditions for uniform sampling rates as given in [20] is:

$$\frac{2f_u}{n} \leq f_s \leq \frac{2f_l}{n-1} \tag{2.1}$$

where f_s is the sampling frequency, the information band is confined to the frequency range (f_l,f_u) i.e the bandwidth, B = f_u - f_l and $1 \leq n \leq \frac{f_u}{B}$. In [20], it is shown that the increase in the rate reduction factor, k, leads to narrowing down the valid region of the sampling rate. Hence the sampling rate for undersampling increases beyond $2B$. Also the sampling of a multiband signal using uniform sampling is found to be difficult due to the varying range of the sampling rate for each individual bands.

2.3.3 Periodic Non-uniform Sampling (PNS)

In [21] and [22] the possibility of sampling and reconstruction of bandpass and multiband signals using PNS is reported. In PNS the input signal enters m parallel branches which sample the signal uniformly with period T but shifted in time with respect to each other. The sampling rate of a PNS system achieves Landau's rate [23] which is no lower than the sum of the bandwidths, i.e. NB where N is the number of information bands and B is the bandwidth. Bands of different widths are treated by viewing the bands as consisting of narrower intervals that are integer multiples of a common length making it into equal width. In [1], PNS is mentioned as a time interleaved ADC, thereby leading to the need of ADCs in each sampling branch with Nyquist rate of input signal.

2.4 Union of subspaces

In [24], it is given that the signals of interest live in a fixed union of subspaces that is defined as

$$\mathcal{X} = \bigcup_{\gamma \epsilon \Gamma} S_\gamma \tag{2.2}$$

where S_γ are subspaces of $\mathcal{H}$, the Hilbert space, and Γ is an index set. In union of

subspaces modelling, two input cases are assumed for sub-Nyquist sampling, one is the multiband input signal with unknown frequency support in which S_γ corresponds to the signals with specific carrier positions and the union consists of all the possible carriers. In the definition of multiband model [9], $\mathcal{M}$ is given as "The set $\mathcal{M}$ contains all signals *x(t)* , such that the support of the Fourier transform *X(f)* is contained within a union of disjoint intervals (bands) in $\mathcal{F} = [-1/2T. + 1/2T]$, and each of the bandwidths does not exceed B" . The other input case is the multitoned signal that consists of several echoes of a known pulse shape, where the delays and attenuations are *a priori* unknown and in which S_γ corresponds to all the possible delays. Multitone signals are bandlimited, continuous-time, periodic signals that contain multiple frequency waveforms combined in a single waveform [10]. Two possible techniques have been proposed in [1] for the recovery of these signals, they are MWC and random demodulator.

2.4.1 MWC

This sub-Nyquist strategy combines the advantages of RF demodulation and the blind recovery model, CTF, and allows sampling and reconstruction of multiband signals whose band locations are unknown. In this strategy the input signal is mixed with a periodic waveform by the RF front end to overcome the bandwidth requirements of ADC techniques. This mixing helps in folding the input signals to the baseband similar to that in undersampling. Here the reconstruction of the unknown spectral support is carried out using CTF block. The recovered solution gives the spectrum slices containing signal energy. In CTF it is done via a greedy algorithm termed as the Orthogonal Matching Pursuit (OMP) algorithm. MWC [9] is selected for blind reconstruction of the support of multiband signals from sub-Nyquist samples and will be detailed in Chapter 5.

2.4.2 Random Demodulator

This method determines the sparse multitoned signals by exploring the CS techniques discussed in Section 2.6. In the random demodulator the input signal, of a certain Nyquist rate is mapped to low rate measurements via binary random sampling. Using a suitable recovery technique, the vector obtained after the integration of the low rate samples gives the unknown carrier frequencies. The architecture of random demodulator is used as an acquisition hardware and the recovery technique for multitoned signals using WCRR [8] is detailed in Chapter 3.

2.5 Classic sub-Nyquist Sampling Vs Union of Subspaces

Table 2.1 shows a comparative study on the sub-Nyquist sampling techniques and consists of information taken from [1]. The sub-Nyquist sampling techniques can be of two types, Classic sub-Nyquist sampling and union of subspaces method. Some of the Classic methods are Demodulation, Undersampling and PNS method. In the demodulation technique, the recovery can be done using low rate ADCs but only if the band locations of the multiband input are known. The Undersampling technique can be used for a single band and only if the maximum frequency is lower; since our requirement is to use ADCs of lower rate which are less expensive. PNS is limited because of the analog bandwidth, each sampling branch requires Nyquist rate ADCs. Single subspace methods cannot be used when the carrier positions are unknown. As our aim is blind recovery, the options are one or more of the union of subspaces strategies like MWC and random demodulator which uses ADCs of low bandwidth.

From the table it can be seen that the techniques which require low ADC bandwidth are demodulation, MWC and random demodulator. In demodulation technique, the recovery can be done only if the band locations of the multiband input are known. Since we need to recover even when the carrier locations are unknown, we go for MWC and random demodulator techniques. The low rates here corresponds to a rate

Table 2.1: Sub Nyquist Strategies (Spectrally Sparse)

Strategy	**Model**	**Required ADC Bandwidth**
Shannon-Nyquist	Bandlimited	Nyquist
Classic		
Demodulation	Multiband	Low rate
UnderSampling	Bandpass	Nyquist
PNS	Multiband	Nyquist
Union of Subspaces		
MWC	Multiband	Low
Random Demodulator	Sparse Harmonic	Low

lower than the Nyquist rate.

2.6 Compressive Sampling

Compressive Sampling (CS) alternatively known as compressive sensing or compressed sensing plays an efficient role by sampling at much lower rate than that recommended by Shannon's theorem. CS may be represented as a generalised form of a point-sampling technique in which inner products are selected between an unknown signal vector and a set of user defined test vectors. For a certain set of random ensembles, compressive sampling is considered as a universal sampling procedure as it is proven to be efficient in encoding information in any sparse signal [25]. In CS it may be observed that in case of the reconstruction of the original signal, the number of samples required is much fewer than the dimension at which the signal vector is acquired. This is achieved mainly because the CS technique relies on sparsity and incoherence. Sparsity pertains to the signals of interest and incoherence pertains to the sensing modality [2].

The sparsest solution of the compressive sensing problem is given by Equation 2.3 based on the properties mentioned above [26].

$$(P_0) \quad \min_{v=R^m} \|v\|_0 \text{ subject to } \Phi v = y, \tag{2.3}$$

where Φ is the coding/sampling matrices with rows $\Psi_j \in R^m$, $\|v\|_0$ is the size of the support of v and y is the sampled vector. A minimization problem of the same kind is however observed to be NP-hard [27] since exhaustive searches are required over all subsets of Φ columns. But as a matter of fact, most of the researchers [27–30] reported that the P_0 given by Equation 2.3 is equivalent to an *l1*-norm minimization problem, and thus can easily be recasted as a linear problem. Typical examples that can illustrate the applications of the above discussed principles may be found in [2].

2.7 CS Based Wideband Spectrum Sensing

The basics of compressive sensing are discussed here followed by recovery algorithms used in compressive sensing that help in wideband spectrum sensing.

2.7.1 Compressive Sensing Basics

Sparsity

Sparsity is vital in CS as it determines the efficiency by which the signals can be acquired non-adaptively. It determines the ”information rate” in case of a continuous time signal or the required number of ”degrees of freedom” in case of discrete time signals. The required information rate of a continuous time signal may be expressed to be much lower than that suggested by its bandwidth or in case of a discrete time signal, the number of degrees of freedom required may be much lesser than the finite length of the signal considered [2]. One of the most common definitions of sparsity in compressive sensing is expressed by Equation 2.4 [2].

Let the recorded values of a signal *f(t)* be denoted by the vector $\mathbf{f} \in R^m$, that can be expanded into an orthonormal basis $\Psi = [\psi_1 \psi_2 \dots \psi_m]$ as given below.

$$f(t) = \sum_{i=1}^{m} x_i \psi_i(t) \tag{2.4}$$

where x is the sequence of coefficients of f, $x_i = \langle f, \psi_i \rangle$. Let Ψ denote the $m \times m$ matrix with $\psi_1 \ldots \psi_m$ as columns.

When a signal has a sparse expansion, it is implied that the small coefficients may be ignored by maintaining most of the required information from the signal. If the sparse expansion of a signal has a maximum of, say, K non-zero entries, then the signal is called K-sparse. Many of the signals can be concisely represented when expressed in a proper Ψ basis and can thus be exploited to a large extent by CS with regards to their sparsity or compressibility.

Incoherent Sampling

Incoherence is the characteristic which expresses the relation between time and frequency of a signal and in relation to objects having sparse representations in Ψ, these characteristics are expressed to be spread out in a domain from which they are acquired [2].

Consider that the pair (Φ, Ψ) be the orthobasis of R^m, where Φ represents sensing modality and Ψ represents the signal model. Equation 2.5 represents a relation that shows the coherence between Φ and Ψ.

$$\mu(\Phi, \Psi) = \sqrt{m}. \max_{1 \leq k,j \leq m} \left| \langle \varphi_k, \psi_j \rangle \right| \tag{2.5}$$

The largest correlation between any two elements Φ and Ψ is measured using this coherence in Equation 2.5. If there are correlated elements contained in Φ and Ψ, then it can be stated that the coherence is large or otherwise it is small. Also, from linear algebra [2], $\mu(\Phi, \Psi) \in \left[1, \sqrt{m}\right]$.When each of the measurement vectors represented by the rows of Φ are spread out in the Ψ domain, the value of μ will be closer to its lowest

minimum value of 1. It can be proved [2] that reconstruction of a K-sparse signal is possible in any domain corresponding to test vectors with coherence of the order of 1. The sensing waveforms have an extremely dense representation in the basis Ψ making incoherence equally important as sparsity.

Random Sampling

Compressibility of a signal can be estimated by its sparsity and incoherence in the sense that a signal having a larger sparsity in some domain Ψ and lesser coherence in the sensing domain Φ is said to be more compressible. This may be argued to be less feasible for most sensing devices as it is computationally more expensive to transform from a denser domain to a sparser domain. But if random matrices are selected, it can be observed that they are largely incoherent with any fixed basis Ψ, where the coherence is $\sqrt{2\ log\ m}$ for a randomly selected uniform orthobasis Φ [2]. This randomly selected Φ can be used for the orthonormalization of m vectors sampled uniformly and independently on a unit sphere. Similarly a very low coherence is exhibited by random waveforms having independent and identically distributed (i.i.d) entries with any fixed representation Ψ. Gaussian or Bernoulli distributed random entries are examples of such entries. When Φ can be made unstructured with respect to Ψ, it is generally possible to make measurements having incoherence in the sparsity domain Ψ. As an optional strategy for acquiring sparse signals in some sense, near minimal number of random measurements [31–33] can be taken and the constants appearing in the analysis are small.

One of the theorems presented in [2] is reproduced here in support of the above discussions:

Theorem 1 [2]: Fix $u \in R^m$ and suppose that the coefficient sequence x of u in the basis Ψ is K-sparse. Select n measurements in the Φ domain uniformly at random. Then if

$$n \geq C \cdot \mu^2(\Phi, \Psi) \cdot K \cdot \log m \tag{2.6}$$

for some positive constant C, the sparsest solution to recover u is exact with overwhelming probability. This in other words proposes that the minimum number of samples, n to be selected in case of a previously known signal which is K-sparse in some domain Ψ is $O(C \cdot \mu^2(\Phi, \Psi) \cdot K \cdot \log m)$ when the samples are randomly selected from the domain Φ. Thus the acquisition protocol suggested by the theorem is to assume an incoherent domain and perform non adaptive sampling, followed by linear programming, once the acquisition step has been completed. This process will acquire a compressed signal that can be decompressed with the help of a suitable decoder, such as *l1* minimisation [2].

2.7.2 CS Recovery Algorithms

Some of the recovery algorithms that are commonly used in compressive sensing are briefly described below.

l1-norm Minimization

A report of the study conducted in [31] demonstrates the effectiveness in the recovery of sparse signals from a limited number of measurements by the *l1*-norm minimisation process. This minimisation process can be represented as given in Equation 2.7 that follows the notation *(P_0)* mentioned in Equation 2.3

$$(P_1) \quad \min_{v=R^m} \|v\|_1 \text{ subject to } \Phi v = y, \tag{2.7}$$

where $\|v\|_1 = \sum_j |v_j|$. Equation 2.7 represents a problem *(P_1)* that can be solved by linear programming techniques. Furthermore there are a number of algorithms such as Fixed Point Continuation (FPC) [34], interior point methods [35] and homotopy methods [36] that are specifically used for solving the *l1*-norm minimisation problem mentioned above. Even though some of those recovery algorithms may take a longer

period to converge to the sparsest solution, they are considered accurate and robust for the reconstruction of sparse signals.

The *l1*-norm recovery algorithm may also converge to an exact solution for a K-sparse signal when $K < (1 + 1/M)/2$, where M is the coherency parameter of the measurement matrices Φ and the signal model Ψ. Based on this it is possible [37] to construct deterministic matrices of Φ with $K \approx \sqrt{n}$.

1-Bit Compressive Sensing

In a recent study conducted by [38] it was shown that by modifying a *l1*-norm minimisation algorithm, signals can be recovered by preserving only the sign information of the random measurements. In 1-bit compressive sensing, less expensive and fast 1-bit quantizers are utilised for CS. The FPC algorithm discussed in [34] is adapted here as the reconstruction algorithm with mainly two modifications. Computation of the gradient descent step ensuring that the gradient of one sided quadratic penalty is projected on the unit sphere $\|x\|_2$=1 serves as the first modification and the introduction of a renormalisation step on every iteration of the algorithm enforcing the solution to be on the unit sphere serves as the second modification.

Similar modifications are used in [39] while stabilising the reconstruction of sparse signals in the sense that amplitude information from the signal is eliminated by both sign measurements and zero crossings. Signal dependency of the zero crossings is one of the major differences in [39] that may be identified when compared to compressive sensing as it is signal independent.

Matching Pursuit

Matching Pursuit recovery [40] is a concept that considers signal recovery as a dual to the sparse approximation problem. In this case the measurement vector is obtained as a linear combination of m columns from the sensing domain Φ as the signal has only

K non zero components. This ensures that sparse signals can be recovered by using sparse approximation algorithms. Determination of columns of Φ that participate in the measurement vector is an identification of the ideal signal. The sparse approximation algorithm used in [40] can pick those columns of Φ such that on each iteration there is a strong correlation with the remaining part of the measurement vector. Iteration is then carried out on the residual measurement vector after subtracting such correlating columns from the measurement vector. This method is advantageous in the sense that complexity of the algorithm is significantly reduced.

2.8 ModelSim

ModelSim is widely known as a simulation tool that can be programmed with high level languages such as VHDL, Verilog and SystemVerilog. It can verify and support mixed language designs as well. An overview of the concept of the ModelSim simulation environment taken from [41] is briefly described in this section under four subsections. First three subsections deal with the basic flow of the simulation, project flow and multiple library flow. The fourth subsection deals with some important debugging tools in ModelSim.

2.8.1 Basic Simulation Flow

Basic steps involved in the process of simulating a design is represented as a block diagram in Figure 2.1.

Creating the Working Library

ModelSim requires that every design be compiled into a separate library and a new simulation is by default created in a working library called ”work” that is identified by the compiler as the default destination of the compiled design units.

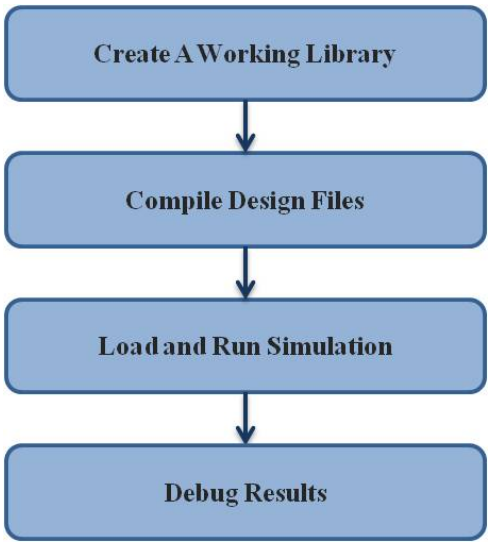

Figure 2.1: Basic Simulation Flow

Compiling the Design

Once the work library is created, sufficient coding can be carried out to formulate the required design in any high level language supported by ModelSim. A compiler compiles these codes of the design to a machine understandable language and creates design units in the work library that may be used across any supported platform without needing to recompile the library again and again.

Loading and Running the Simulation

Further to the successful completion of the compiling process, the simulator module is to be loaded with the compiled design units by invoking it on a top-level module (Verilog) or a configuration or an architecture pair (VHDL). When the simulation is successfully loaded and the simulation time is set to zero, a run command can be entered to begin the simulation process.

Debugging the Results

ModelSim is equipped with a robust debugging environment that can be made use of for tracking down any unexpected or nil results after the simulation.

2.8.2 Project Flow

It is not mandatory to use projects in ModelSim, but starting a project will definitely ease the interaction with the tool and may help by organizing files and specifying customised simulation settings.

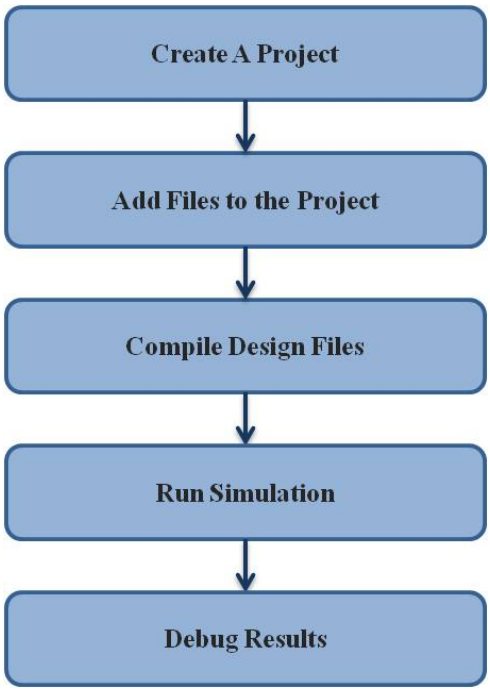

Figure 2.2: Project Flow

Figure 2.2 represents the basic steps involved in the simulation of a design within a ModelSim project. It can be clearly interpreted from Figure 2.1 that Project flow is almost similar to the basic simulation flow except that it is not required to manually create a work library and that the projects are persistent or need not be opened manually every time ModelSim is invoked.

2.8.3 Multiple Library Flow

Libraries in ModelSim are considered in two different ways; as a local working library containing all the compiled versions of design files and as a resource library. While the contents of a local library keep changing with every update of the design once the recompilation is done, a resource library is typically static and is considered as part of the source of the design. Resource libraries can be created and customised to meet the requirements of the design or may be incorporated from external designs. There are options to select the required resource libraries for a particular design and rules can be created to mention the order of preference for a particular library to be searched. A simple illustration of the simultaneous use of a local and a resource library is where a gate level design and test bench are compiled to a work library, while gate level models are referenced from a separate resource library. It is also possible to link a project to multiple libraries as and when required.

Diagram shown in Figure 2.3 corresponds to the basic steps in simulation with multiple libraries.

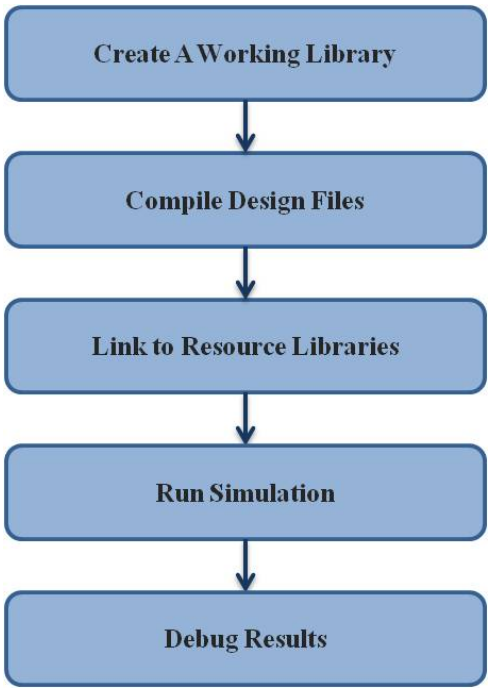

Figure 2.3: Multiple Library Flow

2.8.4 Debugging Tools

ModelSim offers numerous tools for debugging and analyzing your design. Several of these tools are:

- Using projects
- Working with multiple libraries
- Setting breakpoints and stepping through the source code
- Viewing waveforms and measuring time
- Viewing and initializing memories
- Creating stimulus with the Waveform Editor
- Automating simulation

2.9 Summary

In this chapter a literature survey has been conducted on the topics of sub-Nyquist sampling techniques, compressive sensing and recovery algorithms. From the sub-Nyquist sampling techniques survey we identified that the MWC and random demodulaor which comes under union of sub-spaces method helps to recover the multiband and multitoned signals respectively. In CS, we have included the topics of sparsity and incoherence that are inter-related to one another as far as compressive sensing technique is concerned. This chapter also includes a survey of various aspects of the simulation environment used in ModelSim that helped in developing a design of the working simulation of the methods mentioned above. Thereby these aspects form a strong foundation that leads to the development of the ModelSim simulation models of two methods namely the WCRR which uses random demodulator architecture and the mixed analog digital system which uses MWC detailed in Chapter 3 and 5 respectively.

Chapter 3

Wideband Compressive Radio Receiver

In this chapter the concept of a generic wideband receiver is presented as a prerequisite for discussing the architecture and design parameters of WCRR. Various components of the simulation model for WCRR are also discussed here using necessary algorithms, flow diagrams and VHDL codes.

3.1 Introduction

In Chapter 1, the steps involved in the modelling process of a computerised simulation model is discussed in Section 1.5. This chapter details the steps involved in the modelling process of the WCRR that processes the multitoned signals at sub Nyquist rate without needing to have the signal reconstructed *a priori* and reduces the high computational effort implied for the signal reconstruction process [8]. The problem considered here is one part of the problem statement given in Section 1.2 which is stated to develop a model for spectrum sensing of multitoned signals using sub Nyquist sampling.

In this study we aim to develop a conceptual model after which a validation process is necessary to determine the theories and assumptions underlying the model are satisfactory. For conceptual model validation, the technique used here is the historical data validation given in [14]. In this validation technique the data collected from the literature explained in Section 3.3 is used for building the model as well as to check whether the behaviour of the model is similar to that of the system. The data collected from the literature helps in developing the conceptual model and is detailed in Section 3.4 as algorithms and flow diagrams. The VHDL code which serves as the computerised model for implementing the simulation model in ModelSim is discussed along with the conceptual models. The computerised model verification and operational validation is done in Chapter 4.

3.2 Generic Wideband Receiver

Figure 3.1 shows the block diagram representing the functioning of a generic wideband receiver [8]. As seen in the diagram, a generic wideband receiver first isolates the wide

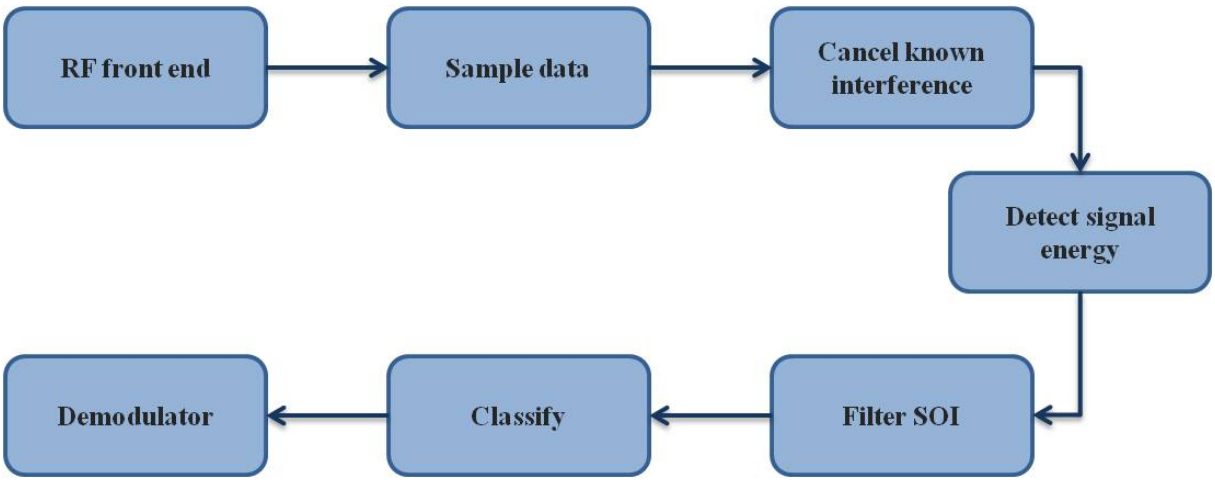

Figure 3.1: Generic Wideband Receiver

collection bandwidth after tuning to it with the help of an analog hardware component. Digital samples acquired at rates greater than the Nyquist rate are then generated from the analog output of the RF front end. Now it is the duty of the receiver to identify the

presence of signals in the monitored bandwidth once the effects of known interference are compensated. While it is possible to apply numerous techniques such as spectral energy detection in single channel receivers in order to identify unknown signals, in general cases the receiver is supplied with a priori information about the presence of Signals Of Interest (SOI)s or the position of the SOIs, making it easier to detect their presence. When a SOI is successfully detected, an appropriate demodulation algorithm is applied for the type of SOI detected to retrieve the information contained in the signal.

3.3 Wideband Compressive Radio Receiver

As our objective is to detect the carrier frequencies present in the sparse wideband multitoned signals, only the sampling and detection block from the generic wideband receiver will be focussed in the next subsections.

3.3.1 Multitone Signal

Multitone signals are bandlimited, continuous-time, periodic signals that contain multiple frequency waveforms combined in a single waveform. The Fourier series expansion from [10] representing a multitone signal, *x(t)* is as follows

$$x(t) = \sum_{n=-N/2}^{N/2-1} X(n) e^{j\frac{2\Pi}{T_x}nt}; \;\; for\; n \,\epsilon\, \mathbb{Z} \tag{3.1}$$

where *X(n)* denotes the Fourier series coefficients of x(t), T_x denotes the period of x(t) in seconds, and N is assumed to be a positive even integer. The summation limits are finite because the harmonics of the fundamental tone $1/T_x$ are assumed to be bounded thereby making the signal bandlimited. A multitone signal is said to be sparse if a small number of the Fourier series coefficients are non zero.

3.3.2 Random Demodulator

A WCRR [8] acquires and tracks signals that may be present in a wide frequency bandwidth and uses a random demodulator architecture [42] for compressive sampling. In Figure 3.2, the block diagram given represents a random demodulator that acquires sparse bandlimited signals.

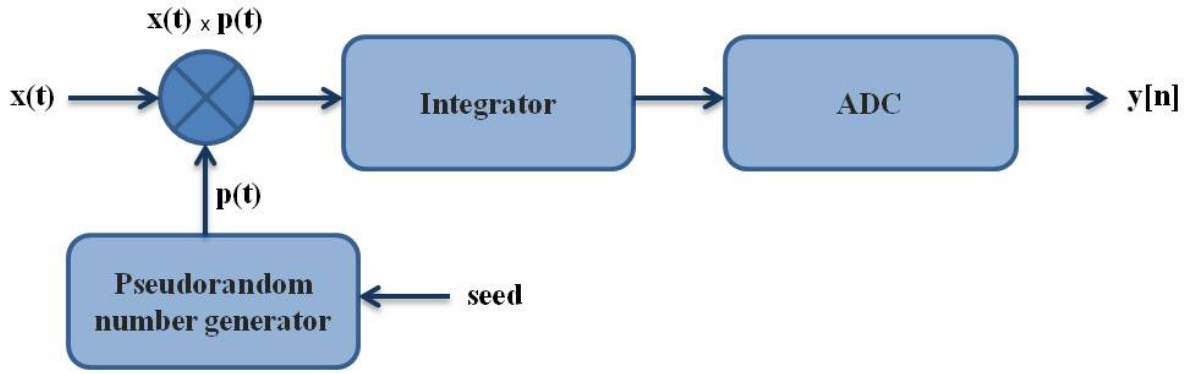

Figure 3.2: Random Demodulator

The mixer multiplies the input signal, *x(t)* with *p(t)*, where $p_j = \pm 1$ sequence is generated by a pseudo-random chipping sequence generator to produce P that spreads out the sparse signal partially into the spectrum.

$$P_j = x_j(t) \times p_j(t); \quad j = 1, 2, \ldots N \tag{3.2}$$

An integrator then does low pass filtering, the output of which is then subjected to sampling with a low rate ADC producing *y[n]*. It is to be noted that even though the back end ADC is operating at low rate, the chipping sequence generator and the modulator are operating at above Nyquist rate.

$$y[n] = \sum_{i=1}^{L} [(n-1)L + i]; \quad n = 1, 2, \ldots M \tag{3.3}$$

Advanced production technology for high rate modulators and sequence generators are more available than for a high rate ADC. The decimation factor, L or the ratio of the Nyquist rate to the sampling rate of the ADC in the random demodulator [8] can be calculated as

$$L = N/M \tag{3.4}$$

From [8] this random demodulator is described mathematically as a linear operator, Φ that maps Nyquist rate samples of $x(t)\ \epsilon\ \mathbb{R}^N$ to $y[n]\ \epsilon\ \mathbb{R}^M$ representing a discrete sequence of measurements and then quantizing them. The operator Φ is an M $\times$ N matrix and can be represented as

Phi, Φ =

$$\begin{bmatrix} p_1 \dots p_L & & \\ & \ddots & \\ & & p_{N-L+1} \dots p_N \end{bmatrix} \tag{3.5}$$

where p_j values are the N pseudo random numbers in p[N]. The mapping operation from an N dimensional vector to an M dimensional vector is described by the equation 3.6.

$$y = \Phi\ x \tag{3.6}$$

where y and x indicate the vectors y[m] and x(t) respectively.

3.3.3 Carrier Detection

The method of carrier detection in WCRR given in [8] is to search within the bandwidth of interest and to detect the frequencies of the SOI at which information is present. Let f_k where k = 1,2,...K be the frequency set expected to have the carrier within the

measured bandwidth.

The correlation equation from [8] given by Equation 3.7 shows that carrier detection is done by correlating $\Phi e^{j2\pi f_k t}$ with the sampled signal y. In other words we correlate the output of the the random demodulator for a series of single tone sinusoid inputs at a selected set of frequencies, f_k, with the output of the random demodulator for the multitoned signal, *x(t)*.

$$S(k) = \left| \left\langle \Phi \, e^{j2\pi f_k t}, y \right\rangle \right|^2 = \left| y^T \Phi \, e^{j2\pi f_k t} \right|^2 \tag{3.7}$$

where *S(k)* is a length K vector containing the correlation coefficients corresponding to the set of frequencies *f(k)*. The correlation coefficients give an estimate of the power in signal *x(t)* at frequency *f(k)*.

3.4 Prototype Architecture

Various parameters used in the simulation of the WCRR system are briefly discussed in this section. It also presents the algorithms, flow diagrams and VHDL codes used for constructing the simulation models of various essential components of the system such as the input model, the random sequence generator, mixer, integrator and frequency correlator for carrier detection.

3.4.1 System Parameters

In this section a table representing the parameter notation and its description is presented. The discussion following the table shows the equations which are used for the calculation of these parameters.

As can be seen from Table 3.1, the total collection bandwidth of the WCRR system is

Table 3.1: System Parameters for WCRR.

Parameter	Description
W	Total collection bandwidth of the system
f_{nyq}	Nyquist frequency
T_{nyq}	Nyquist rate
L	Decimation factor
ν_{eff}	Effective Sampling Rate

denoted by W. Therefore the Nyquist rate of the system , f_{nyq} can be obtained from Equation 3.8.

$$f_{nyq} = 2 \times W \tag{3.8}$$

Sampling rate suggested by f_{nyq} is denoted by T_{nyq} and can be calculated from the Equation 3.9.

$$T_{nyq} = 1/f_{nyq} \tag{3.9}$$

To calculate the effective sampling rate denoted by ν_{eff}, the following equation from [43] is used

$$\nu_{eff} = f_{nyq}/L \tag{3.10}$$

where L is the decimation factor.

3.4.2 Generation of Multitoned Signal

Design of the input model for simulation is carried out using the Algorithm 1 given below. As WCRR is used for the carrier detection of multitoned signals, the input to the system is a model that generates multitoned signals. In [44] a multitoned sig-

nal is defined as a composite of several sine waves, where each sine wave can have distinct amplitude, phase and frequency. Input to the algorithm comprises of carrier frequency, f_c (Hz) at which the sine wave alternates, the number of elements in the carrier frequency vector, l, selected dimension of Nyquist rate samples, N, and the time length of the Nyquist frequency, t_n (s). Output of the algorithm is the sine wave *x[N]* alternating at the frequency of f_c, which is then given as one of the inputs to the mixer. Figure 3.3 and HDL Code 3.1 represents the flow diagram and VHDL code of the input model respectively.

Algorithm 1 Algorithm for generation of multitoned signals

1. Start
2. Assign $j = 1$
3. If $j \leq N$, GOTO Step 4
   else GOTO Step 10
4. Assign $i = 1$
5. If $i \leq l$, GOTO Step 6
   else GOTO Step 9
6. Calculate $\theta = 2\Pi f_c(i)t_n$
7. Calculate $x_j = x_j + \cos\theta$
8. Increment i and GOTO Step 5
9. Increment j and GOTO Step 3
10. Stop

HDL Code 3.1: Generation of multitoned signals

```
for i2 in 1 to N loop
    for i3 in 1 to l loop
        theta := (2.0*3.141592*real(i2)*fc(i3))/fnyq;
        x(i2) := x(i2) + cos(theta);
    end loop;
end loop;
```

3.4.3 Pseudo-random Chipping Sequence Generator

The pseudo-random chipping sequence, *p[N]* that needs to be generated must have the length the same as that of the input signal, *x[N]*; which is equal to the selected

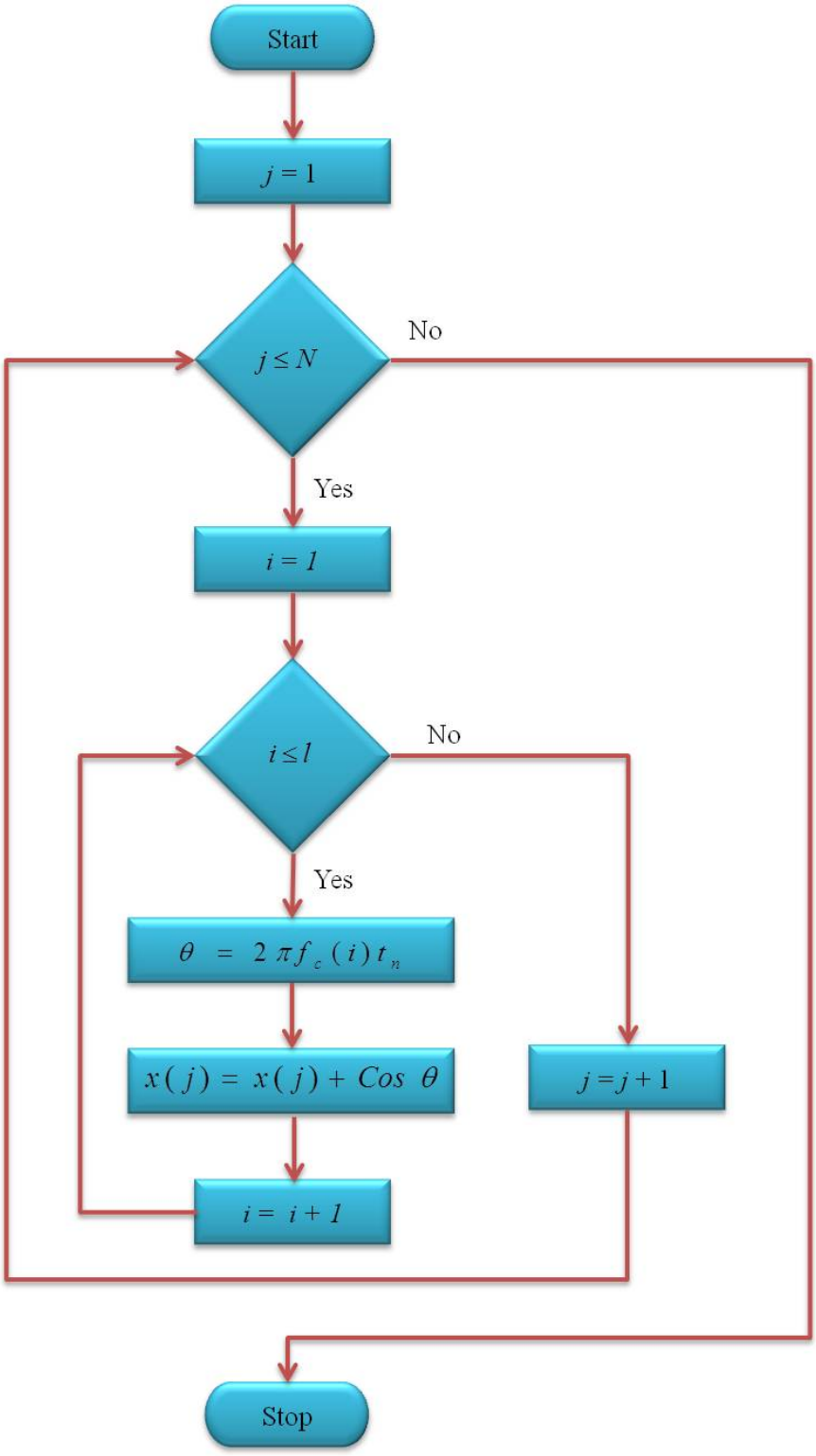

Figure 3.3: Flow diagram for generation of multitoned signals

dimension of the Nyquist rate samples, N. The pseudo-random sequence generator is designed based on Algorithm 2 given below. First a random number is generated using an inbuilt function from the programming environment, then the value of the generated random number is compared with 0.5. According to our algorithm,p_j will be assigned -1 if R is less than 0.5 else p_j will be +1. This process will be repeated until j in p_j reaches N starting from 1. Figure 3.4 and HDL Code 3.2 represents the flow diagram and VHDL code of the pseudo-random chipping sequence generator respectively.

Algorithm 2 Algorithm for Pseudo-random Chipping Sequence Generator

1. Start
2. Assign j = 1
3. If $j \leq N$, GOTO Step 4
   else GOTO Step 10
4. Generate **R** ,random number
5. If $0 \leq R \leq 1$, GOTO Step 6
   else GOTO Step 4
6. If $R < 0.5$, GOTO Step 7
   else GOTO Step 8
7. Assign p_j = -1 and GOTO Step 9
8. Assign p_j = +1
9. Increment j and GOTO Step 3
10. Stop

HDL Code 3.2: Pseudo-random Chipping Sequence Generator

```
for i4 in 1 to N loop
    UNIFORM(seed1,seed2,rand);
    R := rand;
    if( R < 0.5 ) then
        p(i4) := -1.0;
    else
        p(i4) := 1.0;
    end if;
end loop;
```

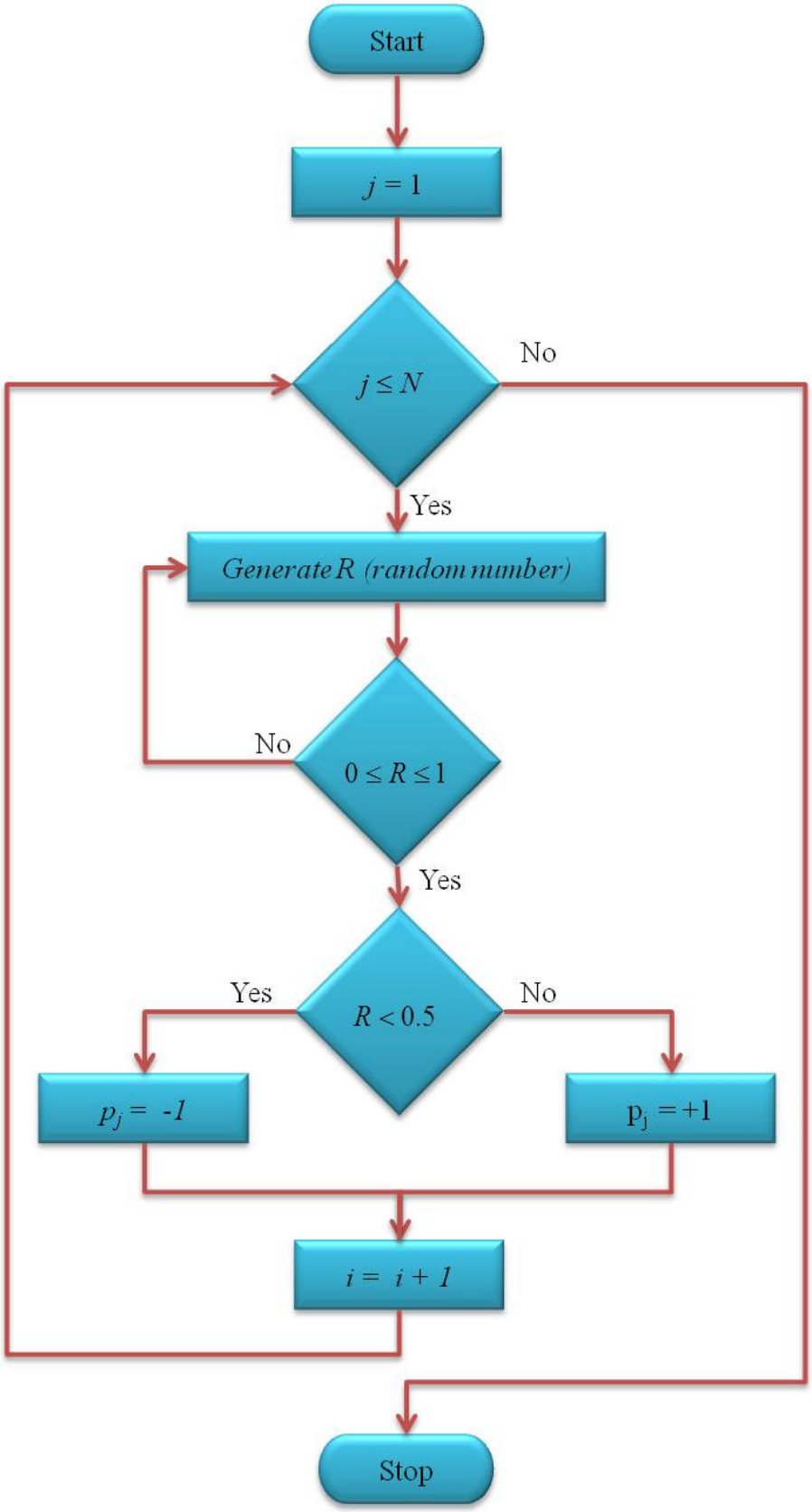

Figure 3.4: Flow diagram for Pseudo-random Chipping Sequence

3.4.4 Mixing

The function of the mixing block is to modulate *x[N]* obtained from Algorithm 1 with *p[N]* obtained from Algorithm 2. In Algorithm 3 each element from *x[N]* will be multiplied with the corresponding element from *p[N]* giving the modulated output, P, of the order of N. Figure 3.5 shown below represents the flow diagram of the described mixing algorithm. VHDL code for the simulation model of mixing algorithm is given in HDL Code 3.3.

Algorithm 3 Algorithm for mixer

1. Start
2. Assign $j = 1$
3. If $j \leq N$, GOTO Step 4
   else GOTO Step 6
4. Calculate P $= x_j \times p_j$
5. Increment j and GOTO Step 3
6. Stop

HDL Code 3.3: Mixer

```
for i5 in 1 to N loop
    P(i5) := x(i5)*p(i5)
end loop
```

3.4.5 Integration

Algorithm 4 shows the basic logic behind the design of integrator and dump circuit that serves as a low pass filter. The functioning of this integrating algorithm is to calculate the sum of every L number of outputs from the modulator, *P[N]*. Since the length of the modulated output is of the order of N, the sum vector generated from the integrator can be calculated using Equation 3.11. Figure 3.6 shows the flow diagram for the integration algorithm and the corresponding VHDL code is given in HDL Code 3.4.

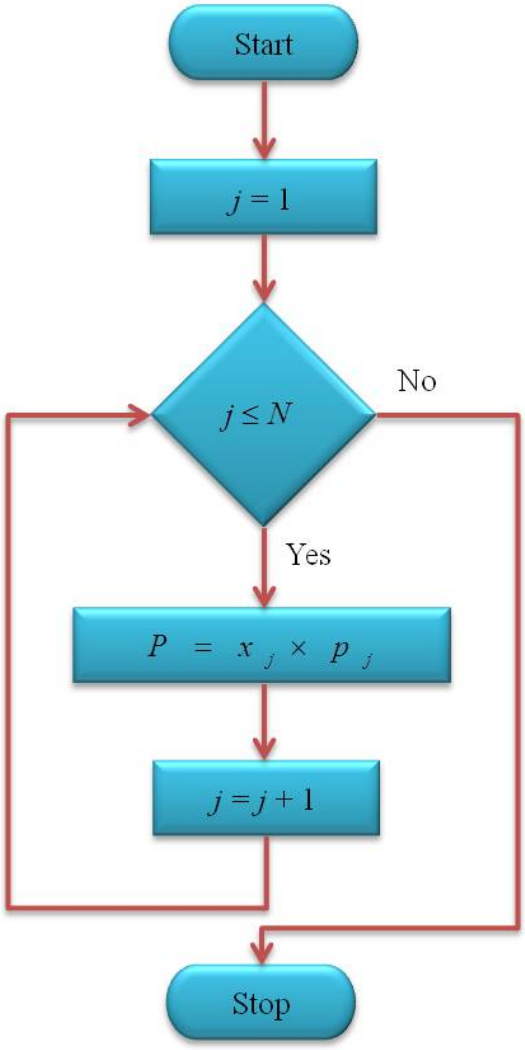

Figure 3.5: Flow diagram for mixing

$$M = N/L \tag{3.11}$$

Algorithm 4 Algorithm for Integrator

1. Start
2. Assign i = 0 , i_1 = 1 and i_2 = L
3. If $i \leq M$, GOTO Step 4
   else GOTO Step 11
4. Assign sum = 0 and $j = i_1$
5. If $j \leq i_2$, GOTO Step 6
   else GOTO Step 8
6. Calculate sum = sum + P_j
7. Increment j and GOTO Step 5
8. Assign $i_1 = i_1$ + L and $i_2 = i_2$ + L
9. Assign y_{i+1} = sum
10. Increment i and GOTO Step 3
11. Stop

HDL Code 3.4: Integrator

```
for i6 in 1 to M loop
        m1 := i6-1;
        for i7 in 1 to L loop
            y(i6) := y(i6) + P( m1*L + i7);
        end loop;
end loop;
```

3.4.6 Generation of Φ

The linear operator Φ represented in Equation 3.5 which is the mathematical representation of the random demodulator is generated from the chipping sequence *p[N]* using Algorithm 5. Flow diagram and VHDL code for Φ generation is given in Figure 3.7 and HDL Code 3.5 respectively.

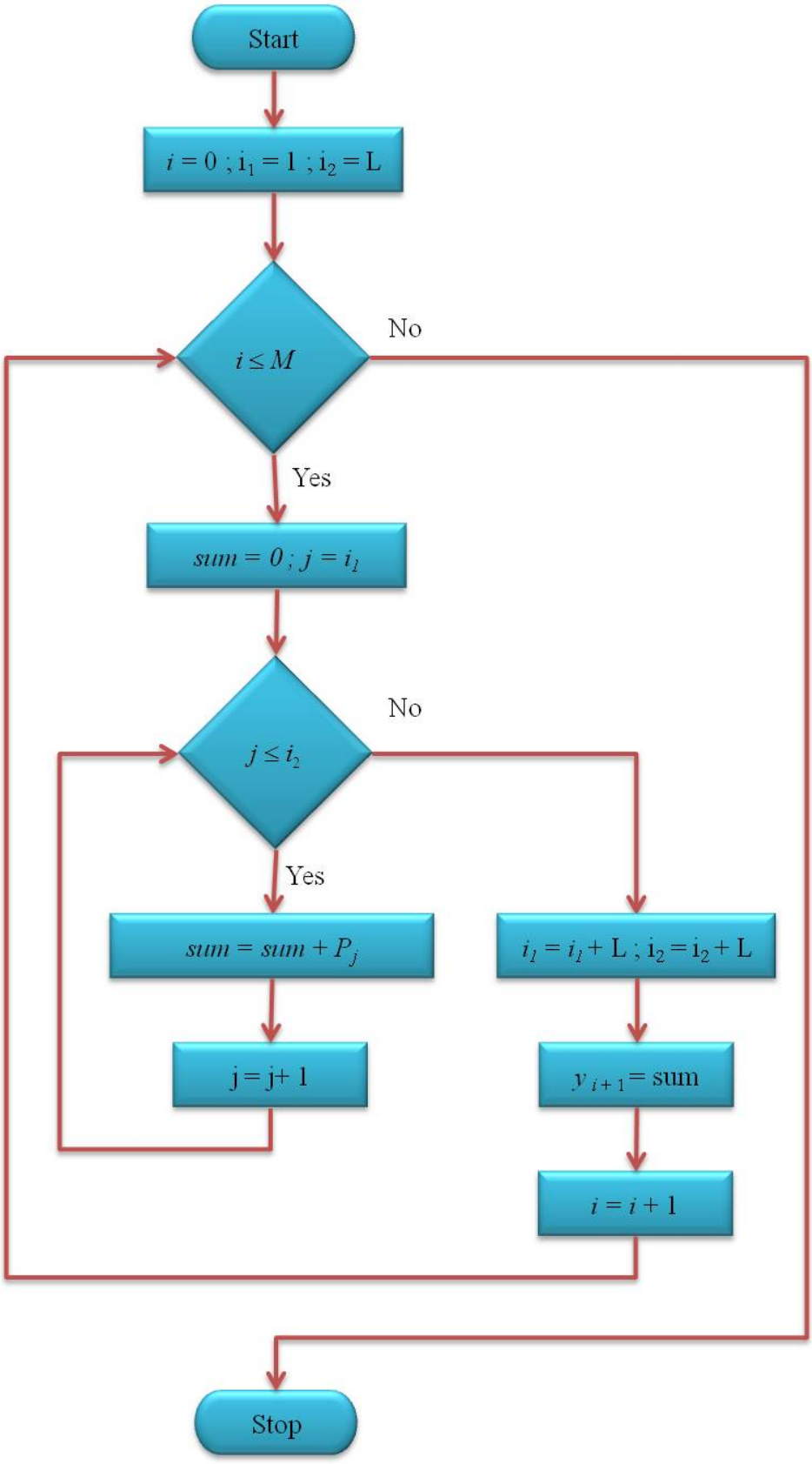

Figure 3.6: Flow diagram for integration

Algorithm 5 Algorithm for Φ Generation

1. Start
2. Assign $i = 1$
3. If $i \leq M$, GOTO Step 4
   else GOTO Step 11
4. Assign $j = i$-1
5. Assign $k = 1$
6. If $k \leq$ L, GOTO Step 7
   else GOTO Step 10
7. Assign $s = j \times L + k$
8. Calculate $\Phi_{is} = p_s$
9. Increment k and GOTO Step 6
10. Increment i and GOTO Step 3
11. Stop

HDL Code 3.5: Φ Generator

```
for i8 in 1 to M loop
        n1 := i8-1;
        for i9 in 1 to L loop
            phi(i8,n1*L + i9) := p(n1*L + i9);
        end loop;
end loop;
```

3.4.7 Frequency Set

Algorithm 6 given below sets the framework for generating a frequency set with a minimum frequency, f_1 and a maximum frequency, f_2 as range and in a pre-chosen resolution making a series of frequency values given by f_{pc}. This frequency set resolution that is the inter frequency spacing between the adjacent values of the frequency set should be chosen in such a way that the frequency set contains values small enough to detect narrow band pulses, keeping in mind that as the frequency set becomes denser the computational effort required for increased number of iterations increase. Figure 3.8 shows the flow diagram and HDL Code 3.6 shows the VHDL code representing the algorithm.

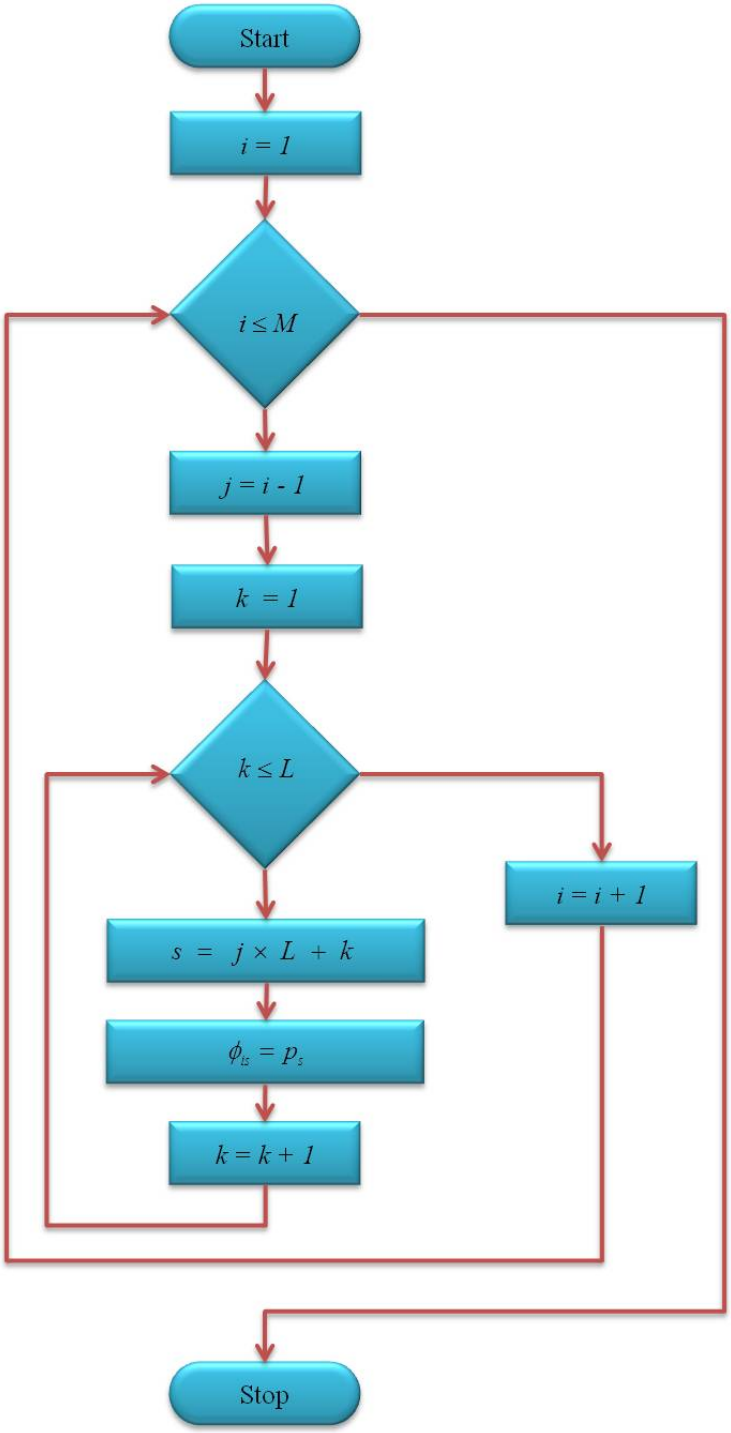

Figure 3.7: Flow diagram for Generating Φ

Algorithm 6 Algorithm for Frequency Set

1. Start
2. Assign $i = 1$
3. Calculate K = $\frac{f_2 - f_1}{resolution}$
4. Assign $f_i = f_1$
5. If $i > K$, GOTO Step 8
   else GOTO Step 5
6. Assign $f_{pc}(i) = f_i$
7. Calculate $f_i = f_i$ + resolution
8. Increment i and GOTO Step 4
9. Stop

HDL Code 3.6: Frequency Set

```
K := (f2 - f1)/resolution;
fi := f1;
for i10 in 1 to K loop
        fpc(i10) := fi;
        fi := fi + 1.0*resolution;
    end loop;
```

3.4.8 Correlation for Carrier Detection

The Algorithm 7 used for detecting the carrier requires the linear operator Φ, length of the frequency set, K, and the frequency set, f_{pc}, as inputs. In this algorithm and corresponding flow chart given in Figure 3.9, detection of carrier is calculated by pre multiplying the transpose matrix y obtained as the integrator output with the matrix y_{pc} and taking the square of the absolute value as can be inferred from Equation 3.7. y_{pc} is calculated by multiplying the linear operator Φ with the transpose of the exponential term x_{pc} calculated as per Equation 3.12. VHDL code for this algorithm is shown in HDL code 3.7.

$$x_{pc} = exp(2\pi f_{pc} t_n) \tag{3.12}$$

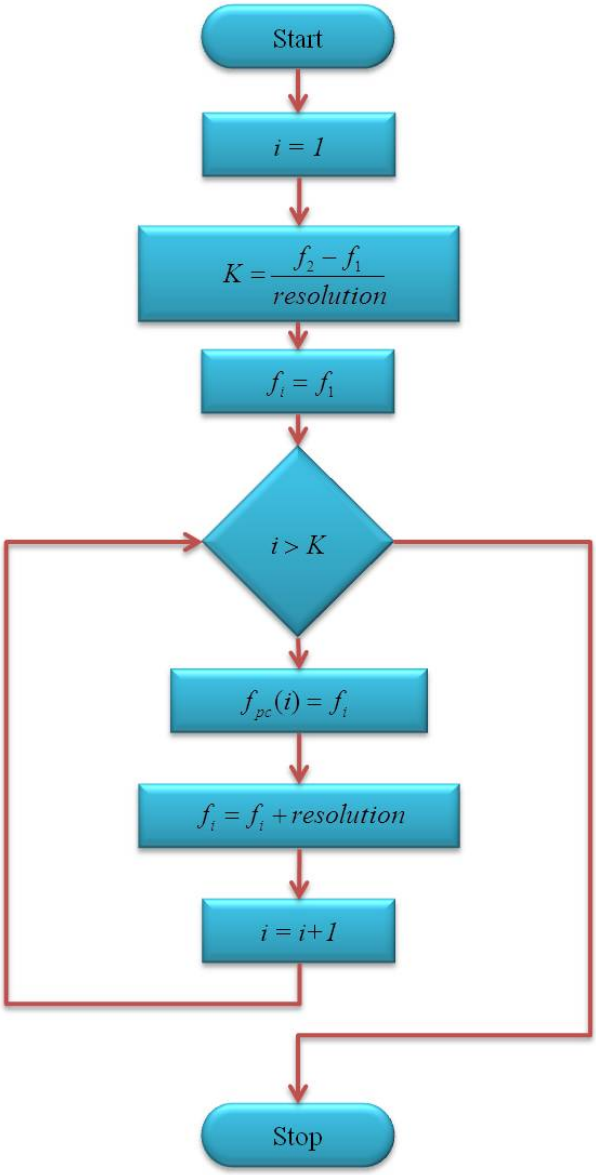

Figure 3.8: Flow diagram for correlating frequency

Algorithm 7 Algorithm for Carrier Detection

1. Start
2. Assign $i = 1$
3. If $i \leq K$, GOTO Step 4
   else GOTO Step 7
4. Calculate $y_{pc} = \Phi \times (x_{pc})^T$
5. Calculate $S_i = \mid y^T \, y_{pc} \mid^2$
6. Increment i and GOTO Step 3
7. Stop

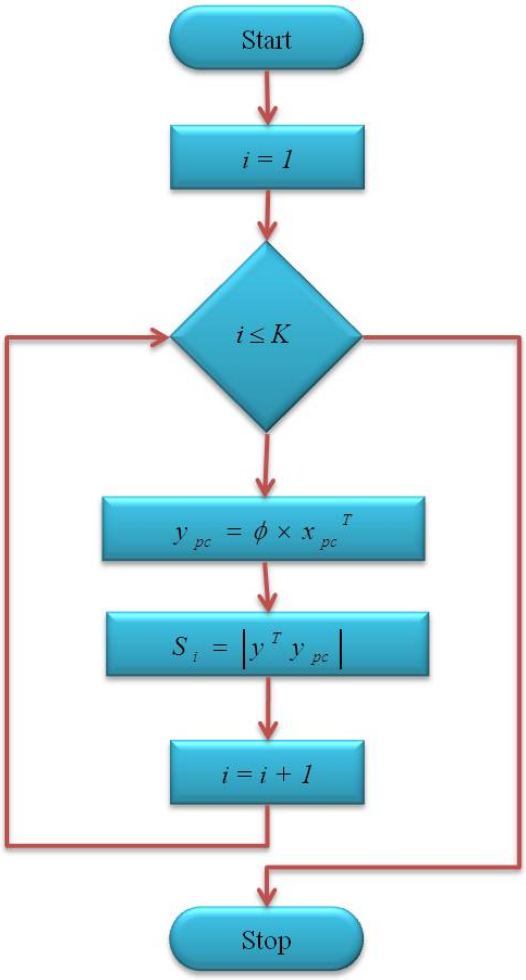

Figure 3.9: Flow diagram for carrier detection

HDL Code 3.7: Carrier Detection

```
for i12 in 1 to K loop
        for i11 in 1 to N loop
            div2 := (-2.0*3.141592*fpc(i12)*real(i11))/fnyq;
            xpc_cos(i11) := cos(div2);
            xpc_sin(i11) := sin(div2);
        end loop;
        for i13 in 1 to M loop
            for i14 in 1 to N loop
                ypc_cos(i13) := ypc_cos(i13) + phi(i13,i14)*xpc_cos(i14);
                ypc_sin(i13) := ypc_sin(i13) + phi(i13,i14)*xpc_sin(i14);
            end loop;
            ypc_sin(i13) := -1.0*ypc_sin(i13);
        end loop;
        for i15 in 1 to M loop
            S_cos(i12) := S_cos(i12) + y(i15)*ypc_cos(i15);
            S_sin(i12) := S_sin(i12) + y(i15)*ypc_sin(i15);
        end loop;
        S(i12) := S_cos(i12)**2 + S_sin(i12)**2;
end loop;
```

3.5 Summary

This chapter presents a brief outline about the Generic Wideband Receiver in Section 3.2 with the help of a block diagram given in Figure 3.1. This is followed by a basic description and related mathematical background of WCRR in section 3.3. Section 3.4 deals with all the relevant details and description of the architecture of the prototype for simulation which essentially discusses about various algorithms and flow diagrams used for designing the essential components of the receiver such as input model, pseudo random chipping sequence generator, mixer, integrator and carrier detection. The testing, validation and verification of this model and the obtained results are discussed in Chapters 4.

Chapter 4

Verification and Validation of WCRR

This chapter deals with the verification of a computerised model and operational validation developed for the WCRR. Test parameter choices have been assigned to carry out the simulations and the results obtained are compared with the original test case for the detection of carrier. In the simulation of the WCRR, three different Nyquist frequencies and varying values of decimation factor have been considered for the assessment of results using a frequency correlation graph. Finally these results are validated with the help of probability study of the occurrences of success or failure in carrier detection.

4.1 Introduction

The WCRR discussed in Chapter 3 accepts a multitoned signal as input and uses different sub blocks to detect the carrier frequency corresponding to the maximum power of the measurement. In this chapter a numerical investigation of different blocks of algorithms of the WCRR discussed in Chapter 3 has been conducted using test parameter choices to verify the correctness of the functioning of the simulation model. This is done so as to verify that the programming and implementation of the conceptual

model presented in Chapter 3 is correct. As the WCRR consists of different sub blocks, the method which we use for model verification is the bottom-up strategy. Bottom-up testing is defined in [14] as a method of testing the sub models first and then the overall model.

This chapter also deals with the operational validation for further assessment and validation of this model that will ensure successful carrier detection by WCRR. The method used for this purpose is parameter variability - sensitivity analysis. This technique described in [14] determines the effect upon the model's behaviour and its output by changing the values of the input and internal parameters of a model. The same relationships should occur in the model as in the real system.

4.2 Verification: WCRR Simulation Model

This section aims for the verification of mathematical functioning of sub blocks of the WCRR simulation model in successful carrier detection. If all the sub block algorithms function correctly, the overall model could successfully detect the carrier frequency, f_c, that was given as an input while generating multitoned signal. The output vector S from the carrier detection block indicates the power of each measurement. The index position of elements of S with maximum value must be noted. Then, if the frequency from the frequency set, f_{pc}, corresponding to this index position is equivalent to the input carrier frequency, f_c, the simulation model for WCRR indicates successful carrier detection.

4.2.1 Parameter Choices

A set of test parameter choices has been selected and is presented in Table 4.1 that contains notations explained in Table 3.1. This set of values is used for testing the mathematical functioning of simulation model for successful carrier detection when it is executed without any unforeseen errors or bugs. The values used for testing are not

realistic values since the matrices become too large when using frequencies of MHz range.

Table 4.1: Parameter Choices for Verification of Simulation

Notations and chosen values for testing	
W(Hz)	5
f_{nyq}(Hz)	10
T_{nyq} (s)	0.1
L	2
ν_{eff}(Hz)	5

4.2.2 Testing: Input Model Generation

The Algorithm 1 that has been designed for the purpose of generating an input model is fed with inputs of carrier frequency, f_c(Hz) , the number of elements in the carrier frequency vector, l, dimension of Nyquist rate samples, N, and the time length of the Nyquist frequency, t_n(s). The values that are assigned for the parameters for testing this block are as follows: N = 10,f_c = [6], l = 1 and t_n =[0.10 0.20 0.30 0.40 0.50 0.60 0.70 0.80 0.9 1]. For the correct implementation of this algorithm, the output should be a one dimensional matrix of length N in accordance with the cosine function evaluated through step 6 and 7 and is given as follows.

Input Signal, x(t) =

$$\begin{bmatrix} -0.8090 & 0.3090 & 0.3090 & -0.8090 & 1.0 \\ -0.8090 & 0.3090 & 0.3090 & -0.8090 & 1.0 \end{bmatrix}$$

This generated vector for x(t) is used as input for the mixing algorithm.

4.2.3 Testing: Pseudo Random Sequence Generation

In this block of the simulation model, a signal pattern is generated as per Algorithm 2 by taking the value of N as length and a standard pseudo random generating function. As per the testing choice of N=10, the generated matrix is as shown below.

Pseudo-random chipping sequence, p(t) =

$$[1 \quad 1 \quad 1 \quad -1 \quad 1 \quad -1 \quad -1 \quad -1 \quad 1 \quad -1]$$

This generated matrix as expected is of length *N* and is required as one of the inputs of the mixing algorithm.

4.2.4 Testing: Generation of Mixed Signal

In this block of the simulation model, the incoming input signal *x(t)* is mixed with the pseudo random chipping sequence *p(t)*. The output of Algorithm 3 is the mixed signal obtained by multiplying every element in *x(t)* with the corresponding element in *p(t)* and that generated from the sample test data is as given below. The correctness of this vector can be verified by comparing the elements of the vectors *x(t)* and *p(t)* given in sections 4.2.2 and 4.2.3 respectively.

Mixed Signal, P =

$$\begin{bmatrix} -0.8090 & 0.3090 & 0.3090 & 0.8090 & 1.0 \\ 0.8090 & -0.3090 & -0.3090 & -0.8090 & -1.0 \end{bmatrix}$$

4.2.5 Testing: Simulation Model for Integration

The mixed signal obtained from the mixing algorithm is given as input here to be integrated and down sampled into a vector of length M. The value assigned for M is 5 and the output from the Algorithm 4 is as given below.

Integrator Output, y =

$$[-0.4999 \quad 1.1180 \quad 1.8090 \quad -0.6180 \quad -1.8090]^T$$

4.2.6 Testing: Generation of Φ

The linear operator Φ is generated from Algorithm 5 which is required for the detection of carrier frequency. The pseudo random chipping sequence p(t) is used here as the input and the generated output of order $M \times N$ is as given below.

Phi, Φ =

$$\begin{bmatrix} 1 & 1 & 0 & 0 & 0 & 0 & 0 & 0 & 0 & 0 \\ 0 & 0 & 1 & -1 & 0 & 0 & 0 & 0 & 0 & 0 \\ 0 & 0 & 0 & 0 & 1 & -1 & 0 & 0 & 0 & 0 \\ 0 & 0 & 0 & 0 & 0 & 0 & -1 & -1 & 0 & 0 \\ 0 & 0 & 0 & 0 & 0 & 0 & 0 & 0 & 1 & -1 \end{bmatrix}$$

This matrix as expected is a representation of Equation 3.5 of order $M \times N$.

4.2.7 Testing: Frequency Set Generation

This block generates a set of frequencies that may contain the carrier frequency to be detected by the simulation model. This generated frequency set, $f_{pc}(Hz)$, is assigned a resolution that is the inter frequency spacing of 0.25 Hz and has lower and upper limits of f_1 = 5 Hz and f_2 = 7 Hz for testing purposes. The output obtained from Algorithm 6 is a one dimensional matrix of length K calculated as $(f_2$ - $f_1)$/resolution = (7-5)/0.25 = 8 and is given below.

Frequency set f_{pc} =

$$[5 \quad 5.25 \quad 5.5 \quad 5.75 \quad 6 \quad 6.25 \quad 6.5 \quad 6.75\,]$$

4.2.8 Testing: Carrier Detection

This block of the simulation model represented by Algorithm 7 generates the final frequency correlation for carrier detection. The output, y generated from the integration block is used here as the input and is correlated against a vector y_{pc} to calculate a vector S of length K indicating the power of measurements. In order to calculate y_{pc}, Φ generated from the phi generation block and x_{pc} calculated from Equation 3.12 are required. The vectors x_{pc} and y_{pc} calculated for the testing purpose are given below.

x_{pc} -

$$\begin{bmatrix} -.454+.891i & -.588-.809i & .988-.156i & -.309+.951i & -.707-.707i \\ .951-.309i & -.156+.988i & -.809-.588i & .891-.454i & -3.43e-15+1i \end{bmatrix}$$

y_{pc} -

$$\begin{bmatrix} -1.042-.082i & 1.297+1.108i & -1.658+.398i & .965+.399i & .891+1.454i \end{bmatrix}^T$$

The output vector S from the carrier detection algorithm is as given below

S -

$$\begin{bmatrix} 5.000 & 16.375 & 43.502 & 68.765 & 74.633 & 57.236 & 30.099 & 11.252 \end{bmatrix}$$

4.3 Model Verification: WCRR Simulation Model

The testing of the computerised model for WCRR has given an output based on the sample input given for verifying the functioning of the model. Now it is to be identified whether the overall model could successfully detect the carrier frequency that was given as an input for the input model generation block. This frequency f_c was given a value of 6 Hz. Now the output S from the carrier detection block is a vector with 8 elements that indicates the power of each measurement. The maximum value of

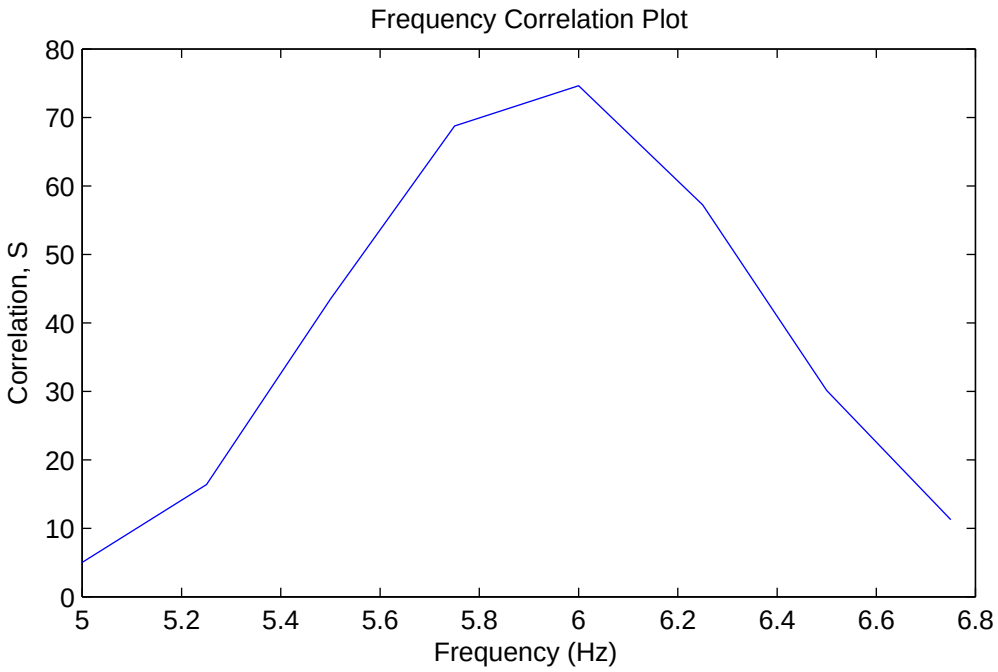

Figure 4.1: Frequency Correlation Graph for Test Data

elements of S can be found to be 49.981 and its index position in the vector is 5. Now when the 5^{th} index position of the frequency vector f_{pc} generated from the frequency set generation block of the model is checked, it is seen that the value there is 6 Hz which is equivalent to the input carrier frequency, f_c. This indicates that the simulation model for WCRR has successfully detected the carrier frequency and the same can be observed from the frequency correlation graph given in Figure 4.1.

The WCRR simulation model was again tested with carrier frequencies ranging from 5 Hz to 6.75 Hz. In all the cases the calculated correlation was maximum for the corresponding carrier frequency and was sufficient enough to indicate successful carrier detection. Thus this computerized model is hereby verified for its correct functioning using the sample test data.

4.4 Operational Validation of WCRR

The results and conclusions of the numerical investigation of ModelSim simulation model for WCRR are discussed in this section. The validation process of parameter variability - sensitivity analysis [14] has been conducted for successful carrier detection with different Nyquist frequencies, carrier positions and varying frequency sets and are presented in section 4.5. An attempt to predict the probability of successful carrier detection has also been performed in section 4.6.

The ModelSim Simulation has been carried out for the WCRR system and the results can be verified and validated by comparing the original carrier frequencies with detected carrier frequencies for different values of frequency grids and Nyquist frequencies. A total of 2500 executions have also been performed for verifying the simulation results when the Nyquist frequency is varied. The simulations have also been carried out by varying the decimation factor ; the number of executions was in the range of 2500 to 25000 based on the convergence of percentage of successful carrier detection in each case.

4.4.1 Parameter Choices for the numerical investigation of WCRR

Different parameters are required in the simulation of WCRR and the corresponding parameter choices are shown in Table 4.2. Notations given in this table can be referred from Table 3.1.

Table 4.2: Parameter Choices

Notations and chosen values			
W(MHz)	500	1000	1200
f_{nyq} (GHz)	1.0E	2.0E	2.4E
T_{nyq} (s)	1.0E-09	5.0E-10	4.2E-10
L	100	100	100
ν_{eff} (MHz)	10	20	24

4.4.2 Frequency Correlation for a f_{nyq} of 1 GHz

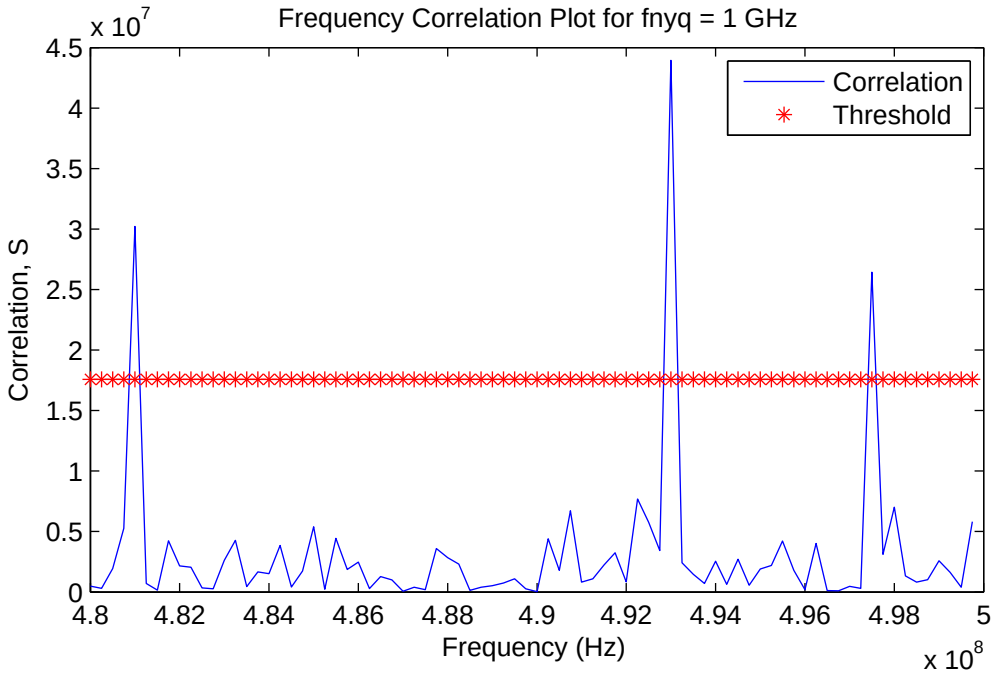

Figure 4.2: Frequency Correlation Graph for f_{nyq} = 1GHz

In Figure 4.2 the frequency correlation graph obtained from the simulation of WCRR has been presented. The aim of this investigation is to detect the carrier when the total bandwidth of the system is maintained at 500 MHz. The Nyquist frequency of the system is fixed and can be calculated as twice the maximum frequency i.e 2×500 MHz = 1 GHz. By keeping the Nyquist frequency fixed at twice the maximum frequency of the band of interest, the carrier frequencies present anywhere within the total bandwidth can be detected without any change in the input multitone signal and pseudorandom generator. In this case, by using a decimation factor, L = 100, a lower value of 10 MHz was determined using the Equation 3.10 for the effective sampling rate, ν_{eff}. The frequency set has been chosen with a lower limit of 480 MHz and an upper limit of 500 MHz and the inter frequency spacing is selected as 0.25 MHz. Our selection of frequency set does not significantly affect the decimation rate or Nyquist frequency of the lower limit of the band. The carrier frequencies have been pre assumed as 481, 493 and 497.5 MHz for detection. It is expected that the simulation of the WCRR model gives peak measurement powers at these carrier frequency positions.

As far as the WCRR is concerned, a successful carrier detection is accepted only when a peak measurement power greater than the threshold value of the correlation is obtained at each and every pre-selected value of carrier frequency. Two methods which can be used for obtaining the threshold value are by calculating the average of the power of measurements obtained in vector S and by a dynamic thresholding algorithm such as discussed in [43]. The demerit in averaging of power measurements occurs when the number of carriers selected is much less than the total number of signals calculated. In that case the average value calculated will be in a position closer to the lower power values resulting in the detection of local peaks generated due to sampling noise resulting in faulty carrier detection. When the dynamic thresholding algorithm discussed in [43] is used, the calculated threshold measurement power is above the local peaks generated by the correlation function for the selected frequency grid. The dynamic thresholding algorithm is termed as dynamic since for each iteration the matrix S generated will be different depending on the pseudo random number obtained. In Figure 4.2 the threshold measurement power calculated for one of the iterations is marked. From the figure it can be concluded that the model has successfully identified the carrier frequencies and is functioning correctly for the selected Nyquist frequency of 1 GHz.

It can be seen from the figure that all the pre assumed carrier frequencies have been successfully identified by the simulation by referring to the peak measurement powers of the correlation graph at these frequency positions.

4.4.3 Frequency Correlation for a f_{nyq} of 2 GHz

The aim of this investigation is to detect the carrier when the Nyquist frequency is maintained at 2 GHz. The effective sampling rate calculated using Equation 3.10 obtained in this case by choosing a decimation factor of 100 is as low as 20 MHz. The frequency set has been chosen with a lower limit of 970 MHz and an upper limit of 1000 MHz and the inter frequency spacing that is the resolution is selected as 0.25 MHz. The carrier frequencies have been pre assumed as 970.5, 982.75 and 999.5 MHz

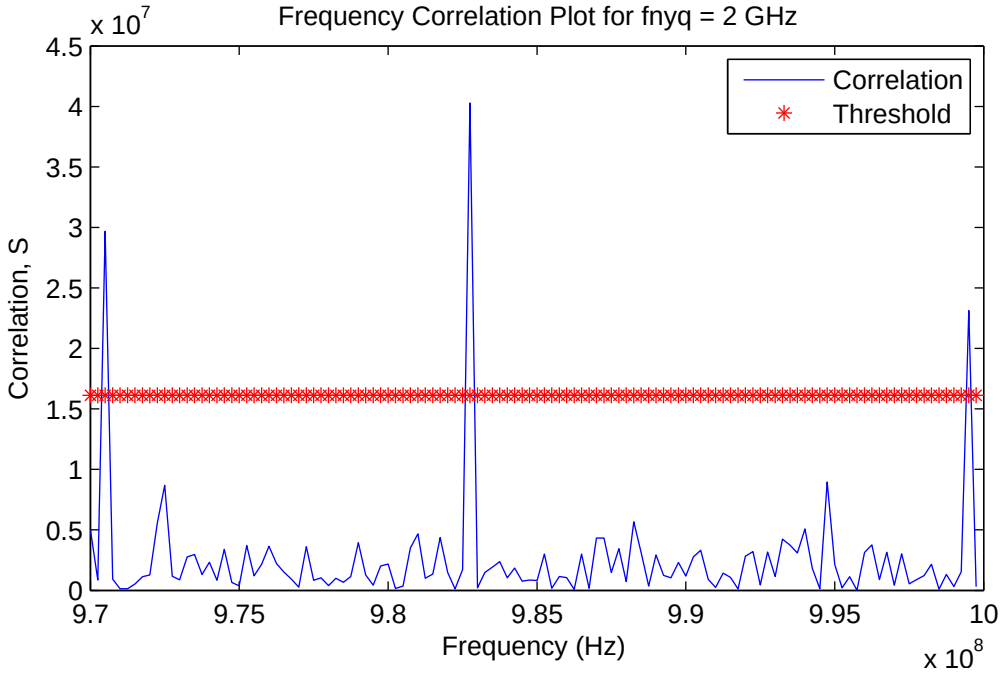

Figure 4.3: Frequency Correlation Graph for f_{nyq} = 2GHz

for detection. It is expected that the simulation of the WCRR model gives peak measurement powers at these carrier frequency positions. It can be seen from the Figure 4.3 that all the pre assumed carrier frequencies have been successfully identified by the simulation by referring to the peak measurement powers of the correlation graph at these frequency positions. It can also be seen that the peak measurement powers at these frequency positions exceed the threshold measurement power calculated based on the dynamic thresholding algorithm discussed in [43]. So it can be concluded that the model has successfully identified the carrier frequencies and is functioning correctly for the selected Nyquist frequency of 2 GHz.

4.4.4 Frequency Correlation for a f_{nyq} of 2.4 GHz

In Figure 4.4 the frequency correlation graph obtained from the simulation of WCRR has been presented. The aim of this investigation is to detect the carrier when the Nyquist frequency is maintained at 2.4 GHz. In this case, by using a decimation factor, L = 100, a lower value of 24 MHz was determined for the effective sampling rate, ν_{eff}

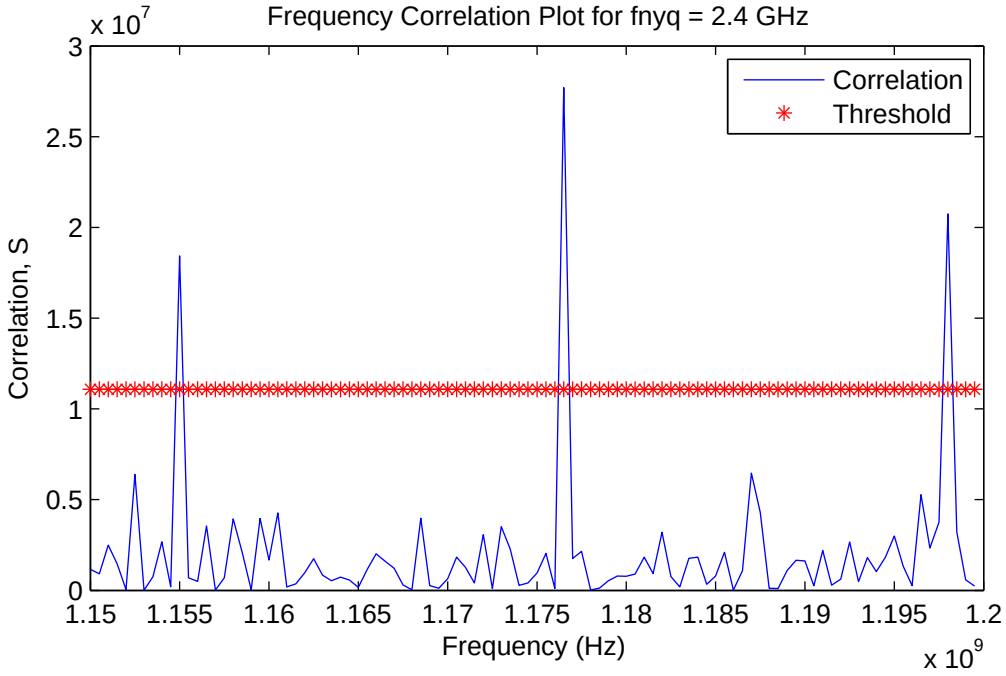

Figure 4.4: Frequency Correlation Graph for f_{nyq} = 2.4GHz

calculated using Equation 3.10. The frequency set has been chosen with a lower limit of 1.15 GHz and an upper limit of 1.2 GHz and the resolution as 0.5 MHz. The carrier frequencies have been pre assumed as 1.155, 1.1765 and 1.198 GHz for detection. It is expected that the simulation of the WCRR model gives peak measurement powers at these carrier frequency positions. It can be seen from the figure that all the pre assumed carrier frequencies have been successfully identified by the simulation by referring to the peak measurement powers of the correlation graph at these frequency positions. It can also be seen that the peak measurement powers at these frequency positions exceed the threshold measurement power calculated based on the dynamic thresholding algorithm discussed in [43]. So it can be concluded that the model has successfully identified the carrier frequencies and is functioning correctly for the selected Nyquist frequency of 2.4 GHz.

4.4.5 Percentage Variation of Successful Detection with Decimation Factor

The purpose of this investigation is to determine the percentage variation of successful carrier detection with respect to the varying decimation factor of the WCRR model simulation when the selected dimension of Nyquist rate samples N is 10000. As per the results from [43] it is expected that the percentage of success should be decreasing with increasing decimation factor, L. The results shown in Figure 4.5 also shows a decreasing behaviour for the percentage of successful detection. It can be observed that up to a value of 100 for L the percentage success remains at 100%. This percentage success then gradually decreases to 0 when the value of L increases from 100 to 10000.

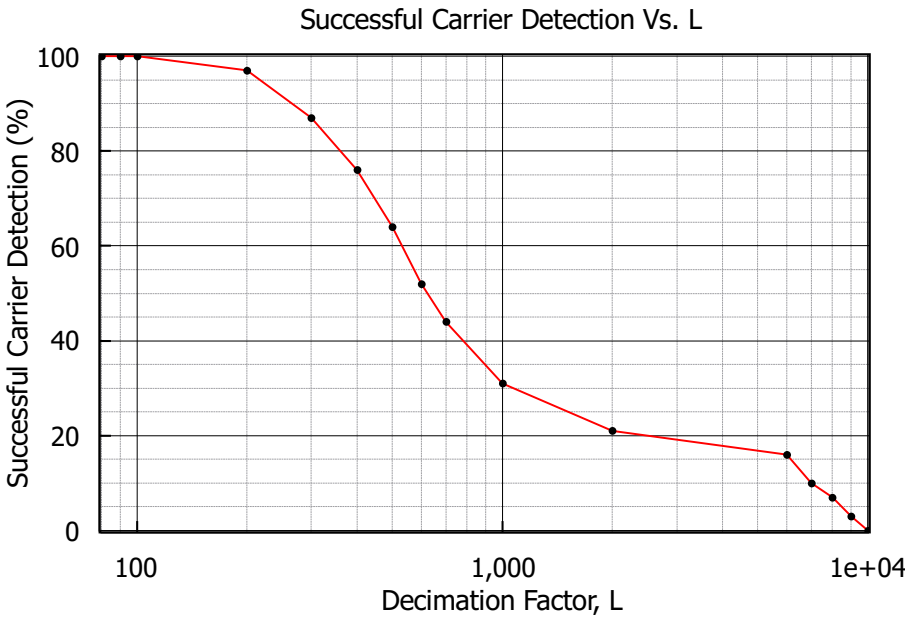

Figure 4.5: Successful Carrier Detection Vs Decimation Factor for f_{nyq} = 2.4GHz

From this it can be concluded that the WCRR simulation model as expected gives a decreasing trend of successful carrier detection with increase in decimation factor, L.

4.5 Verification of Successful Carrier Detection

The purpose of this investigation is to verify the carriers detected using the ModelSim simulation of WCRR with the original carrier frequency set. This study has been conducted for different frequency sets and Nyquist frequencies.

Table 4.3: Successful Carrier Detection for f_{nyq} = 1 GHz

Original Carrier Frequency	Detected Carrier Frequency
[480.5, 485, 495, 499]	[480.5, 485, 495, 499]
[482.5, 487, 492, 497.5]	[482.5, 487, 492, 497.5]
[484, 486, 490, 494]	[484, 486, 490, 494]

Table 4.3 shows a comparison between the pre-selected carrier frequencies and detected carrier frequencies for a frequency grid of 480 to 500 MHz when f_{nyq} is 1 GHz. It may be noted that the given three sets of detected carrier frequencies exactly match with the pre-selected carrier frequency sets indicating clear cases of successful carrier detection. Three cases can be identified pertaining to unsuccessful carrier detection. In the first case the detected carrier frequency set will not contain all the pre-selected carrier frequencies. In the second case the detected carrier frequency set contains atleast one frequency that was not contained in the pre-selected carrier frequency set and in the last case, the detected carrier frequencies will not contain atleast one of the frequencies that was contained in the pre-selected carrier frequencies and will contain atleast one frequency that was not contained in the pre-selected carrier frequencies.

Table 4.4 shows the frequency sets detected by the simulation for Nyquist frequency of 2 GHz when the frequency grid has been maintained with a lower to upper limit of 970 to 1000 MHz. It can be seen here that the pre-selected frequency set is exactly the same as that of the detected carrier frequency set which indicates successful carrier detection.

Table 4.4: Successful Carrier Detection for f_{nyq} = 2 GHz

Original Carrier Frequency	Detected Carrier Frequency
[970.5, 985, 995, 999]	[970.5, 985, 995, 999]
[972.5, 987, 992, 997.5]	[972.5, 987, 992, 997.5]
[974, 986, 990, 994]	[974, 986, 990, 994]

Table 4.5 corresponds to the successful carrier detection in the case when Nyquist frequency is 2.4 GHz and for a frequency grid of 1150 to 1200 MHz. The detected carrier frequency set has a total of four elements in each case and all of them match with that of the corresponding original carrier frequency sets.

Table 4.5: Successful Carrier Detection for f_{nyq} = 2.4 GHz

Original Carrier Frequency	Detected Carrier Frequency
[1155, 1165, 1180, 1195]	[1155, 1165, 1180, 1195]
[1156.5, 1175, 1188.5, 1196.5]	[1156.5, 1175, 1188.5, 1196.5]
[1160.5, 1168.5, 1191.5, 1199]	[1160.5, 1168.5, 1191.5, 1199]

It could be concluded from this investigation of the results that the execution of simulations could detect the carrier frequencies successfully in all the cases of frequency grid values and Nyquist frequencies. Thus the results could be verified for its correctness.

4.6 Validation of Successful Carrier Detection

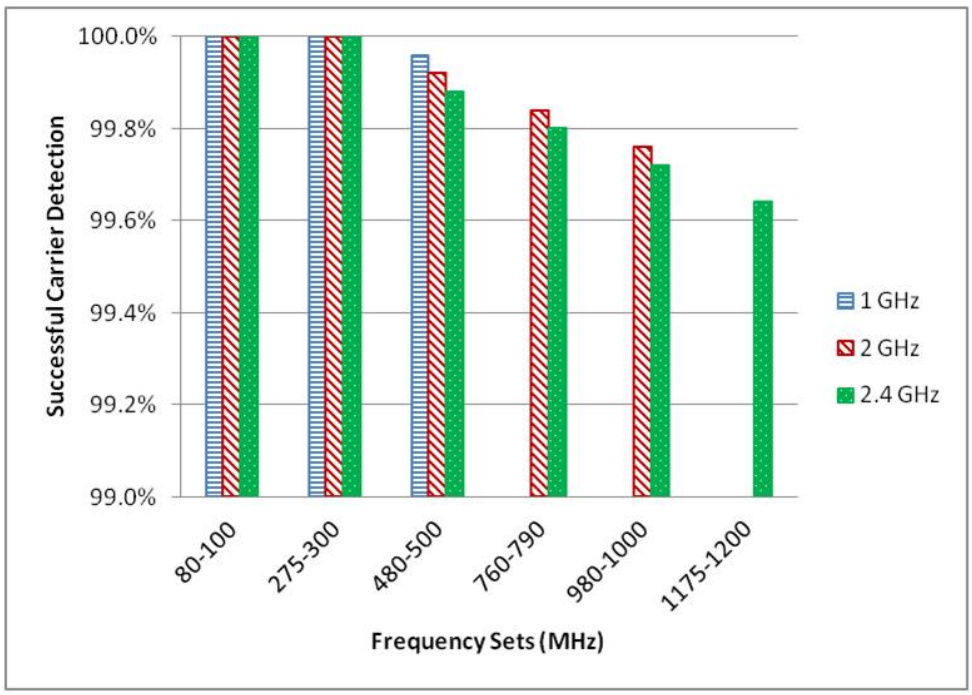

Figure 4.6: Percentage of Successful Carrier Detection

The purpose of this investigation is to validate the WCRR simulation model by con-

ducting a probability study of the occurrences of success or failure in carrier detection. This has been conducted by executing the simulation for 2500 independent trials and calculating the total number of successful carrier frequency detections. For a decimation factor, L, equals 150 is chosen so as to provide some errors, the frequency set is varied from a lower range to a higher range of (80-100)MHz to (1150-1200)MHz at different Nyquist frequencies of 1 GHz, 2 GHz and 2.4 GHz. A tendency of a decrease in percentage can be observed within the range of 99.6% to 100%. It can be observed from the bar diagram given in Figure 4.6 that the minimum percentage of success is 99.6% when all the selected cases are considered. A common decreasing trend of variation of percentage of success could be identified from the study. This is because of the decrease in the relative decimation for the lower range to the higher range of SOI in the selected band of interest. Also the effective sampling rate, ν_{eff} using Equation 3.10 can be calculated as 6.67 MHz, 13.33 MHz and 16 MHz for f_{nyq} of 1 GHz, 2 GHz and 2.4 GHz respectively. From the calculated ν_{eff} the actual maximum frequencies that could be sampled are 2.33 MHz, 6.66 MHz and 8 MHz instead of 500 MHz, 1000 MHz and 1200 MHz, thereby making the WCRR system sampling at sub-Nyquist rate for frequency ranges (2.33-500) MHz, (6.66-1000) MHz and (8-1200) MHz. Thus it could be concluded that the simulation model generates successful results at sufficiently high rates and the model is thereby validated.

4.7 Summary

The first section of this chapter deals with the numerical investigation process carried out in the simulation models of the WCRR. The purpose of this investigation was to verify that the developed model functions correctly for the given test parameter choices. Since the WCRR model discussed here is non-deterministic in nature, a single execution of the simulation cannot verify the functioning of the model. So statistically more number of executions have been carried out with the test parameter choices and for verifying the model. In the later sections for operational validation of the WCRR model, assessment of the frequency correlation graph for Nyquist frequency of 1 GHz,

2 GHz and 2.4 GHz has been carried out. Studies have also been conducted separately by executing the simulation by varying the decimation factor. In the last section of this chapter, the results obtained from the probability studies of successful carrier detection have been discussed. These studies, conducted for 2500 number of iterations of the simulation, has been utilised to verify and validate the results of the simulation model for practical purposes.

Chapter 5

Modulated Wideband Converter

In this chapter the concept of a mixed analog digital system is presented in sections such as the multiband signal model, MWC and CTF block. Various components of the simulation model for the above mentioned components are also discussed here using the necessary algorithms, flow diagrams and their corresponding VHDL codes.

5.1 Introduction

This chapter focuses on the steps involved in the modelling process of a mixed analog digital system that operates at sub-Nyquist sampling rates. The sub Nyquist sampling algorithm used by this system, alternatively known as the MWC [9], does not require wideband inputs at higher Nyquist rates to gather sufficient samples for representing the original signal. This system is less complex when compared to a Shannon's sampling system as it does not assume that the SOI are confined to a discrete set of frequencies. The identification of support is done in this system by making use of a simple detection system known as the CTF [11] block rather than relying on traditional recovery methods such as *l1* minimization.

The problem entity considered here is one part of the problem statement given in Section 1.2 which is mentioned to develop a ModelSim simulation model for spectrum sensing of multiband signals using sub Nyquist sampling. In order to develop a conceptual model, a validation process is necessary to determine that the theories and assumptions underlying the model is satisfactory. For conceptual model validation, the technique used here is the same as that used in Chapter 3, i.e the data validation process given in [14]. In this validation technique, the data collected from the literature, as presented in Sections 5.2, 5.3, 5.4 and 5.5, is used for building the model as well as to check whether the behaviour of the model is similar to that of the system. The data collected from the literature helps in developing the conceptual model and is detailed in Section 5.6 in the form of algorithms and flow diagrams. The VHDL code which serves as the computerised model for implementing the simulation model in ModelSim is discussed along with the conceptual model. The computerised model verification and operational validation is done in Chapter 6.

5.2 Mixed Analog Digital System

The spectrum sensing method based on the mixed analog digital system discussed in [11] and [9] has several advantages when compared to previous architectures. Firstly, the mixed analog digital system has a fixed analog front end. The ADCs and the DSP rates of this system are substantially below Nyquist. The sensing resources of the system are shared with the reception path of the CR, so that the low rate streaming samples can be used for communication purpose of the device, in addition to the sensing functionality it provides.

A block diagram representing the major functions of a mixed analog digital system is shown in Figure 5.1. A suitable signal model having the required specifications of the multiband signal is first defined and fed to the system as input. This is shown in the first block of the diagram shown in the figure and is detailed in Section 5.3. The second block in the diagram represents the analog system with the help of which the

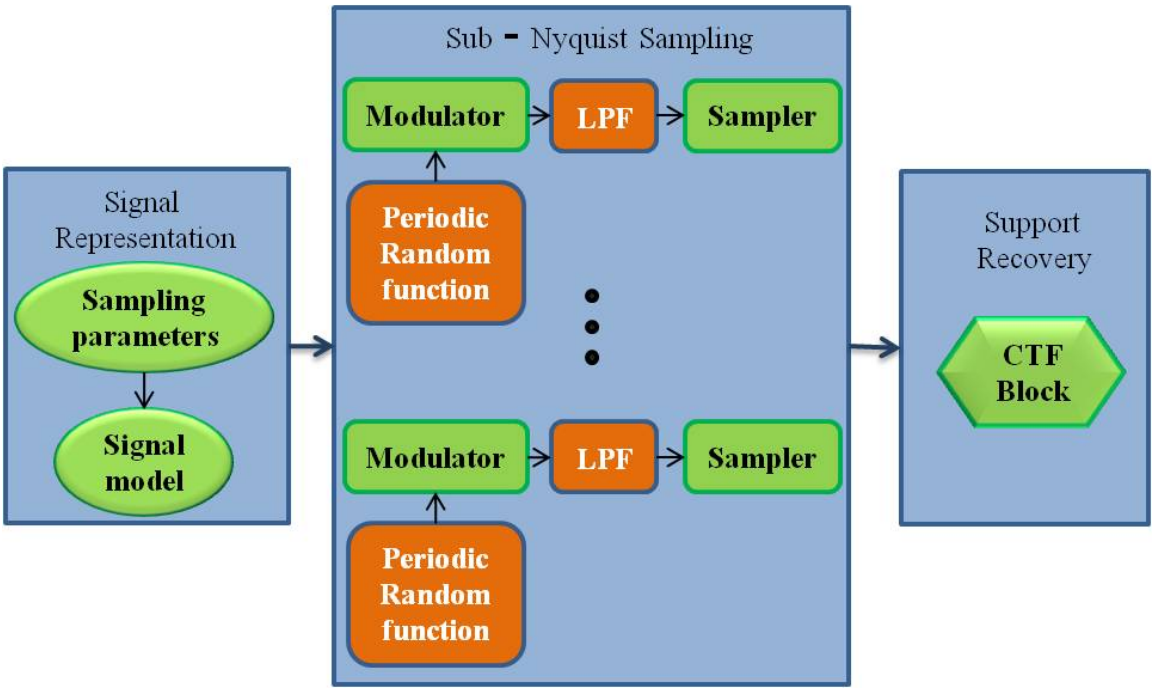

Figure 5.1: Mixed Analog Digital System

parameters essential for the modulated wideband converter discussed in Section 5.4 are designed. Once the signal is converted, it is the function of the support recovery system to identify the support and recover it. This is done using CTF as described in Section 5.5.

5.3 Multiband Signal Model

The input signal represented by *x(t)* and detailed in Equation 5.1 belongs to the multi band model $\mathcal{M}$, in such a way that the support of its Fourier transform *X(f)* can be identified from within a union of N disjoint intervals in [-1/2T_{nyq}, +1/2T_{nyq}] with each of the bandwidths not exceeding BW [11].

$$X(f) = \int_{-\infty}^{+\infty} x(t) e^{-j2\pi ft} dt \tag{5.1}$$

Figure 5.2 represents a typical spectral support of a multiband signal $x(t) \epsilon \mathcal{M}$.

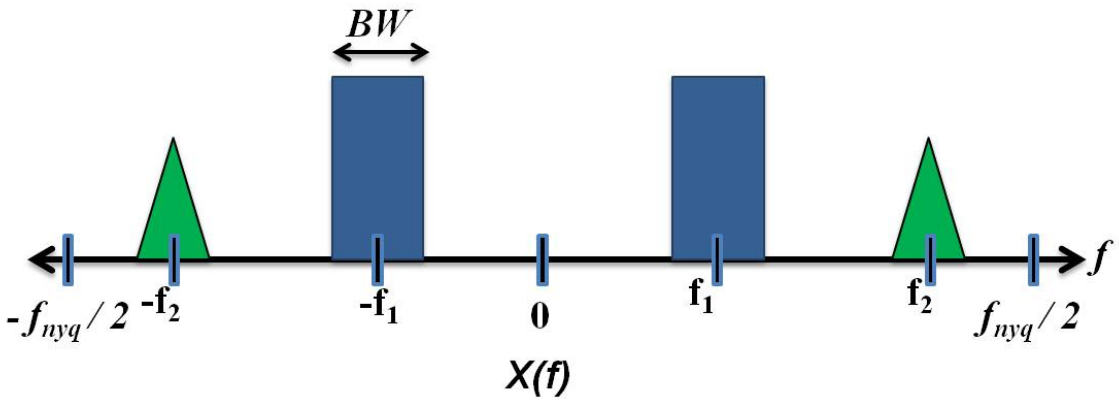

Figure 5.2: Typical Spectrum Support of $x(t) \epsilon \mathcal{M}$

5.4 Modulated Wideband Converter

The Modulated Wideband Converter system [11] detailed in this chapter operates on multiband analog signals and generates samples of any information band of interest at sub Nyquist rates and thereby makes baseband processing possible. The MWC is designed with an analog front end and a digital back end.The analogue front end of an MWC is used to alias the spectrum, by making use of spread spectrum techniques, in such a way that the base band contains spectrum portions from each band.

The RF front end of the sampling stage has a bank of multiple channels consisting of modulators and Low Pass Filter (LPF)s where input signals enter simultaneously. Low analog bandwidths are handled by low rate ADCs that are present on all channels following the RF front ends.

The mathematical expressions and equations shown below are taken from [9] and repeated here for the functional clarity and completeness of the MWC. Figure 5.3 represents the functional block diagram of an MWC where the input signal $x(t)$ enters the system simultaneously to m number of different channels.

This input signal at the i^{th} channel is mixed as per Equation 5.4 with a piecewise con-

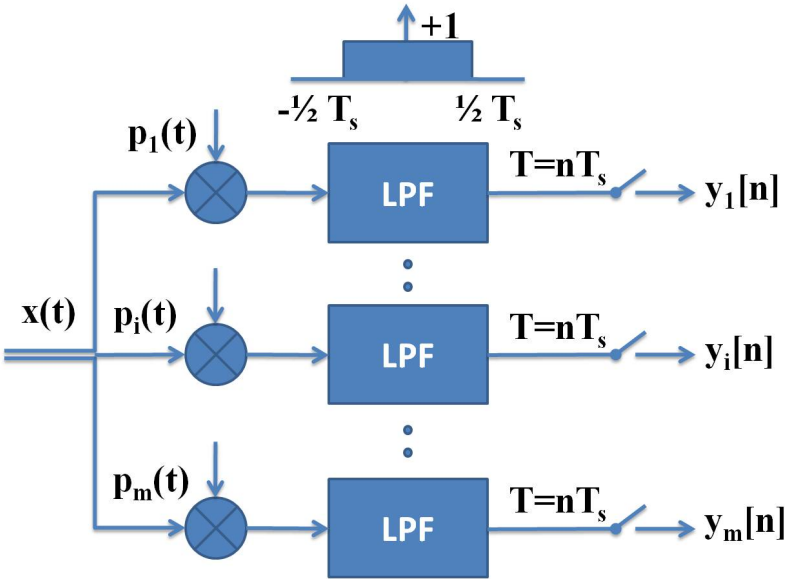

Figure 5.3: Modulated Wideband Converter

stant function $p_i(t)$ given in Equation 5.2 which has a period T_p.

$$p_i(t) = \sum_{l=-\infty}^{\infty} c_{il} e^{j\frac{2\pi}{T_p}lt} \tag{5.2}$$

where

$$c_{il} = \frac{1}{T_p} \int_0^{T_p} p_i(t) e^{\frac{-j2\pi}{T_p}lt} dt \tag{5.3}$$

$$\tilde{x}_i(t) = x(t) p_i(t) \tag{5.4}$$

The Fourier transform of this analog mixing sequence can be evaluated as [9]

$$\begin{aligned}\tilde{X}_i(f) &= \int_{-\infty}^{\infty} \tilde{x}_i(t) e^{-j2\pi ft} dt \\ &= \int_{-\infty}^{+\infty} x(t) \Big(\sum_{l=-\infty}^{\infty} c_{il} e^{j\frac{2\pi}{T_p} lt} \Big) e^{-j2\pi ft} dt \\ &= \sum_{l=-\infty}^{l=+\infty} c_{il} X(f - lf_p) \end{aligned} \tag{5.5}$$

This mixed signal spectrum then enters a low pass filter with a cut-off $1/(2T_s)$ and is sampled at a sufficiently lower frequency, $f_s = 1/T_s$. Equation 5.6 shows the Discrete Time Fourier Transform (DTFT) expression of the sampled output.

$$Y_i(e^{j2\pi fT_s}) = \sum_{l=-L_0}^{l=+L_0} c_{il} X(f - lf_p), f \epsilon \mathcal{F}_s \tag{5.6}$$

where $\mathcal{F}_s = [-f_s/2, +f_s/2]$ and L_0 is chosen as the smallest integer such that the sum contains all nonzero contributions of $X(f)$ over $\mathcal{F}_s$. Equation 5.6 can be represented in matrix form as

$$y(f) = Az(f), f \epsilon \mathcal{F}_s \tag{5.7}$$

y(f) is a vector of length m with i^{th} element $y_i(f) = Y_i(e^{j2\pi fT_s})$, A is a known matrix of order $m \times L$ and can be represented as Equation 5.8 which contains the coefficients c_{il} and z is an unknown vector of length L that is used to recover the signal.

$$A = S \times F \times D \tag{5.8}$$

S is the random pattern of ± 1 denoted by p_{ij} of order $m \times M$.
F is a discrete Fourier transform matrix of order $M \times L$ with columns $\left[\bar{F}_{L_0}..., \bar{F}_0, ..., \bar{F}_{-L_0}\right]$; where $\bar{F}$ can be obtained from Equation 5.9.

$$\bar{F}_i = \left[\theta^{0.i}, \theta^{1.i}, ..., \theta^{(M-1).i}\right]^T \tag{5.9}$$

$$\text{where } \theta = e^{\frac{-j2\pi}{M}} \text{ and } 0 \leq i \leq M-1$$

D is a diagonal matrix of order $L \times L$ with diagonal elements $[d_{L_0}, ..., d_0, ..., d_{-L_0}]$; where d_i is defined by Equation 5.10

$$d_i = \begin{cases} 1/M \; ; \; i = 0 \\ \frac{1-\theta^i}{2\pi j i} \; ; \; i \neq 0 \end{cases} \tag{5.10}$$

$$\text{where } -L_0 \leq i \leq L_0$$

5.5 Continuous To Finite Block

Support recovery is done using a digital algorithm by the continuous to finite block [9] that isolates the problem to a one-time execution of a polynomial time algorithm [45]. It solves a finite dimensional sparse representation problem after constructing a frame as per Equation 5.11, using the input samples thereby making it possible to detect the correct support set and their positions by using this digital recovery algorithm.

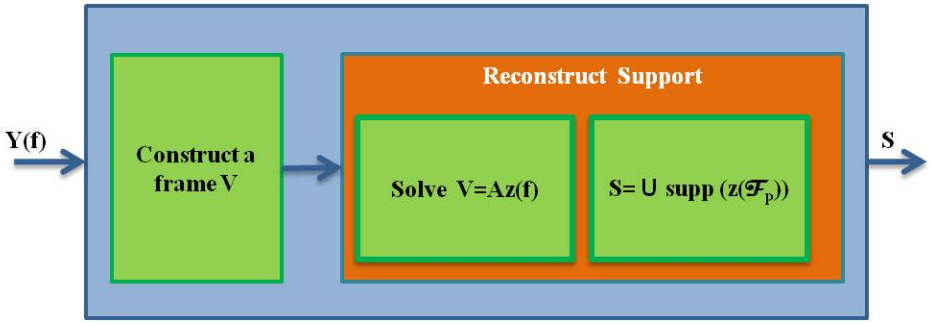

Figure 5.4: Continuous To Finite Block

$$Q = \sum_{n=-\infty}^{+\infty} y[n]y^T[n] \tag{5.11}$$

where $y[n]=[y_1[n],...,y_m[n]]^T$ is the vector of samples at time instances nT_s. Then any matrix V, for which $Q = V\,V^H$, is a frame for $y(\mathcal{F}_s)$ [46] is constructed and the support of the input signal is reconstructed using an OMP algorithm. There are mainly two major inputs A and v, required for the OMP algorithm, first one of which can be calculated from Equation 5.8 and the second major input v of this algorithm is a function of data samples obtained after down-sampling the signal and can be represented as given in Equation 5.12

$$v = V \times e \tag{5.12}$$

where V contains the eigenvectors corresponding to the non-zero eigenvalues of Q obtained from Equation 5.11 when arranged in descending order and e is the diagonal matrix generated from the square root of non-zero eigenvalues of Q arranged in descending order. The Support S can then be recovered from $z(\mathcal{F}_p)$ using the CTF block as shown in Figure 5.4.

5.6 Prototype Architecture

This section gives the details about the various parameters used in MWC.

5.6.1 System Parameters

Table 5.1 indicates the different parameters used in the simulation of MWC. For a periodic wave represented by p_{ij} of order $m \times M$, frequency is indicated by f_p and can be calculated from the Equation 5.13:

$$f_p = f_{nyq}/L \tag{5.13}$$

Table 5.1: System Parameters for MWC.

Parameter	Description
N	Number of bands
BW	Maximum width of each band
f_{nyq}	Nyquist frequency
T_{nyq}	Nyquist rate
m	Number of sampling channels
f_s	sampling frequency
f_p	frequency of periodic wave,p_{ij}
M	Number of $\pm$ 1 intervals in each period of p_{ij}
L	Number of equally spaced divisions in each period of x

This periodic wave required for mixing the input signal is generated as a pseudo random chipping sequence with M number of $\pm$ 1 in each period, Tp.

5.6.2 Signal Representation

The input signal x belonging to the multiband model $\mathcal{M}$ is a continuous function of time t, the Fourier transform of which is a piecewise continuous function of f_i and is represented by Equation 5.14. The random carrier frequency f_i is generated using a random number algorithm after adapting it for the Nyquist frequency under consideration to ensure that the generated carrier falls within the limit [0,$f_{nyq}/2$].

$$X(f_i) = \int_{-\infty}^{+\infty} x(t) e^{-j2\pi f_i t} dt \tag{5.14}$$

The frequency of periodic wave f_p and frequency of the input signal f_i are the key factors in the calculation of original support S_{orig} given in Algorithm 8. The starting edge of the support is calculated as f_i - $BW/2$ and dividing the value by f_p. This value is shifted by half to 0 and then moved to L_0 + 1 as can be seen from the Step 2 of Algorithm 8 for original support. The standard function *ceil* is used for finding out the nearest integer value on the upper side. The value of L_0 is calculated as per Equation 5.15 for distributing the values symmetrically. The end point is similarly calculated

except that the input frequency f_i is added here to half of the bandwidth BW as can be seen from Step 3 of the above mentioned algorithm .

$$L_0 = \frac{L-1}{2} \tag{5.15}$$

The original support, S_{orig} is obtained by taking the union between the values of the starting edge vector, provided the corresponding values in the ending edge vector are higher or equal in value. As S_{orig} is to be distributed symmetrically, the vector thus calculated as S_{orig} is then merged with the values on the corresponding symmetric position. The VHDL code for the calculation of original support is given in HDL Code 5.1.

Algorithm 8 Algorithm for Original Support

1. Start
2. Calculate$B = ceil\left[\frac{f_i - \frac{BW}{2}}{f_p}\right] - 0.5 + L_0 + 1$
3. Calculate $E = ceil\left[\frac{f_i + \frac{BW}{2}}{f_p}\right] - 0.5 + L_0 + 1$
4. Assign c=1, j=1
5. if $j \leq \frac{N}{2}$ GOTO step 6, else GOTO step 11
6. if $B(j) \leq E(j)$, GOTO step 7, else GOTO step 10
7. K(c)=B(j)
8. Increment B(j)
9. Increment c and GOTO step 6
10. Increment j and GOTO step 5
11. Sorig=Sorig $\bigcup$ K
12. Left=L+1-Sorig
13. Sorig=Sorig $\bigcup$ Left
14. Stop

HDL Code 5.1: Original Support

```
\vline
for i in 1 to (N/2) loop
    B(i) := CEIL(((fi(i)-(BW(i)/2.0))/fp)+L0+1.0-0.5);
    E(i) := CEIL(((fi(i)+(BW(i)/2.0))/fp)+L0+1.0-0.5);
end loop;
j := 1;
for i in 1 to N/2 loop
```

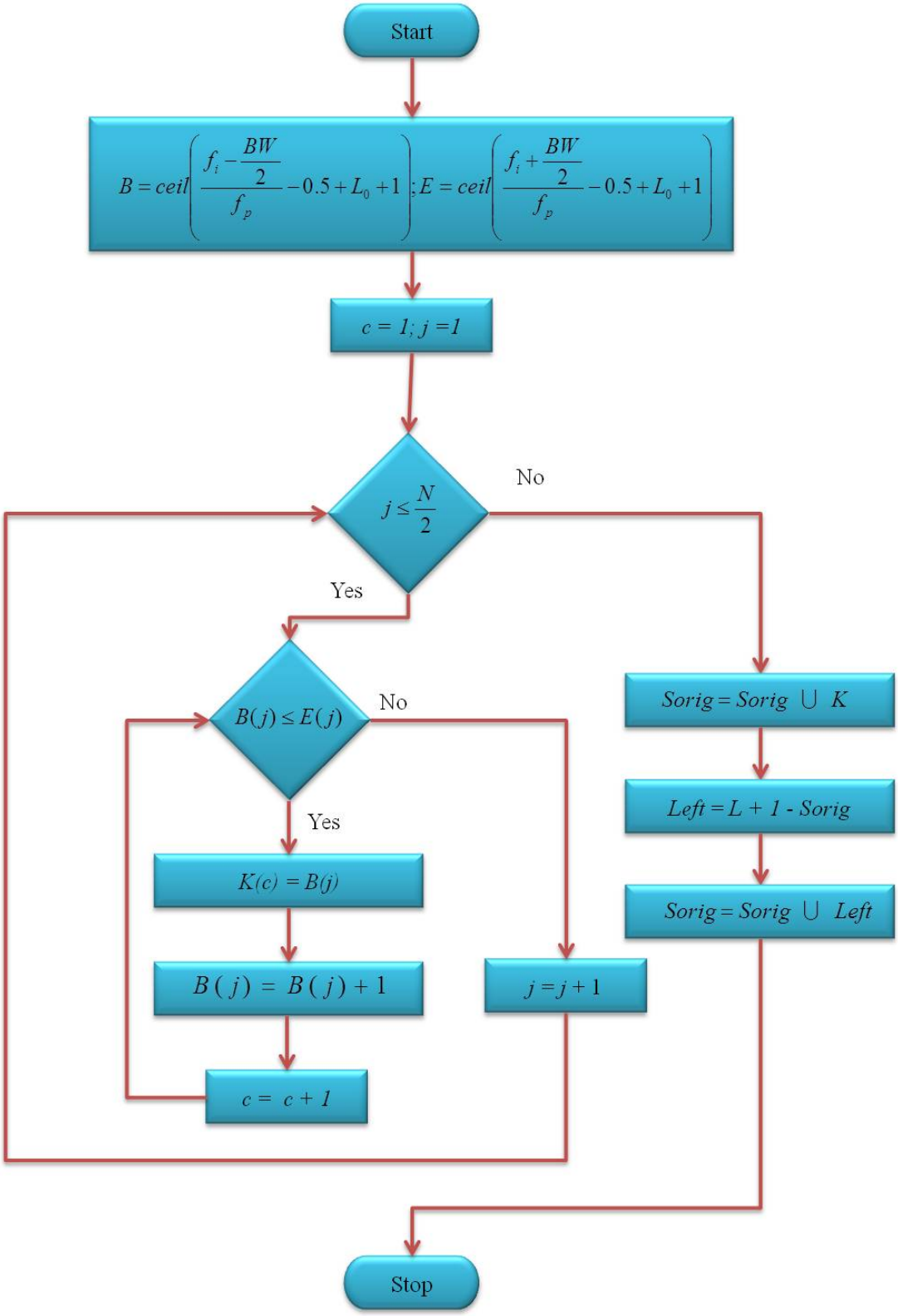

Figure 5.5: Flow diagram for the generation of original support

```
  temp := B(i);
  while (temp <= E(i)) loop
          K(j) := temp;
          temp := ((temp)+1.0);
          j := j + 1;
  end loop;
end loop;
KLen := j - 1;
for i in 1 to KLen loop
  K(j) := (L + 1 - K(i));
  j := j+1;
end loop;
KLen := j - 1;
for i in 1 to (KLen-1) loop
     for j in i+1 to KLen loop
         if (K(i) > K(j)) then
             temp := K(i); K(i) := K(j); K(j) := temp;
         end if;
    end loop;
end loop;
for i in 1 to (KLen-1) loop
    if (K(i) = K(i+1)) then
        count := count + 1;
    end if;
end loop;
length := KLen - count;
len := 1;
if (K(1) /= K(2)) then
    Sorig(1) := K(1); len := 2;
end if;
for i in 2 to KLen loop
    if ((i-1) /= 0) then
        if (K(i) /= K(i-1)) then
         if (len <= length) then
          Sorig(len) := K(i); len := len+1;
        end if;
       end if;
    end if;
end loop;
```

5.6.3 Mixing

The mixing algorithm ensures that for each and every channel, the input signal *x(t)* is mixed with a piecewise constant function *p(t)* that alternates between ± 1 for each of M equal time intervals. In order to calculate the index vector for *p(t)* the maximum length of the time axis, T_{axis} is to be determined. This T_{axis} is a sequential vector starting at zero and increments with a common difference indicated by time resolution until the maximum value of time at which the signal is observed is reached. As can be seen from the Algorithm 9, an index vector of length same as that of T_{axis} is created with elements indicating the column number of *p(t)* in a sequentially repeating order until the number of elements reaches the same as that in T_{axis}. Once the index vector is calculated the elements of *p(t)* is taken for each number of channel, based on the values in the index vector and multiplied with the corresponding values in *x(t)* to generate a two dimensional mixed matrix P_{ij} where i increments up to the number of channels and j increments up to the length of the T_{axis} assigned as *len* in the algorithm. The VHDL coding for this algorithm is given in HDL Code 5.2.

Algorithm 9 Algorithm for Mixer

1. Start
2. Calculate len = length of T_{axis}
3. quotient = $T_{axis}/(T_p/M)$
4. quoToInt = round down (quotient)
5. Index = remainder (quoToInt/M) + 1
6. Assign i = 1
7. if $i \leq m$, GOTO step 8, else GOTO step 13
8. Assign j = 1
9. if $j \leq len$, GOTO step 10, else GOTO step 12
10. $P_{ij} = x_j \times p(i, Index(j))$
11. Increment j and GOTO step 9
12. Increment i and GOTO step 7
13. Stop

HDL Code 5.2: Mixing

```
for i in 1 to m loop
    for j in 1 to len loop
        quotient := (t_axis(j)/real(Tp/M));
```

```
        quoToInt := floor(quotient);
        Index := (integer (quoToInt) mod M) +1;
        P(i,j) := x(j) * real(p(i,Index));
    end loop;
end loop;
```

5.6.4 Analog low-pass filtering and actual sampling

A low pass filter is known to be completely transparent to signals that have frequencies less than a specified cut-off limit. In the implementation of an algorithm to mimic the functions of a LPF, it is necessary to consider a temporary vector that can be interpolated to the specified dimension. In Algorithm 10 a row vector of length (K+K_0) is first generated in an iteration loop. The elements in this vector are chosen in such a way that the first element represents the highest limit, 1, and all other elements are assigned as 0. A standard interpolation function is then used to interpolate this temporary vector to a length same as that of the time axis and is divided by L.

Prior to creating the filtered signal by multiplying the mixed signal with the ideal low pass filter in Algorithm 10, Fourier transforms of each of these vectors are taken. This makes it necessary that the obtained product of the vectors is to be applied with an inverse Fourier transform function to create the filtered signal, FS as a function of time. This process when repeated for the total number of channels will generate a two dimensional matrix. A standard down sampling function is used for down sampling this signal to a length specified by the decimation factor d and this down sampled signal is represented as y_i where i stands for the number of channels. The decimation factor specified with this down sampling function helps to keep the values of FS at every d^{th} sample from the starting point. HDL Code 5.3 represents the VHDL coding for the analog LPF and sampling algorithm.

HDL Code 5.3: Analog LPF and Actual Sampling

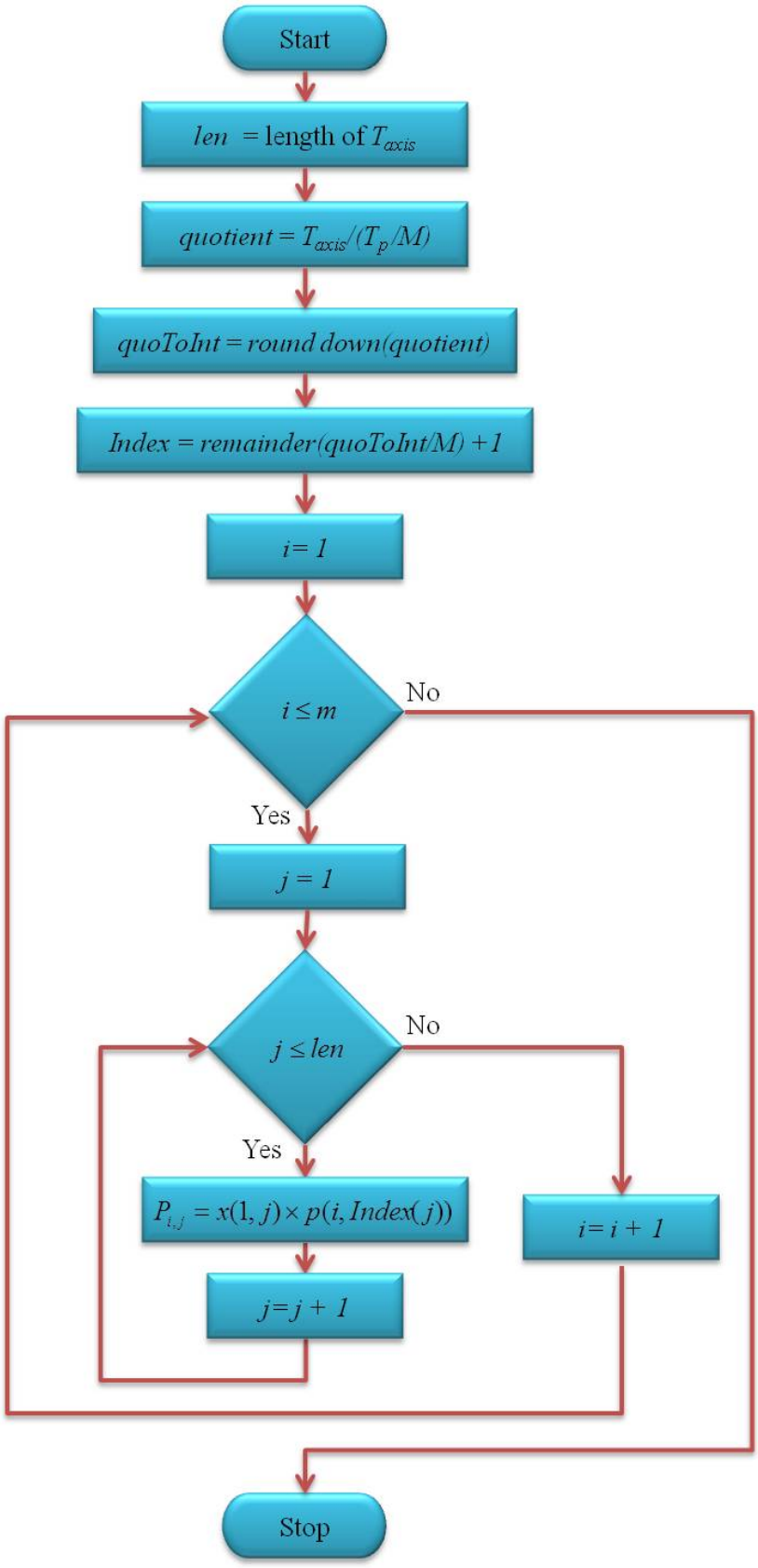

Figure 5.6: Flow diagram for Mixing

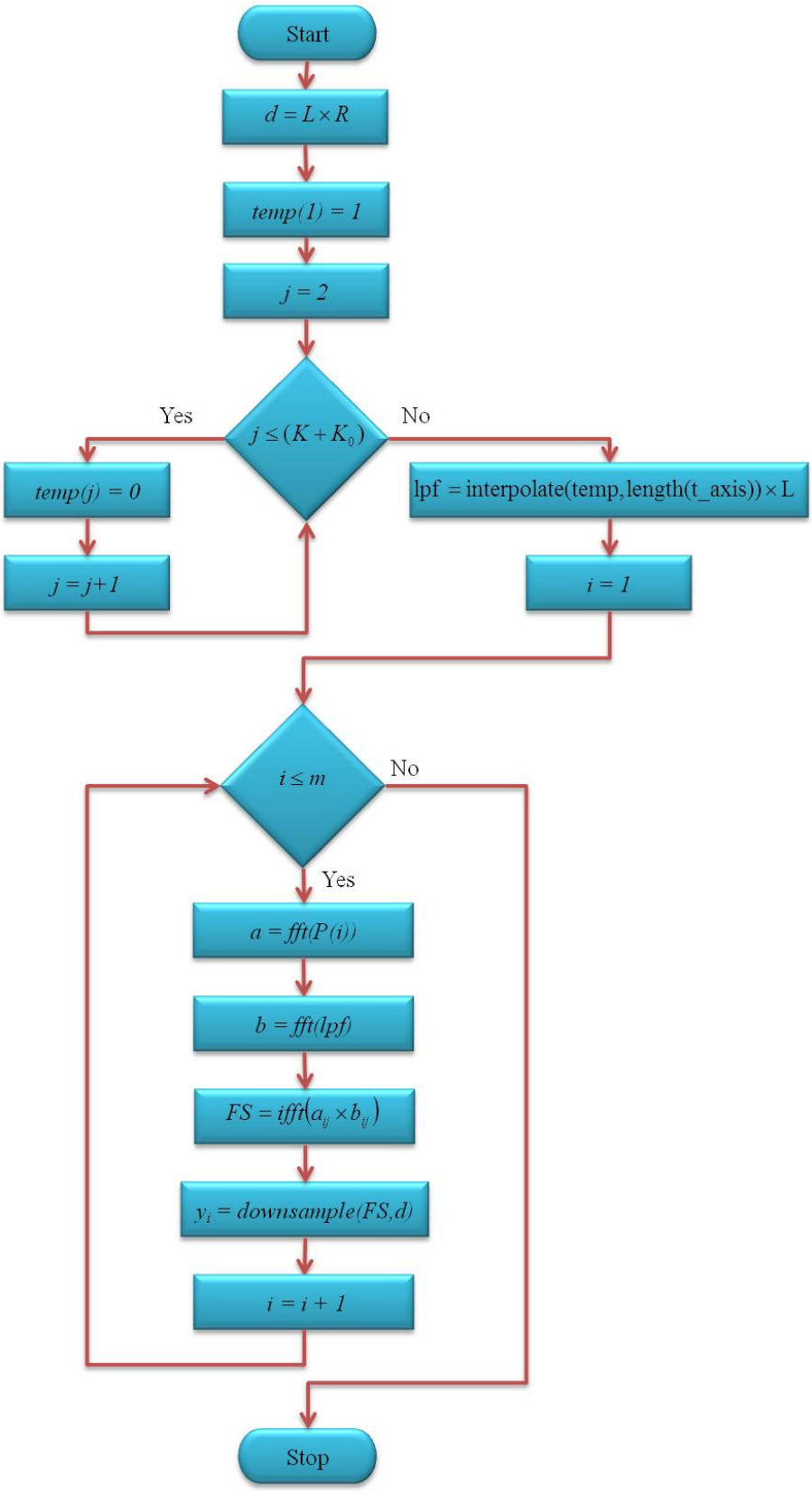

Figure 5.7: Flow diagram for LPF

Algorithm 10 Algorithm for Analog LPF and Actual Sampling

1. Start
2. Calculate decimation factor, $d = L \times R$
3. Assign temp(1)=1 and j=2
4. if $j \leq (K + K0)$, GOTO step 5, else GOTO step 7
5. temp(j)=0
6. Increment j and GOTO step 4
7. lpf= interpolate temp upto a length of T_{axis} and multiply by L
8. Assign i=1
9. if $i \leq m$, GOTO step 10, else GOTO step 15
10. a=Fast Fourier Transform of P(i)
11. b=Fast Fourier Transform of lpf
12. Filtered signal, FS = Inverse of Fast Fourier Transform $(a_{ij} \times b_{ij})$
13. y_i= Down Sample FS based on d
14. Increment i and GOTO step 9
15. Stop

```
d := L*R;
for j in 1 to (K+K0) loop
    if (j = 1) then
        temp(j) := 1;
    else
        temp(j) := 0;
    end if;
end loop;
len := (K+K0) * L;
lpf(i) := interpft(temp(i),len) * L;
for i in 1 to len loop
    theta := MATH_PI*2.0/real(len)*real(i-1);
    for j in 1 to len loop
        exp_c := cos((theta*real(j-1)) mod (MATH_PI*2.0));
        lpf_fft(i) := lpf_fft(i) + lpf(j)*exp_c;
    end loop;
    if(lpf_fft(i) < 0.00001) then
     lpf_fft(i) := 0.0;
     end if;
end loop;
b := lpf_fft;
DigitalLength := len/d;
for k1 in 1 to m loop
    for i in 1 to len loop
        theta := MATH_PI*2.0/real(len)*real(i-1);
            for j in 1 to len loop
                exp_c1 := (cos((theta*real(j-1)) mod (MATH_PI*2.0)),-1.0*sin((theta*real(j↩
                    -1)) mod (MATH_PI*2.0)));
```

```
                P_fft(i) := P_fft(i) + P(k1,j)*exp_c1;
            end loop;
    end loop;
    a := P_fft;
    for i in 1 to len loop
        mult_fft1(i) := a(i) * b(i);
    end loop;
    for i in 1 to len loop
        theta := MATH_PI*2.0/real(len)*real(i-1);
            for j in 1 to len loop
                exp_c1 := (cos((theta*real(j-1)) mod (MATH_PI*2.0)),sin((theta*real(j-1)) ↩
                    mod (MATH_PI*2.0)));
                P_ifft(i) := P_ifft(i) + (mult_fft1(j).RE*exp_c1.RE - mult_fft1(j).IM*exp_c1↩
                    .IM);
            end loop;
        P_ifft(i) := P_ifft(i) / real(len);
    end loop;
    FS := P_ifft;
    for i in 1 to DigitalLength loop
        y(k1,i).RE := FS((i-1)*d+1);
    end loop;
end loop;
```

5.6.5 CTF

CTF block [9] is used to recover the support of active bands by making use of an OMP algorithm from [30]. These two inputs A and v obtained from Equations 5.8 and 5.12 are used by the OMP algorithm to iteratively calculate the value of z given in Step 4 of Algorithm 11 and thereby identifies the location of support which is maximum of the elements in z. This support is again updated based on the symmetric location to generate the Recovered Support vector. VHDL Code for OMP algorithm is shown in HDL Code 5.4.

HDL Code 5.4: CTF

```
R1 := v ;
G := (others => 0.0);
for i in 1 to L loop
```

Algorithm 11 OMP algorithm used in CTF

Input:

- Signal v and matrix A
- Stopping criteria
  1. number of iterations, I reaches N
  2. $R2 > R3$; $R2 = \sqrt{\sum \left(v_{ij}\right)^2}$, $R3 = 0$
  3. $R4 > R5$; $R4 = \frac{R2}{\sqrt{\sum\left(\left[As^{\perp} \times v\right]_{ij}\right)^2}}$, $R5$ = Residual vs Solution Threshold which is pre-initialised

Output

- Recovered support, RS

Algorithm
1. Start by setting residual, $R1 = v$
2. Start iteration for termination criteria
3. Assign $Z1 = A^T \times R1$
4. $z = \frac{\left[\sqrt{\sum_{j=1}^{q} |Z1|^2}\right]_i}{G_i}$; $G = \sqrt{diag\left(A^T \times A\right)}$
and q is the length of $Z1$
5. Best Location, $BL = j$; j is the value of i in $(z_i)_{max}$
6. Recovered Support, $RS = RS \cup BL$
7. Find symmetric location, SL and compare to BL to update RS with SL
8. $As_{ij} = A_{ij}$; $i = 1$ to m and $j = RS(1)$ to RS(length of RS)
9. Now update $R1 = v - \left(As \times As^{\perp} \times v\right)$ where $As^{\perp}$ is the pseudo inverse of As
10. Update $R2$, $R4$ and increment I
11. Goto Step 2 and check for criterias to exit

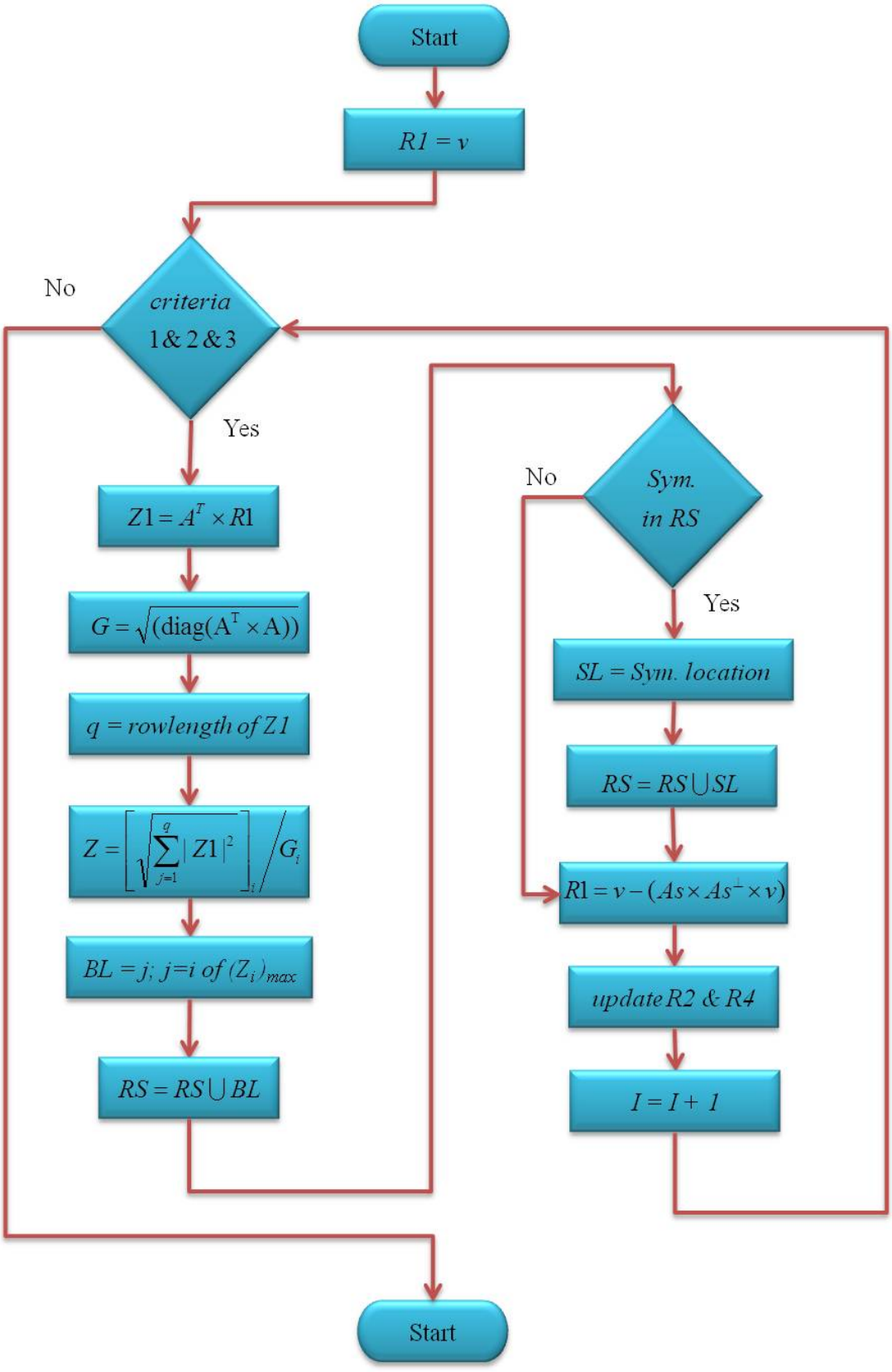

Figure 5.8: Flow diagram for OMP algorithm in CTF

```
  exp_c1 := cmplx(0.0,0.0);
    for j in 1 to m loop
       exp_c1 := exp_c1 + A(j,i)*conj(A(j,i));
    end loop;
    G(i) := sqrt(exp_c1.RE);
end loop;
index := 1;

for iter in 1 to N loop
  if( (R2 > R3) and (R4 >  R5) ) then
        Z1 := (others => (others => cmplx(0.0,0.0)));
        for i in 1 to L loop
            for j in 1 to (2*N) loop
                for k1 in 1 to m loop
                    Z1(i,j) := Z1(i,j) + (A(k1,i))*R1(k1,j);
                end loop;
            end loop;
        end loop;
Z := (others => 0.0);
        for i in 1 to L loop
            for j in 1 to (2*N) loop
                 Z(i) := Z(i) + Z1(i,j).RE*Z1(i,j).RE + Z1(i,j).IM*Z1(i,j).IM;
            end loop;
            Z(i) := sqrt(Z(i)) / G(i);
        end loop;
maxVal := Z(1);
BL := 1;
        for i in 2 to L loop
            if(maxVal < Z(i)) then
                maxVal := Z(i);
                BL := i;
            end if;
        end loop;
RS(index) := BL;
index := index+1;
        if (BL /= (L+1-BL)) then -- SL is (L+1-BL).
            RS(index) := L+1-BL;
            index := index+1;
        end if;
        for i in 1 to (index-1) loop
            for j in 1 to m loop
                As(j,i) := A(j,RS(i));
            end loop;
        end loop;
solution := (others => (others => cmplx(0.0,0.0)));
        for i in 1 to m loop
            for j in 1 to (2*N) loop
```

```
                for k1 in 1 to m loop
                    solution(i,j) := solution(i,j) + ((As*pinv(As))(i,k1))*v(k1,j);
                end loop;
            end loop;
        end loop;
        for i in 1 to m loop
            for j in 1 to (2*N) loop
                R1(i,j) := cmplx(v(i,j),0.0) - solution(i,j);
            end loop;
        end loop;
R2 := 0.0;
        for i in 1 to m loop
            for j in 1 to (2*N) loop
                R2 := R2 + R1(i,j).RE**2;
            end loop;
        end loop;
R2 := sqrt(R2);
R4 := 0.0;
        for i in 1 to m loop
            for j in 1 to (2*N) loop
                R4 := R4 + solution(i,j).RE*solution(i,j).RE;
            end loop;
        end loop;
R4 := R2/sqrt(R4);
    end if;
end loop;
```

5.7 Summary

This chapter presented a brief outline about the Mixed Analog Digital System in Section 5.2 with the help of a block diagram given in Figure 5.1. This is followed by a detailed description of Multiband Signal Model, MWC and CTF block in sections 5.3, 5.4 and 5.5 respectively. Section 5.6 discusses the prototype architecture for simulation which essentially discusses various algorithms and flow diagrams along with the VHDL codes used for designing the essential components.

Chapter 6

Verification and Validation of Modulated Wideband Converter

This chapter deals with the verification of a computerised model and the operational validation of the mixed analog digital system described in Chapter 5. Test parameter choices have been assigned to carry out the execution of simulations and the results obtained are compared with the original test case for identification of support. This is followed by the assessment of the mixed analog digital system for a range of Nyquist frequencies and Signal-to-Noise Ratio (SNR) values. Finally these results are validated with the help of probability studies.

6.1 Introduction

The mixed analog digital system discussed in Chapter 5 accepts a multiband signal as input and uses different sub-blocks to recover the support. In this chapter a numerical investigation of different blocks of algorithms of the mixed analog digital system discussed in Chapter 5 has been conducted using test parameter choices to verify the correctness in the functioning of the simulation model. This is done so as to verify that

the programming and implementation of the conceptual model presented in Chapter 5 is correct. As the mixed analog digital system consists of different sub blocks, the method which can be used for model verification is similar to that used for the WCRR, that is the bottom-up strategy [14] taken from dynamic testing.

This chapter also deals with the operational validation for further assessment and validation of this model that will ensure successful support recovery by the mixed analog digital system. The method used for this purpose is a parameter variability - sensitivity analysis [14] which has been described in Chapter 4.

6.2 Verification: Mixed Analog Digital System Simulation Model

This section deals with the verification of the mathematical functioning of sub-blocks in the mixed analog digital system. If all the sub block algorithms function correctly, the complete computerised model can successfully recover the support. For successful support recovery, the original support set, S_{orig}, generated by using the generation of original support set block given in Algorithm 8, must be a subset of the recovered support set, RS, which is obtained from the CTF block given in Algorithm 11.

6.2.1 Parameter Choices

Parameter choices assigned for testing the simulation model is given in Table 6.1 and the notations mentioned can be referred from Table 5.1. The low values which are not realistic are selected for testing purpose so that the matrices are small enough to present in thesis.

Table 6.1: Parameter Choices for Verification of Simulation

Notations and chosen values for testing	
fnyq (Hz)	100
Tnyq (s)	.01
fp(Hz)	20
fs(Hz)	20
Tp(s)	.05
Ts(s)	.05
BW(Hz)	10
L	5
M	5

6.2.2 Testing: Input Signal Generation

The simulation model of the mixed analog digital system can accept a multiband signal as input for the mixing algorithm to mix it with a pseudo random chipping sequence for a different number of required channels. For the testing purposes we use an input signal belonging to the multiband model, $x(t) \in \mathcal{M}$. The vector corresponding to this input signal used for testing purposes is given below.

Input Signal, $x(t)$ =

$$\begin{bmatrix} 0.00E+00 & 9.05E-03 & 5.96E-02 & -5.19E-02 & 9.78E-02 \\ -3.77E-01 & -1.05E+00 & 1.02E+00 & 1.37E+00 & -6.99E-01 \\ -4.51E-01 & 7.03E-02 & -2.46E-02 & 1.11E-02 & 0.00E+00 \\ 0.00E+00 & 0.00E+00 & 0.00E+00 & 0.00E+00 & 0.00E+00 \end{bmatrix}$$

The vector shown below corresponds to the values in the time axis grid of the input signal.

Time axis, T_{axis} =

$$\begin{bmatrix} 0.00E+00 & 1.00E-02 & 2.00E-02 & 3.00E-02 & 4.00E-02 \\ 5.00E-02 & 6.00E-02 & 7.00E-02 & 8.00E-02 & 9.00E-02 \\ 1.00E-01 & 1.10E-01 & 1.20E-01 & 1.30E-01 & 1.40E-01 \\ 1.50E-01 & 1.60E-01 & 1.70E-01 & 1.80E-01 & 1.90E-01 \end{bmatrix}$$

6.2.3 Testing: Pseudo Random Sequence Generation

This random sequence of $\pm$ 1 s are generated using inbuilt function 'UNIFORM' in ModelSim and the order of the sequence is m $\times$ M. The sequence generated for the testing purpose is given as below.

Pseudo-random chipping sequence, *p(t)* =

$$\begin{bmatrix} -1.00E+00 & 1.00E+00 & -1.00E+00 & -1.00E+00 & -1.00E+00 \\ -1.00E+00 & 1.00E+00 & -1.00E+00 & 1.00E+00 & 1.00E+00 \\ -1.00E+00 & 1.00E+00 & -1.00E+00 & 1.00E+00 & -1.00E+00 \\ -1.00E+00 & 1.00E+00 & 1.00E+00 & 1.00E+00 & -1.00E+00 \end{bmatrix}$$

6.2.4 Testing: Generation of Original Support

The original support calculated as per the Algorithm 8 is given below. It is this vector that will be compared with the final output of the CTF block to determine whether the recovery has been successful or not. It may be noted that in case the recovered support set contains all of the elements given in the vector, S_{orig} below, it may be considered as a successful support recovery. For testing purposes the start point, B of S_{orig} is calculated as 4 and end point, E is calculated as 5 using the equations given in Step 2 and 3 of Algorithm 8 respectively.

Original Support, S_{orig} =

$$\begin{bmatrix} 1 & 2 & 4 & 5 \end{bmatrix}$$

6.2.5 Testing: Mixing Algorithm

In the mixing block of the simulation model, the input signal is mixed with the pseudo random chipping sequence. The elements of the chipping sequence p_{ij} are sequentially

accessed based on the values in the index vector calculated in Step 5 of Algorithm 9 and multiplied with the corresponding element of the input signal, *x(t)*. This is repeated for the total number of channels. The mixed signal thereby calculated by the mixing algorithm should be of the order of $m \times len$ and is given below.

Mixed Signal, P =
Columns 1 through 5

$$\begin{array}{rrrrr}
0.00E+00 & 9.05E-03 & -5.96E-02 & 5.19E-02 & -9.78E-02 \\
0.00E+00 & 9.05E-03 & -5.96E-02 & -5.19E-02 & 9.78E-02 \\
0.00E+00 & 9.05E-03 & -5.96E-02 & -5.19E-02 & -9.78E-02 \\
0.00E+00 & 9.05E-03 & 5.96E-02 & -5.19E-02 & -9.78E-02
\end{array}$$

Columns 6 through 10

$$\begin{array}{rrrrr}
3.77E-01 & -1.05E+00 & -1.02E+00 & -1.37E+00 & 6.99E-01 \\
3.77E-01 & -1.05E+00 & -1.02E+00 & 1.37E+00 & -6.99E-01 \\
3.77E-01 & -1.05E+00 & -1.02E+00 & 1.37E+00 & 6.99E-01 \\
3.77E-01 & -1.05E+00 & 1.02E+00 & 1.37E+00 & 6.99E-01
\end{array}$$

Columns 11 through 15

$$\begin{array}{rrrrr}
4.51E-01 & 7.03E-02 & 2.46E-02 & -1.11E-02 & 0.00E+00 \\
4.51E-01 & 7.03E-02 & 2.46E-02 & 1.11E-02 & 0.00E+00 \\
4.51E-01 & 7.03E-02 & 2.46E-02 & 1.11E-02 & 0.00E+00 \\
4.51E-01 & 7.03E-02 & -2.46E-02 & 1.11E-02 & 0.00E+00
\end{array}$$

Columns 16 through 20

$$\begin{array}{rrrrr}
0.00E+00 & 0.00E+00 & 0.00E+00 & 0.00E+00 & 0.00E+00 \\
0.00E+00 & 0.00E+00 & 0.00E+00 & 0.00E+00 & 0.00E+00 \\
0.00E+00 & 0.00E+00 & 0.00E+00 & 0.00E+00 & 0.00E+00 \\
0.00E+00 & 0.00E+00 & 0.00E+00 & 0.00E+00 & 0.00E+00
\end{array}$$

6.2.6 Testing: Signal Filtering and Sampling

In this block of the simulation model, a filtered signal *FS* is generated using the mixed signal *P* and the vector corresponding to the impulse response of the low pass filter represented as *lpf*. The vector calculated for *lpf* and the corresponding filtered signal, *FS* obtained for testing purposes of Algorithm 10 is given below.

Impulse response of LPF, *lpf* =

$$\begin{bmatrix} 2.00E-01 & 1.86E-01 & 1.46E-01 & 9.33E-02 & 4.05E-02 \\ -5.55E-18 & -2.14E-02 & -2.42E-02 & -1.55E-02 & -4.65E-03 \\ 0.00E+00 & -4.65E-03 & -1.55E-02 & -2.42E-02 & -2.14E-02 \\ -1.11E-17 & 4.05E-02 & 9.33E-02 & 1.46E-01 & 1.86E-01 \end{bmatrix}$$

Filtered Signal, *FS* = Columns 1 through 5

$$\begin{bmatrix} 5.86E-02 & 4.66E-02 & -1.73E-02 & -1.29E-01 & -2.65E-01 \\ 2.05E-02 & 4.65E-03 & -3.26E-02 & -8.37E-02 & -1.34E-01 \\ 6.08E-03 & -3.52E-02 & -9.51E-02 & -1.50E-01 & -1.73E-01 \\ -2.54E-02 & -5.66E-02 & -7.13E-02 & -4.47E-02 & 3.61E-02 \end{bmatrix}$$

Columns 6 through 10

$$\begin{bmatrix} -3.87E-01 & -4.60E-01 & -4.59E-01 & -3.82E-01 & -2.51E-01 \\ -1.67E-01 & -1.71E-01 & -1.42E-01 & -8.65E-02 & -1.97E-02 \\ -1.47E-01 & -6.93E-02 & 4.45E-02 & 1.65E-01 & 2.60E-01 \\ 1.65E-01 & 3.17E-01 & 4.54E-01 & 5.41E-01 & 5.52E-01 \end{bmatrix}$$

Columns 11 through 15

$$\begin{bmatrix} -1.01E-01 & 2.78E-02 & 1.06E-01 & 1.25E-01 & 9.54E-02 \\ 4.03E-02 & 7.86E-02 & 8.82E-02 & 7.21E-02 & 4.15E-02 \\ 3.04E-01 & 2.88E-01 & 2.22E-01 & 1.30E-01 & 4.15E-02 \\ 4.86E-01 & 3.61E-01 & 2.12E-01 & 7.62E-02 & -1.72E-02 \end{bmatrix}$$

Columns 16 through 20

$$\begin{matrix} 4.34E-02 & -9.39E-04 & -1.66E-02 & -2.64E-05 & 3.40E-02 \\ 1.09E-02 & -7.77E-03 & -9.36E-03 & 2.31E-03 & 1.66E-02 \\ -1.81E-02 & -3.86E-02 & -2.62E-02 & -2.64E-05 & 1.66E-02 \\ -5.72E-02 & -5.27E-02 & -2.62E-02 & -3.69E-03 & -2.77E-03 \end{matrix}$$

Once FS is obtained, we down sample it by a decimation factor, d, the value of which used for the testing purpose is 5. The vector representation of the down sampled signal y obtained for the given testing parameter choices is given below.

Down Sampled Signal, y =

$$\begin{bmatrix} 5.86E-02 & -3.87E-01 & -1.01E-01 & 4.34E-02 \\ 2.05E-02 & -1.67E-01 & 4.03E-02 & 1.09E-02 \\ 6.08E-03 & -1.47E-01 & 3.04E-01 & -1.81E-02 \\ -2.54E-02 & 1.65E-01 & 4.86E-01 & -5.72E-02 \end{bmatrix}$$

6.2.7 Testing: CTF Block

The down sampled signal generated using the down sampler is fed into the CTF block as the major input for calculating the matrix Q given below.

Q =

$$\begin{bmatrix} 1.65E-01 & 6.24E-02 & 2.58E-02 & -1.17E-01 \\ 6.24E-02 & 3.02E-02 & 3.68E-02 & -9.19E-03 \\ 2.58E-02 & 3.68E-02 & 1.14E-01 & 1.24E-01 \\ -1.17E-01 & -9.19E-03 & 1.24E-01 & 2.67E-01 \end{bmatrix}$$

The matrix, Q, is used to calculate v which is one of the inputs required to calculate the support by the OMP algorithm.

$v =$

$$\begin{bmatrix} -2.66E-01 & 3.07E-01 & -5.70E-03 & 2.11E-04 \\ -3.90E-02 & 1.69E-01 & 6.22E-04 & -6.81E-04 \\ 2.09E-01 & 2.66E-01 & 7.66E-03 & 1.95E-04 \\ 5.13E-01 & 6.39E-02 & -6.04E-03 & -2.19E-05 \end{bmatrix}$$

In addition to this matrix v, the OMP algorithm uses matrix A calculated by multiplying matrices S, F and D. S is the same as that of the random pattern matrix, p. Matrix F and D generated using Equations 5.9 and 5.10 for testing purpose are given below.

$F =$

$$\begin{bmatrix} 1.00+0.00i & 1.00+0.00i & 1.00+0.00i & 1.00+0.00i & 1.00+0.00i \\ -0.80+0.58i & 0.30+0.95i & 1.00+0.00i & 0.30-0.95i & -0.80-0.58i \\ 0.30-0.95i & -0.80+0.58i & 1.00+0.00i & -0.80-0.58i & 0.30+0.95i \\ 0.30+0.95i & -0.80-0.58i & 1.00+0.00i & -0.80+0.58i & 0.30-0.95i \\ -0.80-0.58i & 0.30-0.95i & 1.00+0.00i & 0.30+0.95i & -0.80+0.58i \end{bmatrix}$$

$D =$

$$\begin{bmatrix} 2.00E-01 & 0.00E+00 & 0.00E+00 & 0.00E+00 & 0.00E+00 \\ 0.00E+00 & 2.00E-01 & 0.00E+00 & 0.00E+00 & 0.00E+00 \\ 0.00E+00 & 0.00E+00 & 2.00E-01 & 0.00E+00 & 0.00E+00 \\ 0.00E+00 & 0.00E+00 & 0.00E+00 & 2.00E-01 & 0.00E+00 \\ 0.00E+00 & 0.00E+00 & 0.00E+00 & 0.00E+00 & 2.00E-01 \end{bmatrix}$$

By multiplying the matrices S, F and D given above, matrix A is calculated and is given below.

$A =$

$$\begin{bmatrix} 2.00E-01 & 0.00E+00 & 0.00E+00 & 0.00E+00 & 0.00E+00 \\ 0.00E+00 & 2.00E-01 & 0.00E+00 & 0.00E+00 & 0.00E+00 \\ 0.00E+00 & 0.00E+00 & 2.00E-01 & 0.00E+00 & 0.00E+00 \\ 0.00E+00 & 0.00E+00 & 0.00E+00 & 2.00E-01 & 0.00E+00 \\ 0.00E+00 & 0.00E+00 & 0.00E+00 & 0.00E+00 & 2.00E-01 \end{bmatrix}$$

The output of the OMP Algorithm 11 used in CTF block is the vector RS corresponding to the recovered support. It is this matrix that is compared with the original support set , S_{orig} to identify whether the recovery is successful or not.

$RS =$

$$\begin{bmatrix} 1 & 2 & 4 & 5 \end{bmatrix}$$

6.3 Model Verification: Mixed Analog Digital System Simulation Model

The computerised model created for identifying the support recovery has generated an output. Now it is to be verified that the output generated is a valid support set. For successful support recovery, the recovered support set RS should be equal to the original support set, S_{orig}. The following Table 6.2 gives the values of S_{orig} and RS. It can be seen from the first row of the table that RS is exactly the same as that of the S_{orig}. This is one of the cases in which successful recovery can be reported. Thus it is hereby verified that for the test parameter choices, the simulation model of the mixed analog digital system has reported an output and it matches the requirement for successful support recovery.

If the model is again tested with test values that have the option of random generation for some of its test parameter choices, a different set of values will be generated for the original support set and the recovered support set. These generated recovered support sets may be the same as that of its corresponding original support sets leading to successful recovery. There are cases when the *RS* set may not be the same as that of the S_{orig} set. In these cases depending on whether the matrix for A_s calculated from step 8 of Algorithm 11 is linearly independent, successful support recovery can also be defined [9] when the recovered support set contains some additional elements other than those which are present in the original support set. For a specific case , this recovery is considered as success since these elements do not interfere with the rights of primary users of CR and these additional elements are named as false positives. The second row of the table shows an example of a case with 2 false positives. In case the support set does not contain all of the elements that are present in the original support, a case of failure in recovering the support is to be reported. An example of a case with 2 false negatives corresponding to failed recovery is shown in the third row of the table.

Table 6.2: Verification of Support Recovery for Test Data

Cases	Original Support	Recovered Support	Recovery Status
0 False Positives	[1,2,4,5]	[1,2,4,5]	Success
2 False Positives	[2,4]	[**1**,2,4,**5**]	Success
2 False Negatives	[1,**2**,**3**,4]	[1,4]	Failure

Thus this computerized model is hereby verified for its correct functioning using the sample test data.

6.4 Operational Validation of Mixed Analog Digital System

This section discusses the results and conclusions of various investigations carried out with the simulation model for the mixed analog digital system using ModelSim. The validation process of parameter variability - sensitivity analysis has been conducted for

successful support recovery with different SNR, Nyquist frequencies and by varying the number of channels and presented in subsection 4.5. An attempt to predict the probability of successful support recovery for a specific parameter selection has also been performed in subsection 4.6.

The ModelSim simulation has been carried out for the mixed analog digital system and the results can be verified and validated by comparing the original support set with the recovered support set for different values of SNR, Nyquist frequencies and number of channels. A total number of 2500 trials of each of the simulations have been executed to investigate the support recovery.

6.4.1 Parameter Choices for the numerical investigation of Mixed Analog Digital System

Different values selected for the parameters involved in the simulation of mixed analog digital system are given in Table 6.3. Notations given in this table can be referred to Table 5.1. Most of the frequencies within radio frequency spectrum is seen to be highly under-utilised by the licensed spectrum users making it accessible for the cognitive radios to free up wireless bandwidth. So our system parameters are chosen to have frequencies within the radio frequency spectrum.

Table 6.3: Parameter Choices

Notations and chosen values							
fnyq (GHz)	0.5	1	2	2.4	3	4	4.8
Tnyq (ns)	2	1	0.5	0.42	0.33	0.25	0.21
BW(MHz)	25	25	25	25	25	25	25
fp(MHz)	25	25	25	25	25	25	25
fs(MHz)	25	25	25	25	25	25	25
L	19	39	75	95	115	155	191
M	19	39	75	95	115	155	191

6.4.2 Variation of minimum Number of Channels required with respect to SNR

In [9], one of the necessary condition stated for exact recovery is that the number of channels should be greater than or equal to twice the number of bands in the multiband input. The purpose of the investigation presented in this section is to identify the variation of minimum number of channels required for successful support recovery when white Gaussian noise is added to the system. The bar diagram given in Figure 6.1 shows the trend in variation of the minimum number of channels required for hundred percentage successful recovery with respect to the signal to noise ratio. As can be inferred from Table 6.4 when the f_{nyq} is fixed at 1 GHz, the minimum number of channels required for full recovery shows a decreasing trend when the SNR is varied from 10dB to a Noise Free condition through an intermediate value of 25dB. For f_{nyq} of 2 GHz, 3 GHz and 4 GHz the same trend can be observed even though the minimum number of channels required for full recovery is less compared to the immediate higher f_{nyq} considered. This trend can be easily understood and is expected based on the fact that it is easier to reach successful recovery when the noise is less.

Table 6.4: Minimum Number of Channels for 100% Support Recovery when N=2

SNR(dB)	1 GHz	2 GHz	3 GHz	4 GHz
10	11	14	16	17
25	9	12	14	15
Noise Free	8	10	12	13

Figure 6.2 shows the variation of the minimum number of channels required for full recovery when N = 4 with respect to SNR for four different f_{nyq} of 1 GHz, 2 GHz, 3 GHz and 4 GHz. Here also a decreasing trend that can be observed in the minimum number of channels for full support recovery. When N is increased from 2 to 4 it can be observed that the minimum number of channels required for full support recovery has increased and can also be seen in Table 6.4 and Table 6.5.

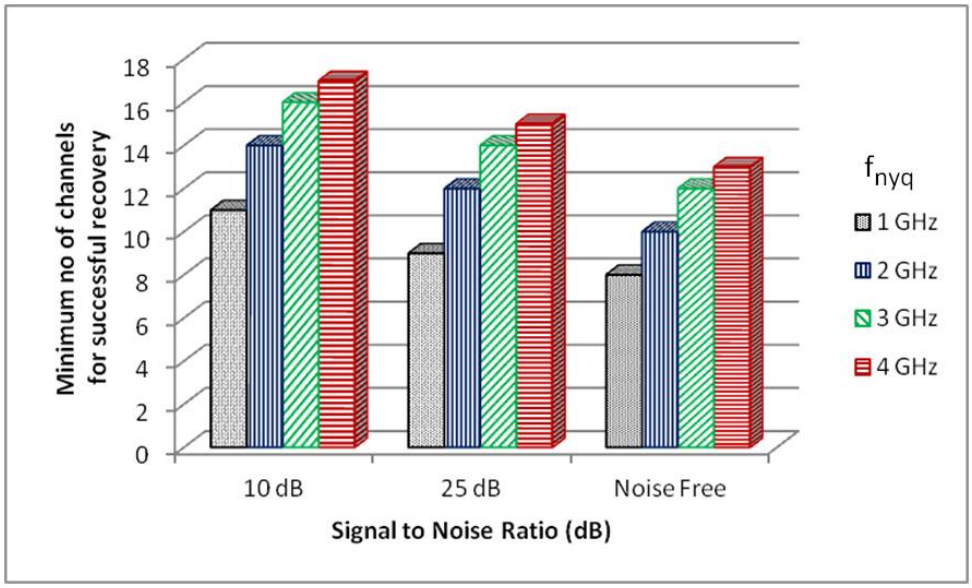

Figure 6.1: Minimum Number of Channels for Fully Successful Recovery Vs SNR for N = 2

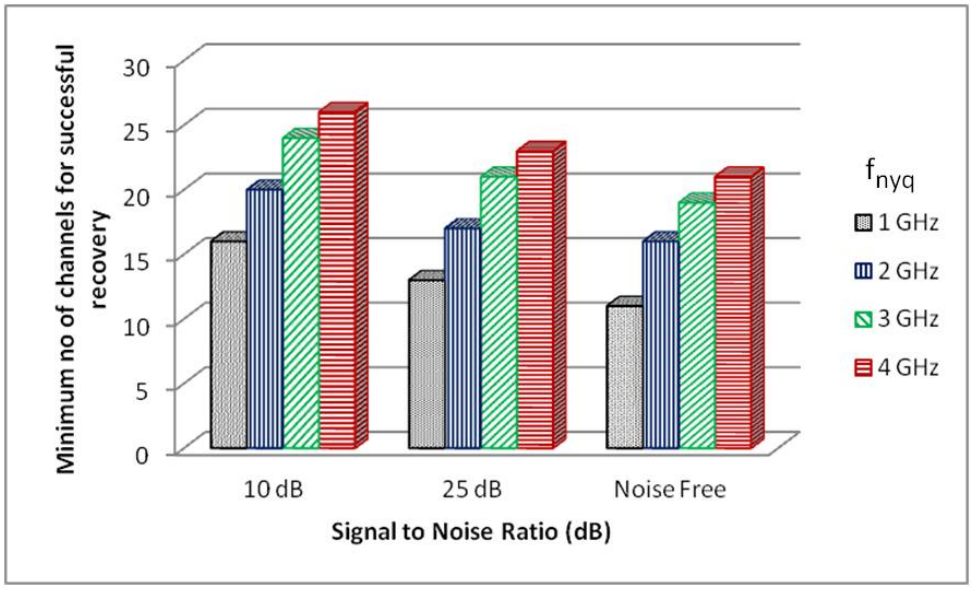

Figure 6.2: Minimum Number of Channels for Fully Successful Recovery Vs. SNR for N = 4

Table 6.5: Minimum Number of Channels for 100% Support Recovery when N=4

SNR(dB)	1 GHz	2 GHz	3 GHz	4 GHz
10	16	20	24	26
25	13	17	21	23
Noise Free	11	16	19	21

From [9], the number of channels required for stable recovery can be calculated using Equation 6.1

$$m \approx 4N \log(M/2N) \tag{6.1}$$

where N is the number of bands and M is the number of ± 1 intervals in each period of p_{ij}. Based on the results, we can conclude that for noise free condition, the number of channels obtained for successful recovery in our simulation model is almost equal to that calculated using Equation 6.1. Also the results shows that the number of channels required when SNR is 10dB and 25dB is slightly above that of noise free condition.

6.4.3 Variation of minimum Number of Channels required with respect to Nyquist Frequency

The purpose of the investigation presented in this section is to determine the trend followed by the minimum number of channels required for 100% successful recovery when the Nyquist frequency is varied. Figure 6.3 shows a plot of the varying minimum number of channels required for full support recovery with respect to the Nyquist frequency for SNR values of 10dB, 25dB and noise free condition for N = 2. For a fixed SNR value, the minimum number of channels required for full support recovery increases with respect to the Nyquist frequency. This increasing tendency can be observed for the other two SNR values also.

The plot shown in Figure 6.4 represents the variation of minimum number of channels required for full support recovery with respect to Nyquist frequency in the case of N

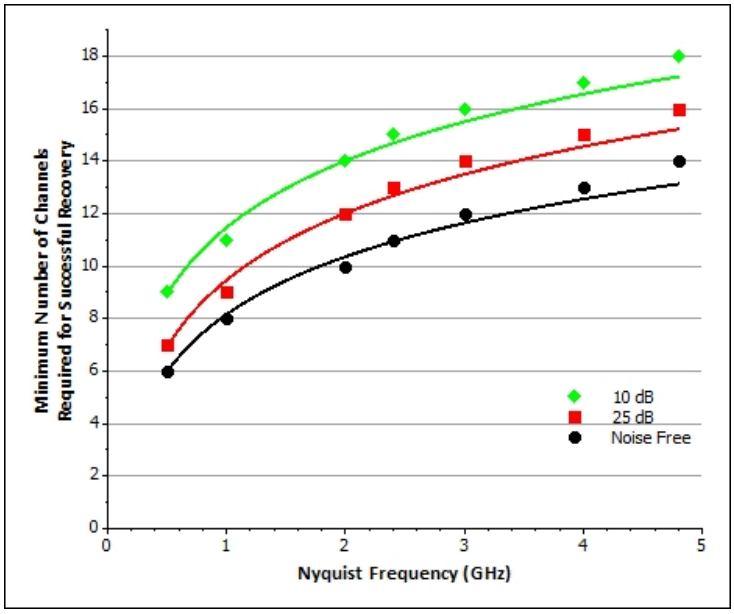

Figure 6.3: Minimum Number of Channels for Full Successful Recovery Vs. Nyquist Frequency for N = 2

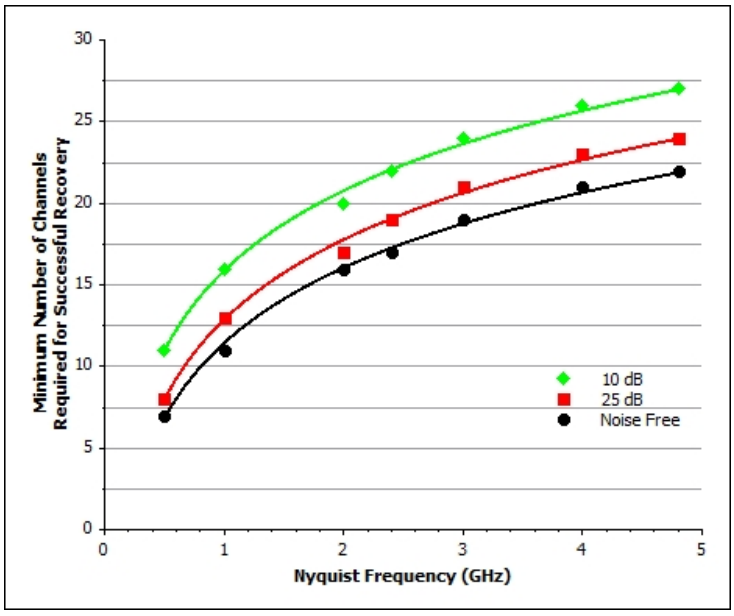

Figure 6.4: Minimum Number of Channels for Full Successful Recovery Vs. Nyquist Frequency for N = 4

= 4. The plot for N = 2 and N = 4 are showing similar variations of minimum number of channels required for full support recovery. The solid line in each of the cases in the graphs are drawn using logarithmic function and the scatter points are those obtained from simulation. Therefore, from the study we can say that the minimum number of channels required followed different logarithmic trends in different noise conditions. Since Equation 6.1 consists of a logarithmic function, we can conclude that the simulation model could successfully identify the logarithmic trend for the minimum number of channels required for full support recovery when Nyquist frequency is varied from 500 MHz to 4.8 GHz for N = 2 and 4.

6.4.4 Percentage Variation of Successful Recovery with Number of Channels

In this section the percentage of successfully recovered support is plotted with respect to the increasing number of channels while considering either the Nyquist frequency or the SNR remaining constant at a time. The study has been conducted for N = 2 and N = 4 by varying the SNR while keeping f_{nyq} constant or by varying f_{nyq} while keeping SNR constant.

Percentage of Recovered Success when SNR is constant

In this section the percentage of successfully recovered support is plotted with respect to the increasing number of channels while the SNR is constant. This is done for three different values of f_{nyq} when the SNR is kept constant for N = 2 and N = 4.

Figure 6.5 shows the variation in percentage of recovered support with respect to increasing number of channels for three different f_{nyq}s of 1, 2 and 2.4 GHz respectively in noise free condition when N = 4. Initially the percentage recovery remains zero up to a certain number of channels and then the percentage increases gradually to full support recovery. As shown in Table 6.6, for f_{nyq} of 1 GHz, successful support recovery is 0%

up to 3 channels and then gradually increases to 100% when the number of channels reaches 11. For f_{nyq} of 2 and 2.4 GHz the success of recovering support remains zero up to 5 channels and then reaches 100 when the number of channels is equal to 16 and 17 respectively.

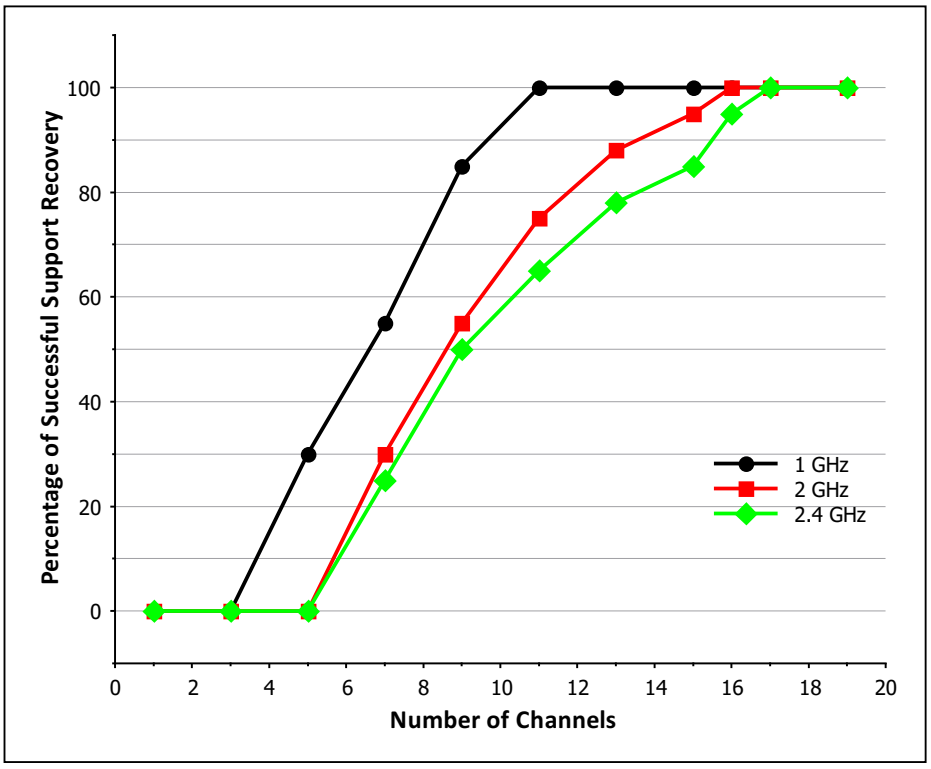

Figure 6.5: Successful Support Recovery Vs. Number of Channels for N=4, NoiseFree

Table 6.6: Percentage of Successful Support Recovery at Noise Free for N=4

No. of Channels	1 GHz	2 GHz	2.4 GHz
1	0	0	0
3	0	0	0
5	30	0	0
7	55	30	25
9	85	55	50
11	100	75	65
13	100	88	78
15	100	95	85
16	100	100	95
17	100	100	100
19	100	100	100

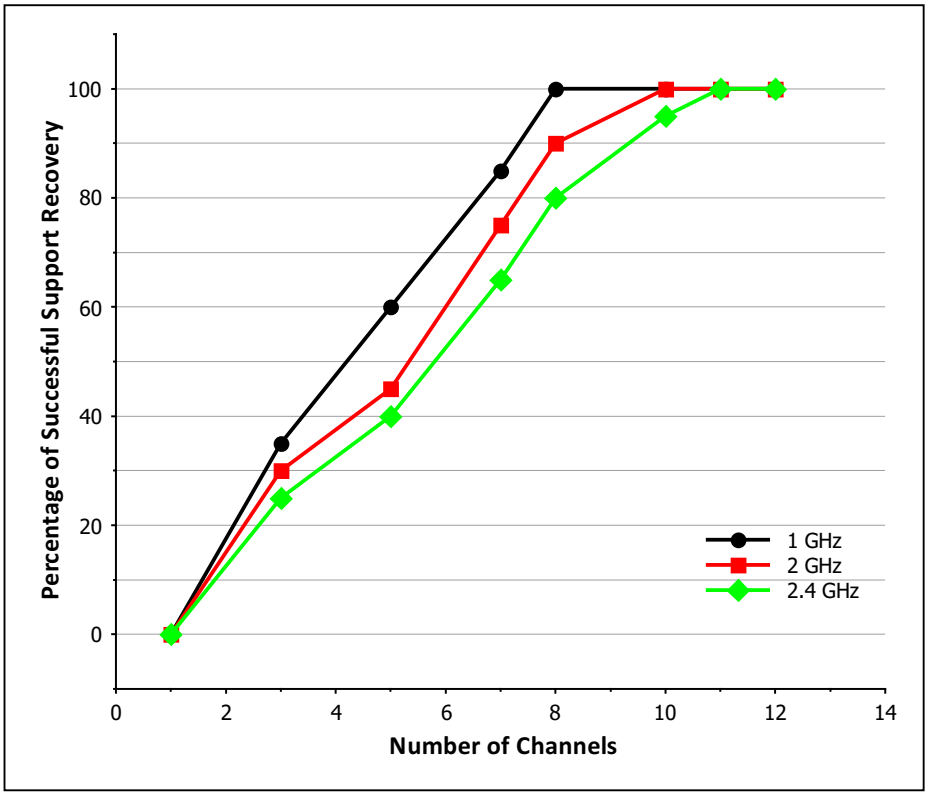

Figure 6.6: Successful Support Recovery Vs. Number of Channels for N=2, Noise Free

Figure 6.6 shows the percentage variation in successful recovery with respect to number of channels in the case of noise free condition when N = 2. In this case, for all the three values of f_{nyq} the percentage support is nil when there is only one channel and increases to 100% when the number of channels increases to 8 for f_{nyq} of 1 GHz, when number of channels are 10 for f_{nyq} of 2 GHz and when number of channels is 11 for f_{nyq} of 2.4 GHz as can be observed from Table 6.7.

Table 6.7: Percentage of Successful Support Recovery at Noise Free for N=2

No. of Channels	1 GHz	2 GHz	2.4 GHz
1	0	0	0
3	35	30	25
5	60	45	40
7	85	75	65
8	100	90	80
10	100	100	95
11	100	100	100
12	100	100	100

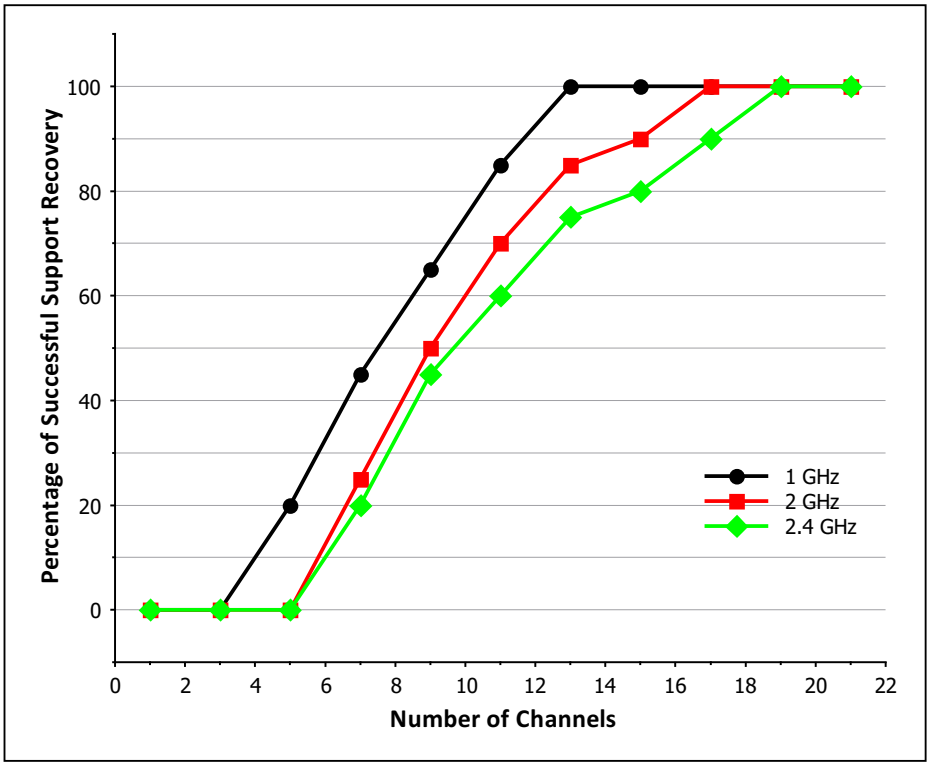

Figure 6.7: Successful Support Recovery Vs. Number of Channels for N=4, SNR=25dB

Figure 6.7 shows the variation of percentage support recovered with respect to number of channels for three different values 1, 2 and 2.4 GHz for f_{nyq} when the signal to noise ratio is 25dB for N = 4. As shown in Table 6.8, for f_{nyq} of 1 GHz, successful support recovery is 0% up to 3 channels and then gradually increases to 100% when the number of channels reaches 13. For f_{nyq} of 2 and 2.4 GHz the success of recovering support

Table 6.8: Percentage of Successful Support Recovery at SNR=25dB for N=4

No. of Channels	1 GHz	2 GHz	2.4 GHz
1	0	0	0
3	0	0	0
5	20	0	0
7	45	25	20
9	65	50	45
11	85	70	60
13	100	85	75
15	100	90	80
17	100	100	90
19	100	100	100
21	100	100	100

remains zero up to 5 channels and then reaches 100 for when the number of channels is equal to 17 and 19 respectively.

Figure 6.8 shows the plot between percentage of successful support recovery and the number of channels for three different values of f_{nyq} when the signal to noise ratio is 25dB for N = 2. Here the percentage recovery increases from zero when the number of channels is 1 and reaches 100% when the number of channels reaches 9 for f_{nyq} of 1 GHz, 12 for f_{nyq} of 2 GHz and 13 for f_{nyq} of 2.4 GHz respectively. The corresponding values of full support can be referred from Table 6.9. It can be seen that the growth of percentage from zero to hundred follows three different paths for the three values of f_{nyq}s. The curve corresponding to f_{nyq} of 1 GHz reaches 100% for a lesser number of channels than for f_{nyq} of 2 GHz and a similar behaviour is observed in the case of f_{nyq}s of 2 and 2.4 GHz also.

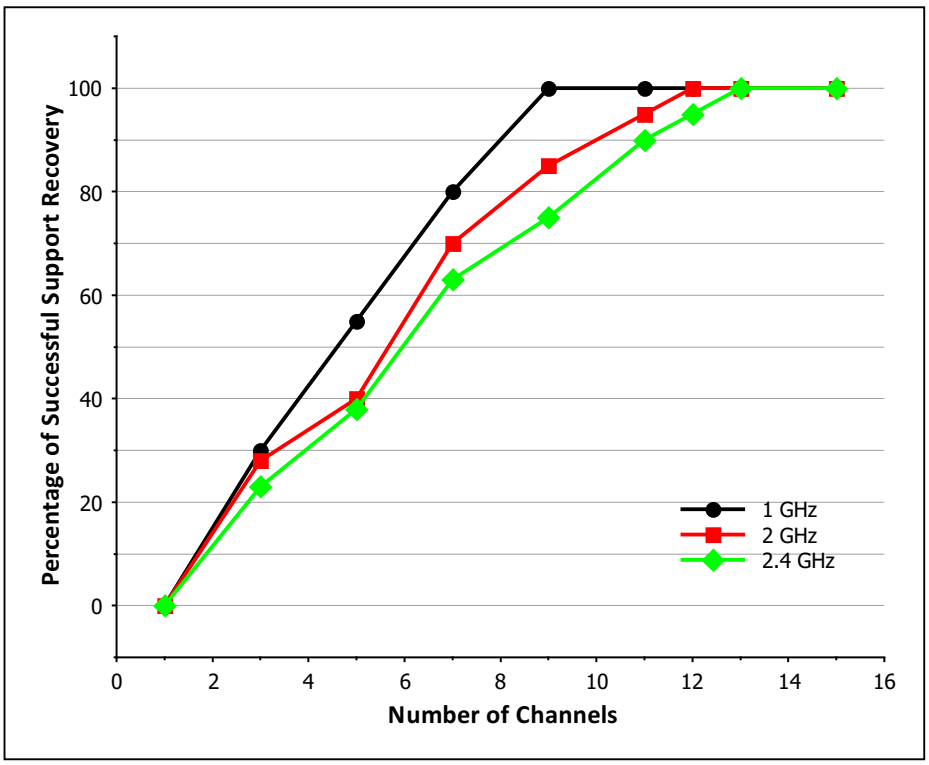

Figure 6.8: Successful Support Recovery Vs. Number of Channels for N=2, SNR=25dB

Figure 6.9 shows the variation of successful support recovery in percentage with respect to increasing number of channels for a signal to noise ratio of 10dB when N = 4.

Table 6.9: Percentage of Successful Support Recovery at SNR=25dB for N=2

No. of Channels	1 GHz	2 GHz	2.4 GHz
1	0	0	0
3	30	28	23
5	55	40	38
7	80	70	63
9	100	85	75
11	100	95	90
12	100	100	95
13	100	100	100
15	100	100	100

The recovered support is seen to be nil for 3 channels when f_{nyq} is 1 GHz, for 5 channels when f_{nyq}s are 2 GHz and 2.4 GHz. The recovery of support reaches 100% when there are 16 number of channels for f_{nyq} of 1 GHz, 18 number of channels for f_{nyq} of 2 GHz and 20 number of channels for f_{nyq} of 2.4 GHz. This can be observed from the results given in Table 6.10.

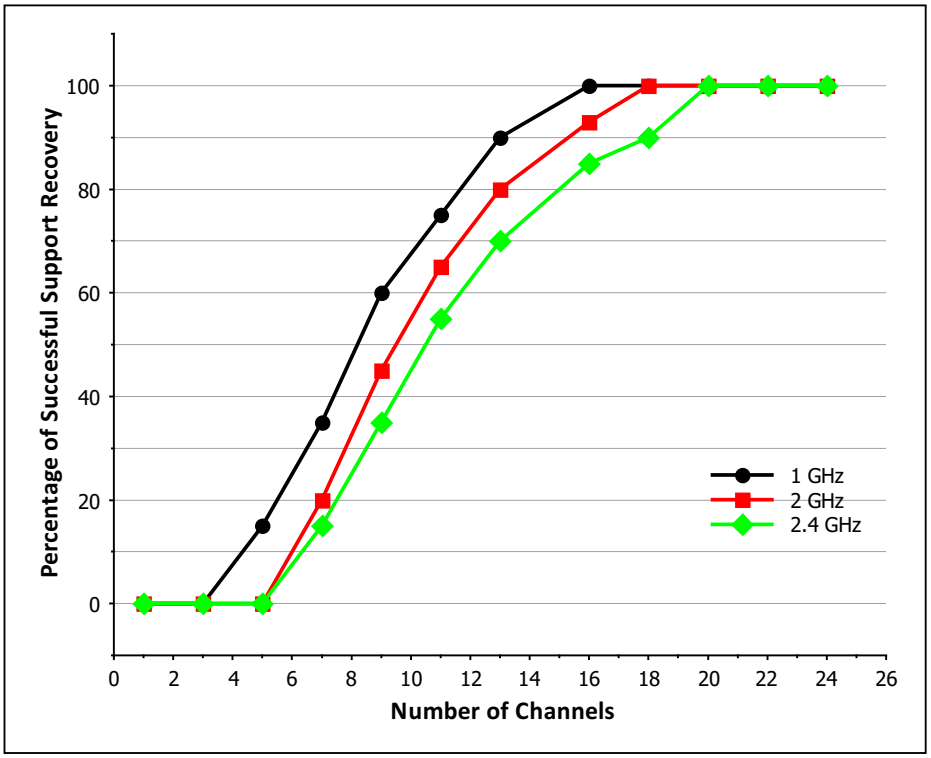

Figure 6.9: Successful Support Recovery Vs. Number of Channels for N=4, SNR=10dB

Table 6.10: Percentage of Successful Support Recovery at SNR=10dB for N=4

No. of Channels	1 GHz	2 GHz	2.4 GHz
1	0	0	0
3	0	0	0
5	15	0	0
7	35	20	15
9	60	45	35
11	75	65	55
13	90	80	70
16	100	93	85
18	100	100	90
20	100	100	100
22	100	100	100
24	100	100	100

Figure 6.10 represents the plot between the percentage of successfully recovered support and the number of channels for three different values of f_{nyq} when SNR is 10dB for N = 2. The curve corresponding to f_{nyq} of 1 GHz is showing zero percentage recovered support for 1 channel and it increases with increase in number of channels to reach the maximum of 100% for 11 number of channels. Corresponding to the value of 2 GHz for f_{nyq} the curve starts at 3 channels showing a zero percentage recovered support and grows to 100% when the number of channels reach 14. In case of 2.4 GHz for f_{nyq}, the curve starts at 3 channels itself with a nil percentage and reaches 100 for 15 number of channels. From the graph we can see an increasing trend in minimum number of channels required for full support recovery. The values plotted in this figure can be referred from Table 6.11.

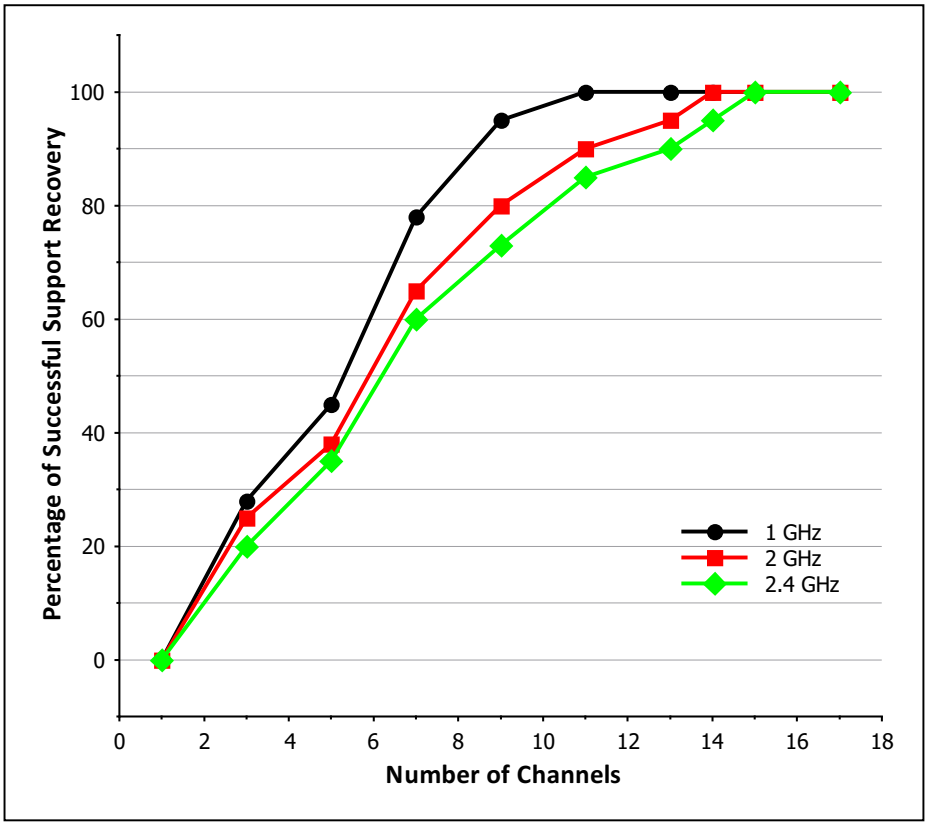

Figure 6.10: Successful Support Recovery Vs. Number of Channels for N=2, SNR=10dB

Table 6.11: Percentage of Successful Support Recovery at SNR=10dB for N=2

No. of Channels	1 GHz	2 GHz	2.4 GHz
1	0	0	0
3	28	25	20
5	45	38	35
7	78	65	60
9	95	80	73
11	100	90	85
13	100	95	90
14	100	100	95
15	100	100	100
17	100	100	100

From the investigation given in this subsection it could be concluded that successful support recovery depends on the number of channels and satisfies the necessary condition given in section 6.5. The percentage of success increases from 0 to 100 when the number of channels is increased for different values of SNR.

Percentage of Recovered Success when f_{nyq} is constant

The purpose of the study conducted in this section is to plot the variation of successful support recovery with respect to increasing number of channels. This is done by varying SNR values keeping f_{nyq} constant.

Figure 6.11 shows the percentage variation of successfully recovered support with increasing number of channels when SNR is varied through 10dB, 25dB and noise free for an f_{nyq} of 1GHz when N = 2. For 3 channels and noise free condition successfully recovered support is observed to be 35%, for an SNR value of 25dB the percentage of support is seen to be 30% and for SNR of 10dB percentage support is seen to be 28%. 11 number of channels corresponds to 100% recovered support for an SNR of 10dB and 9 number of channels corresponds to 100% recovered support for an SNR of 25dB. In noise free condition 100% recovery is obtained at an earlier stage when there are 8 number of channels. From this we can see as the noise in the system decreases, success in support recovery is achieved faster.

In Figure 6.12, the graph is generated by keeping f_{nyq} at 2 GHz for N = 2 and by varying the SNR value for three different cases. The plot represents the variation of successfully recovered support with respect to number of channels in ascending order. It can be observed that the percentage support is 25% for SNR = 10dB when there are only 3 channels while it is 28% for SNR = 25dB and 30% for noise free condition. The percentage of recovered support reaches 100% when there are 10 channels for noise free condition and 12 number of channels for an SNR of 25dB. When the number of channels is increased to 14, it can be seen that the support is recovered fully in all the selected cases of SNR values. For the same number of channels, the noise free condition has the higher probability of achieving higher percentage of recovered support when compared to the other cases under consideration.

In Figure 6.13 f_{nyq} is kept at a constant value of 2.4 GHz for N =2 in view of studying the variation in percentage of recovered support with respect to increasing number of channels for three different cases of SNR values. The percentage recovery for all the

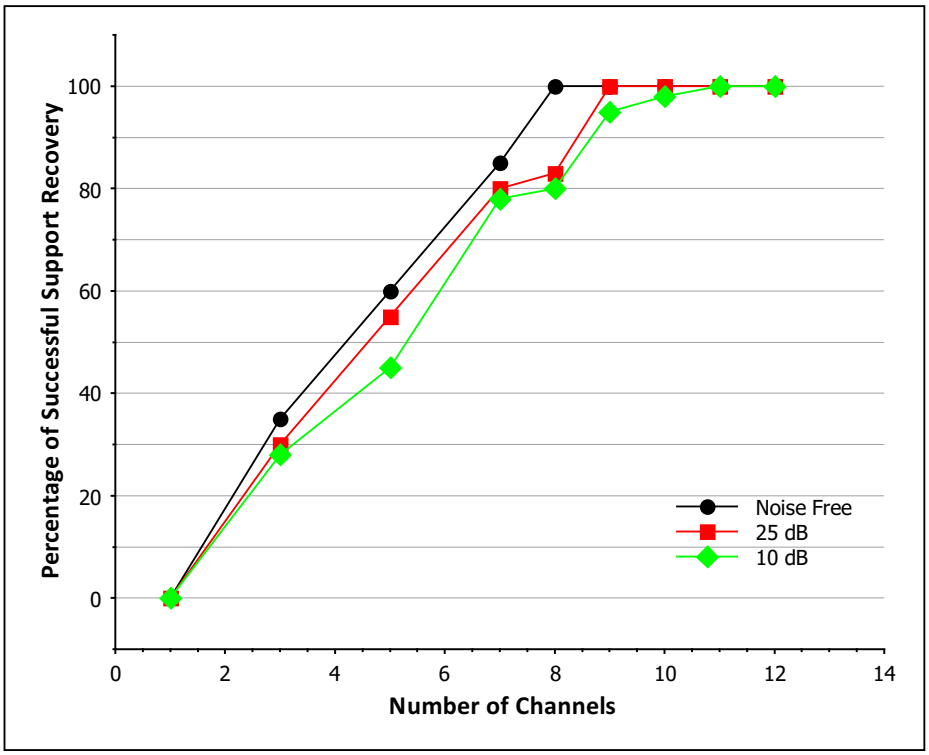

Figure 6.11: Successful Support Recovery Vs. Number of Channels for N=2, $f_{nyq} = 1GHz$

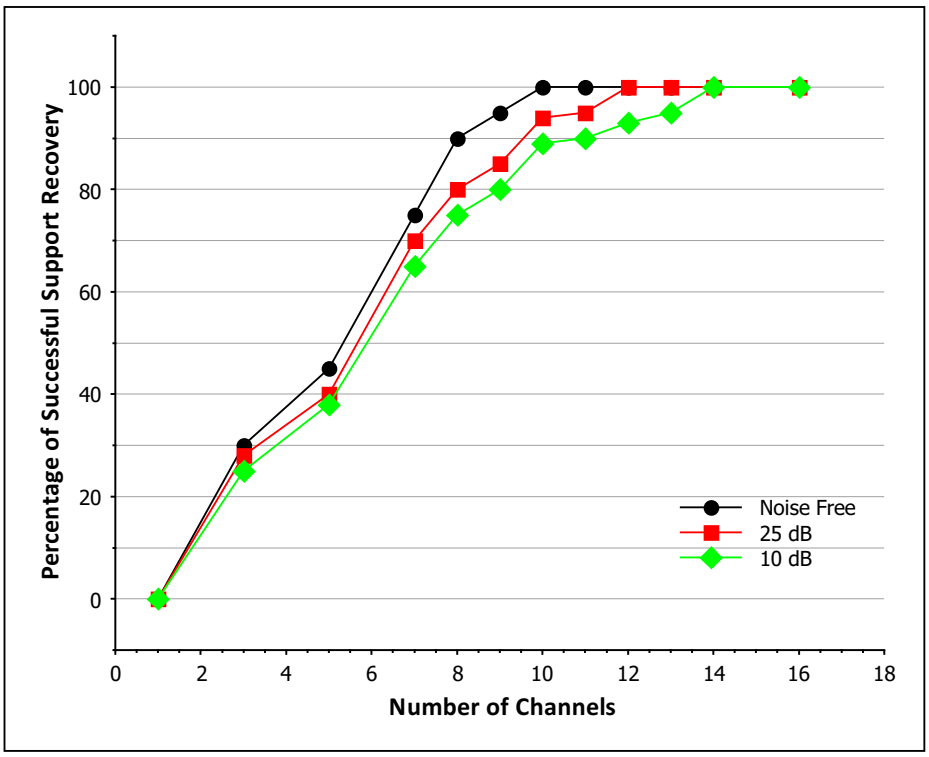

Figure 6.12: Successful Support Recovery Vs. Number of Channels for N=2, $f_{nyq} = 2GHz$

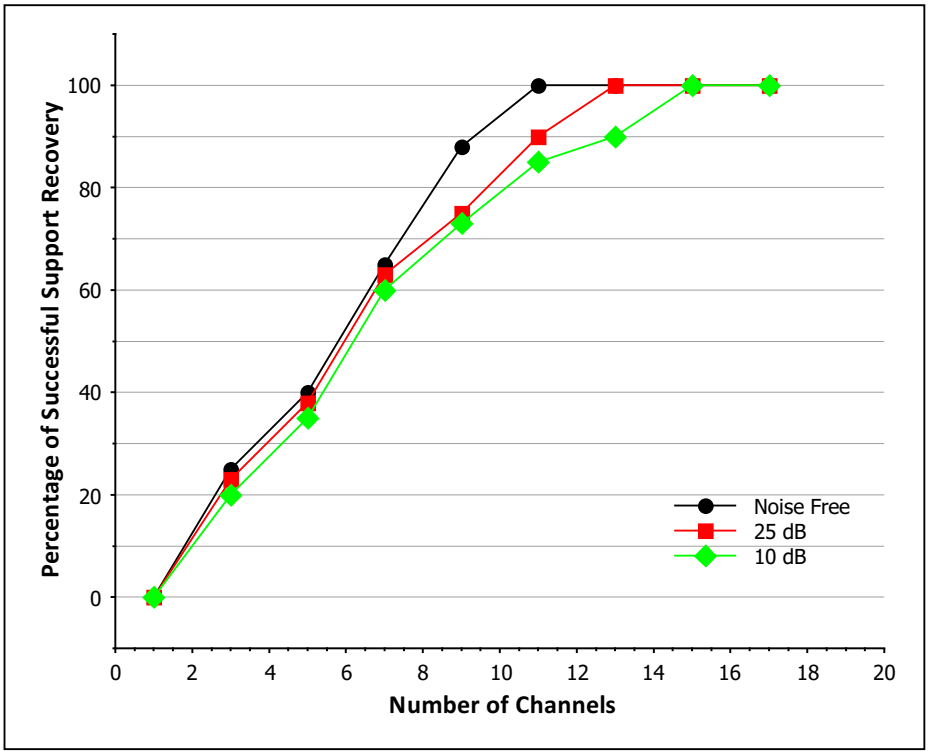

Figure 6.13: Successful Support Recovery Vs. Number of Channels for N=2, $f_{nyq} = 2.4GHz$

three cases of SNR values is seen to be zero when there is only 1 channel and it gradually increases with increase in number of channels. When the number of channels is 11, all the support is recovered for noise free condition while in case of SNR = 25dB, 100% recovery is obtained when the number of channels is 13 . From 15 number of channels onwards all the selected SNR cases are seen to be reporting 100% recovered support.

Figure 6.14 represents the graph with a constant f_{nyq} of 1 GHz when N = 4. It can be seen here that for 5 number of channels, the reported percentage of recovered support for noise free condition is 30% while SNR of 25dB and 10dB reports 20% and 15% respectively. The noise free condition reports 100% recovered support for 11 number of channels and for 13 number of channels in the case of SNR of 25dB. From 16 channels onwards all the selected cases are reporting 100% recovered support.

In the graph shown in Figure 6.15, f_{nyq} is kept at 2 GHz for N = 4. It can be seen here that the reported percentage of recovered support is nil up to 5 channels and it increases to 30% and 25% for 7 channels for noise free condition and 25dB respectively.

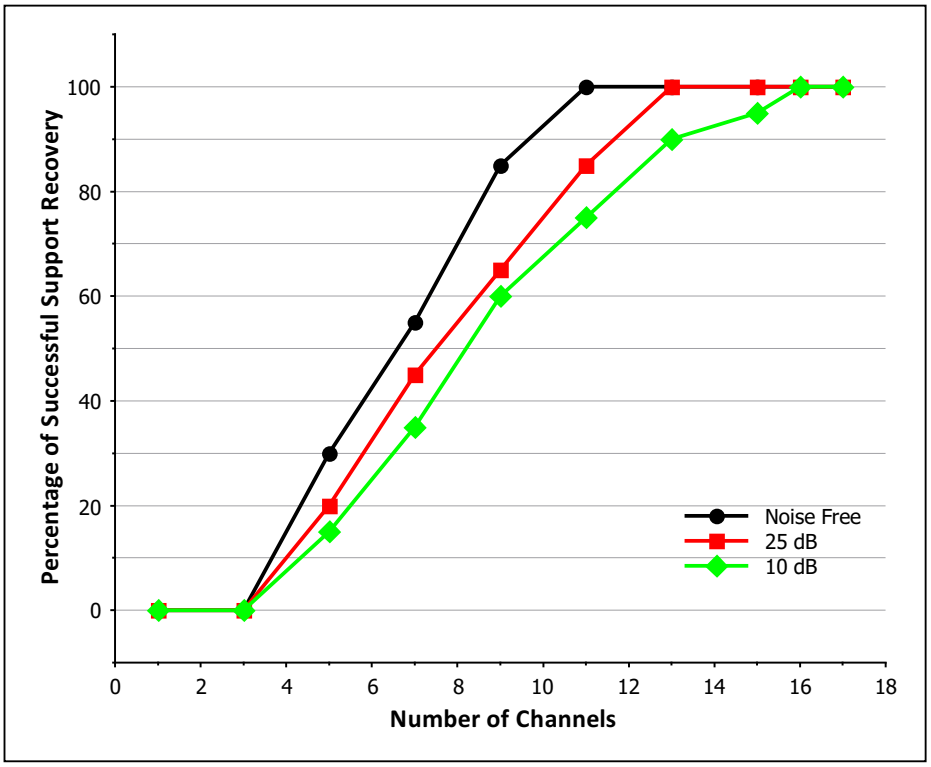

Figure 6.14: Successful Support Recovery Vs. Number of Channels for N=4, $f_{nyq} = 1GHz$

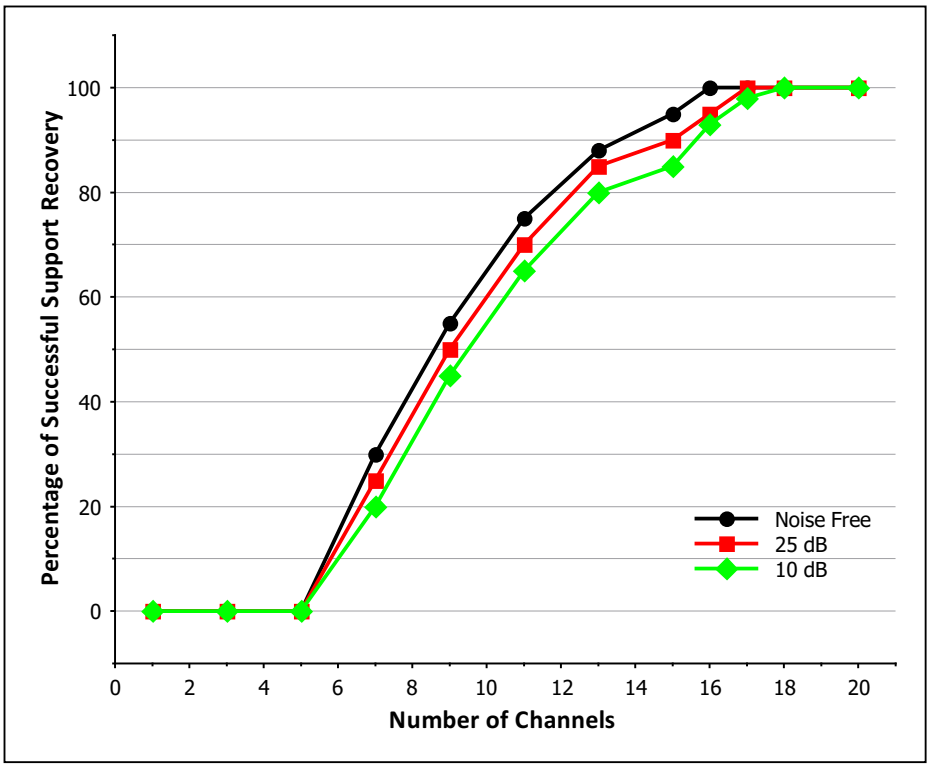

Figure 6.15: Successful Support Recovery Vs. Number of Channels for N=4, $f_{nyq} = 2GHz$

The noise free condition reaches 100% recovered support for 16 channels and for the case of SNR = 25dB 17 channels are required. From 18 channels onwards all the selected cases are reporting 100% recovered support.

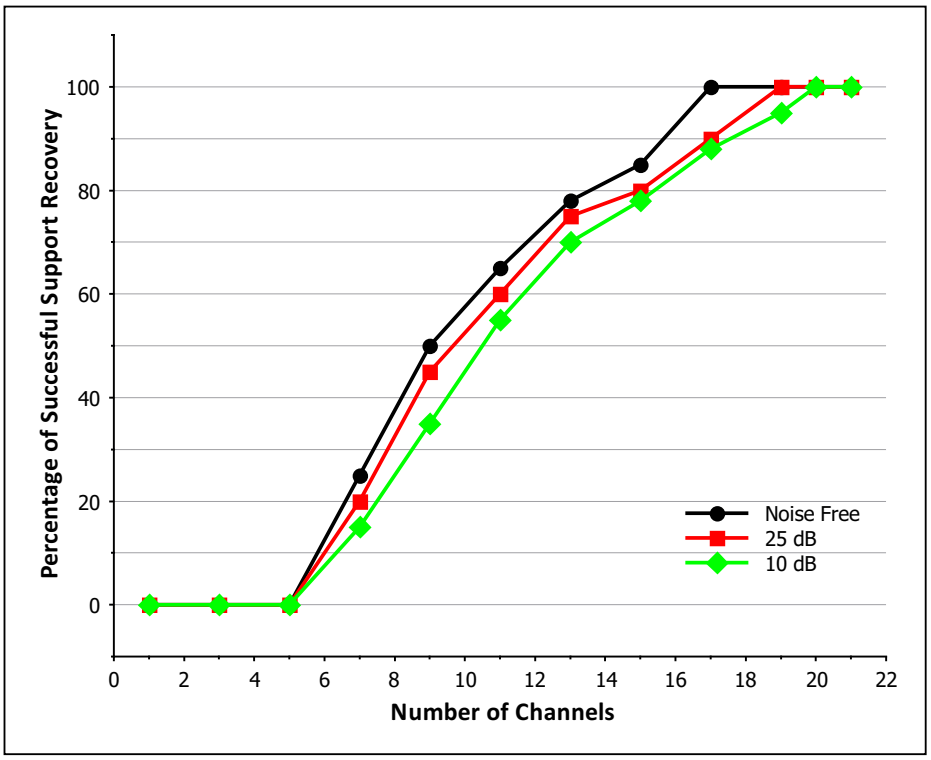

Figure 6.16: Successful Support Recovery Vs. Number of Channels for N=4, $f_{nyq} = 2.4GHz$

The graph shown in Figure 6.16 gives the variation of percentage recovery of support with respect to the increasing number of channels when SNR is varied between 10dB to noise free condition through 25dB for a constant f_{nyq} of 2.4 GHz when N = 4. When there are 17 channels, support is fully recovered for noise free condition while it remains at 90% for SNR of 25dB. When there are 19 number of channels, SNR of 25dB reports 100% recovered support along with noise free condition. This remains the same as the number of channels increases while an increase in percentage of recovered support is reported for the case of SNR = 10dB until it reaches the same as that of the other two selected cases of 100% when there are 20 channels. From 20 onwards all the selected cases are reporting full recovery of support.

6.5 Verification of Successful Support Recovery

The purpose of this investigation presented in this subsection is to verify the results obtained from the ModelSim simulation of the mixed analog digital system by comparing the recovered support set with that of the corresponding original support. This study has been conducted for different Nyquist frequencies.

During the verification process the mixed analog digital system showed both successful and failed recovery of supports based on the selected parameter choices. However one of the necessary conditions for exact spectrum blind recovery as reported by [9] is that the number of channels should be greater than or equal to twice the number of bands. From Figures 6.11 to 6.16 it can be seen that when the number of channels increases beyond a certain limit the percentage of successful support recovery stabilises to be at 100%. So, for the verification of the obtained results it is enough to select sufficiently higher number of channels corresponding to 100% recovery. This will ensure that the failed recoveries will be negligibly rare to be considered.

In terms of the present simulation, as described in Section 6.3, a success is defined when the original support set can be observed to be a subset of the recovered support set while a failure is defined when the original support set is not seen to be a subset of the recovered support set. This definition gives the concepts of false positives and false negatives. When the recovered support set contains elements that are not present in the original support set, then the condition for success is satisfied and such elements are named as false positives. There are cases when the recovered support set contains two or four false positives for a successfully recovered support set. In case if the original support containing elements that are not present in the recovered support, the condition for success is not satisfied leading to a failure recovery and such elements are collectively known as false negatives.

Table 6.12 shows the elements in the successfully recovered support set and original support set for f_{nyq} of 1 GHz. The first row is corresponding to the case when there are no false positives ensuring that the elements in the recovered support set is exactly

the same as that in the original support set. Second row is corresponding to the case when there are two additional elements or false positives in the successfully recovered support set. Similarly the third row of the table shows the elements 4, 7, 31 and 34 in addition to the elements that are commonly present in the original and recovered support set. As far as CR is concerned, a primary user is given higher priority than a secondary user and it is necessary for a secondary user to find transmission holes without interrupting the primary user. It is therefore necessary to exactly identify the frequency supports of the primary users. This means that a false negative should be considered as a failure in support recovery. If there are false positives it can be ignored considering that it indicates non availability of transmission holes even if they are present as it does not interrupt the rights of the primary users.

Table 6.12: Verification of Successful Support Recovery for f_{nyq}=1 GHz

False Positives	Original Support	Recovered Support
0	[2,7,31,36]	[2,7,31,36]
2	[8,9,29,30]	[8,9,**15**,**23**,29,30]
4	[11,18,20,27]	[**4**,**7**,11,18,20,27,**31**,**34**]

Table 6.13 corresponds to the successfully recovered support set and the original support set in the case when f_{nyq} is 2GHz. It can be observed here that the sets corresponding to the recovered support and original support are exactly the same for the first row to ensure successful recovery with zero false positives. Recovered support set given in the second row contains two extra elements of 5 and 33 to make it a case of two false positives. Third row is corresponding to the case of successful support recovery with four false positives.

Table 6.13: Verification of Successful Support Recovery for f_{nyq}=2 GHz

False Positives	Original Support	Recovered Support
0	[4,5,16,17,21,22,33,34]	[4,5,16,17,21,22,33,34]
2	[6,17,21,32]	[**5**,6,17,21,32,**33**]
4	[2,3,35,36]	[**1**,2,3,**11**,**27**,35,36,**37**]

The values shown in Table 6.14 represent the successful support recovery obtained for f_{nyq} of 2.4 GHz. First row represents successful recovery with zero false positives and

second row corresponds to that with two false positives. The additional elements 2, 7, 45 and 50 shown in the recovered support set given in the third row of the table corresponds to the four false positives obtained from the simulation.

Table 6.14: Verification of Successful Support Recovery for f_{nyq}=2.4 GHz

False Positives	Original Support	Recovered Support
0	[12,13,39,40]	[12,13,39,40]
2	[5,6,11,27,32,33]	[**1**,5,6,11,27,32,33,**37**]
4	[4,6,25,26,27,46,48]	[**2**,4,6,**7**,25,26,27,**45**,46,48,**50**]

It could be concluded from this investigation of the results that the execution of simulations could recover the supports successfully in all the cases of Nyquist frequencies. Thus the results could be verified for its correctness.

6.6 Validation of Successful Support Recovery

The purpose of this investigation is to validate the results obtained from the ModelSim simulation of mixed analog digital system by conducting a probability study of the occurrences of false positives when the support is successfully recovered. A total number of 2500 trials of simulations have been executed to investigate these occurrences. Results obtained from the probability study for the occurrence of false positives in the case when N = 4 is given in Figure 6.17. The pie diagram clearly indicates that out of the 2498 successful recoveries obtained, 87.4% of them generated a recovered support set exactly the same as that of the original support set. There were 11.4% of occurrences with two false positives and the occurrences of four false positives were only 1.2%. A study similar to this conducted by varying the Nyquist frequency by 1, 2 and 2.4 GHz yielded results with comparatively negligible differences from that which is shown in the above mentioned pie diagram.

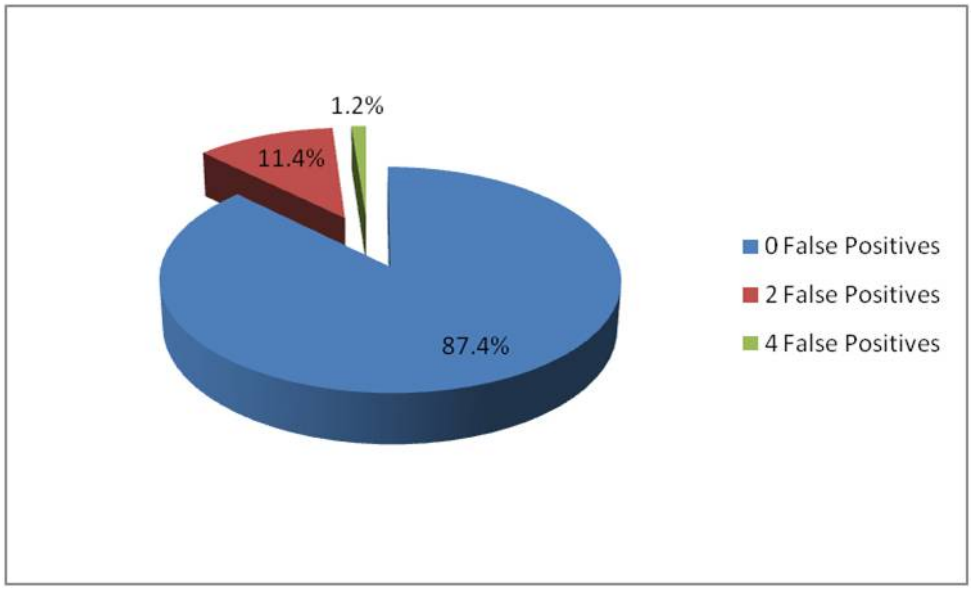

Figure 6.17: Probability for the occurrence of False Positives for N = 4

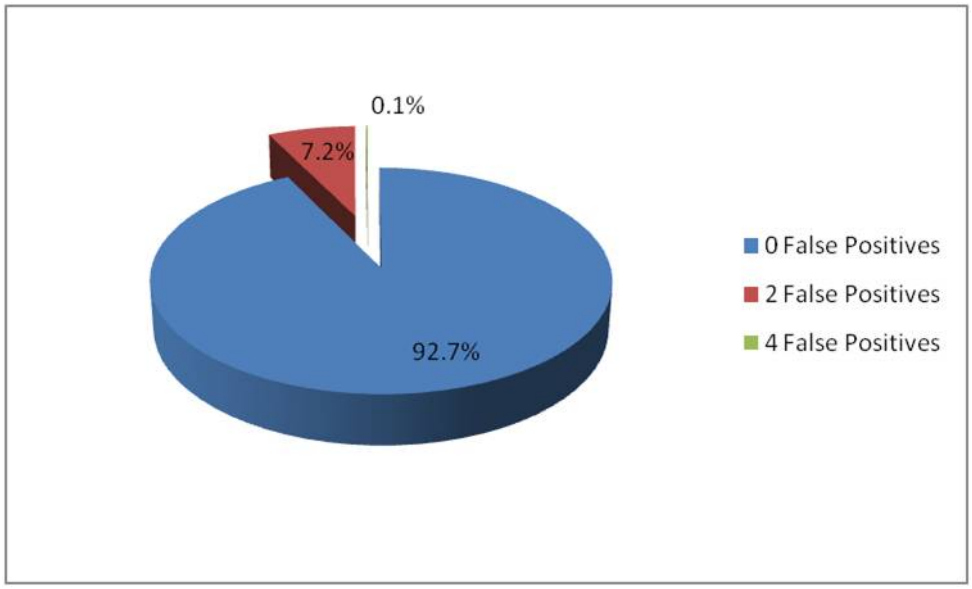

Figure 6.18: Probability for the occurrence of False Positives for N = 2

The pie diagram shown in Figure 6.18 represents the results of a similar probability study conducted for the occurrences of successful support recovery in case of 2500 trials when the value of N is equal to 2. Out of the 2499 successful recoveries reported here, 92.7% of them did not report any false positives. There were 7.2% of occurrences of 2 false positives while the percentage of occurrences of four false positives were

negligible. A change in the Nyquist rate did not yield a comparable difference in the percentage of occurrences of any of the selected number of false positives.

Thus it could be concluded that the simulation model generates successful results at very high rates and the model is thereby validated.

6.7 Summary

The former portions of this chapter deals with the numerical investigation process carried out in the simulation models of the mixed analog digital system. The purpose of this investigation was to verify that the developed model functions correctly for the given test parameter choices. Since the output of the mixed analog digital system contained all the elements of the original support set, it could be verified that the model is working for the test parameter choices. The mixed analog digital system discussed is non-deterministic in nature, a single execution of the simulation cannot verify the functioning of the model. So, statistically more number of executions have been carried out with the test parameter choices for verifying the system. In the later sections of the chapter, operational validation of mixed analog digital system has been carried out by studying the influence of signal to noise ratio and Nyquist frequency in the variation of minimum number of channels required for full support. The variation of percentage of successful support recovery has also been considered here for assessment.

Chapter 7

Conclusion

As a conclusion to this dissertation, this chapter summarises the work done by briefly discussing the problem under consideration and the steps taken to address the problem. It also discusses the contributions of this research and the possibilities of future work

---

7.1 Introduction

This chapter concludes this dissertation titled "Wideband spectrum sensing using sub-Nyquist sampling". In the first section of this chapter an overall summary of the research work has been presented. This is followed by a revisit to the problem statement and the issues to be addressed given in Chapter 1 before discussing the suggested solutions. Further to this, the contributions of this research work and recommendations for future work are discussed. Final sections of this chapter presents the conference contributions and achievements.

7.2 Summary of Work

In this research work, two separate simulation models from literature were selected and implemented in ModelSim. The first model detects the carrier frequencies using the Wideband Compressive Radio Receiver [8]. The second model recovers the support using a mixed analog digital system [9]. The following sections give a brief walk-through of this research that led to the development of the simulation models.

7.3 Problem Statement

The problem statement given in Chapter 1 is as given below:

The aim of this research is to develop a VHSIC hardware descriptive ModelSim simulation model for wideband spectrum sensing of multitoned and multiband signals using sub-Nyquist sampling.

7.4 Issues to be Addressed

The issues that were identified in Chapter 1 are listed below

- Identification of a sub Nyquist sampling system for sparse wideband analog signals;
- Development of a ModelSim simulation model for detection of carrier frequency of multitoned signals from sub-Nyquist samples;
- Blind determination of the support of the multiband signals from sub-Nyquist samples using ModelSim simulation.

7.5 Suggested Solutions

- In order to address the first issue, a literature review has been conducted in Chapter 2 and it was identified that the WCRR and MWC methods can be used to achieve sub Nyquist sampling for sparse wideband signals;
- In order to address the second issue, in Chapter 3 all the required algorithms were implemented for the ModelSim simulation of a WCRR for carrier detection in multitoned signals;
- To address the third issue, in Chapter 5 the ModelSim simulation of the mixed analog digital system was implemented.

7.5.1 WCRR model for Multitoned Signals

In the case of a multitoned signal model, the WCRR technology was used to detect the carrier frequency. First the conceptual design of the model had been carried out. The system was divided into different blocks such as generation of a multitoned signal, generation of a pseudo random chipping sequence, mixing the input signal with the pseudo random chipping sequence, integration of the signal, generation of the linear operator Φ, generation of the frequency set and finally the calculation of the correlation function for energy detection to detect the frequency corresponding to the maximum energy. This was followed by the design of suitable algorithms that could numerically simulate each block mentioned above.

7.5.2 MWC model for Multiband Signals

In the case of a multiband signal model, the MWC was used to recover the support successfully. The methodology behind the development of the simulation model was the same as that of the WCRR. The conceptual design of the model contained different blocks such as the generation of the input signal, calculation of original support,

pseudo random chipping sequence generator, mixing the signal with the chipping sequence, filtering the signal and down-sampling and finally the generation of the recovered support set for identifying the original support.

7.5.3 Testing the Models

Once the algorithms had been verified and made error free, the implementation phase of the algorithm started. In this phase, VHDL codes were developed for creating the computerised simulation model of each block in ModelSim. These codes were verified for any syntax errors and logical errors. For this purpose, a set of test parameter choices had been identified and the codes were numerically investigated by executing the codes using the test parameter choices. Thus when the test results matched with the specified requirements for successful carrier detection, correct functioning of the model could be assumed. Although the procedure was the same for both WCRR and MWC, the test parameter choices were in accordance with the requirements of the inputs of each model under consideration.

7.5.4 Execution of simulation

The simulation model was then executed with practically similar parametric choices and various results were generated.

In case of the WCRR, a parametric study was conducted for three different Nyquist frequencies of 1, 2 and 2.4 GHz to generate the required frequency correlation graphs for each case. For the MWC, studies were conducted with varying Nyquist frequencies to identify the minimum number of channels for which 100% successful recovery was reported in each case. Similarly, the effect of varying the signal to noise ratio was also investigated. These experiments were separately executed for 2 and 4 bands. Once the minimum number of channels required for obtaining 100% successful recovery was determined, all of these cases were executed for 2500 trials to investigate the change in

percentage of 100% successful support recovery.

Parametric studies conducted for the identification of carrier frequencies in the WCRR model generated successful results and the simulation model was verified for different carrier frequencies. The MWC simulation generated successful support recovery and identified the minimum number of channels required for achieving cent percentage successful support recovery for different Nyquist frequencies and SNR values.

7.5.5 Validation of Implementation

In order to validate the results obtained from the simulation of the WCRR model, the frequency value corresponding to the maximum measurement power was identified and compared with the known carrier frequency. This comparison made the decision of whether the detection was successful or not. This is repeated iteratively for 2500 times and the percentage of successful detection was recorded. A threshold value of 90% of successful detection was considered to be sufficient enough to validate the model since the simulation models can cause simulation errors. However the yielded results reported in subsection 4.6 was much higher confirming the validity of the results and that of the simulation model.

In case of the MWC, the repeated iterations of 2500 times with varying parametric choices of practical feasibility generated results of successful recovery that were very high compared to the minimum required threshold value of 90% . Also the logarithmic trend that was obtained for the variation of minimum number of channels required for successful recovery when the Nyquist frequency is varied agreed with the analytical results presented in literature. This has therefore successfully served the purpose of validating the simulation model of mixed analog digital system as discussed in subsection 6.6.

7.5.6 Summary of Results

- A conceptual design was identified and selected for the WCRR model and mixed analog digital system. Logically correct algorithms satisfying the requirements of each block in the conceptual design were implemented.
- VHDL codes were developed and presented for the ModelSim implementation of all the required algorithms.
- WCRR and MWC models are used for carrier detection of multitoned signals and the support recovery of multiband signals respectively. In case of WCRR, we have done parametric studies by varying the Nyquist frequency and decimation factor. While in MWC, parametric studies were conducted by varying Nyquist frequency, number of channels and SNR values. The results thus obtained from the simulations were verified for correctness and suitable statistical analyses were used to validate the model. Resultantly, WCRR detected the carriers and MWC recovered the support for more than 99.9% of the simulation runs. The 0.1% of error is expected to be caused due to the simulation errors caused by the system.

  In [47], it is given that the random demodulator and MWC have remarkably similar structures, but their signal model, sampling functions characterising the systems and reconstruction algorithms strongly differ. WCRR is implemented to sample and detect sparse multitone signals. The modulated wideband converter addresses the sampling of sparse multiband signals and are implemented as multi-channel system and then CTF determines the location of active bands. Both WCRR and MWC samples at sub-Nyquist rate and by some simple modifications can reliably determine inactive frequencies and bands respectively over a wide span of the spectrum thereby making the models useful for spectrum sensing.

7.6 Future Work

This research may be continued further in the following directions that may help in the cost reduction of present day technology used in wide band spectrum sensing and signal recovery. The following ideas may be used:

7.6.1 Extending the Parametric Study

The parametric study of WCRR simulation model conducted in this research by varying the decimation factor can be extended by studying the influence of varying signal strength and SNR values in carrier detection. In this research a parametric study has been conducted for the mixed analog digital system by executing the ModelSim simulation models for different Nyquist frequencies, number of channels and SNR values for two different numbers of bands. This study can be extended further by studying the influence of increasing the number of bands, varying the width of each band present in the multiband model and varying the signal strength.

7.6.2 FPGA Implementation of Simulations

The processes involved in the FPGA implementation of simulation models developed through this research work are as follows:

1. Development of the ModelSim model in VHDL
2. Functional Simulation of the model
3. Timing Simulation of the model
4. Design Synthesis and Implementation

Through this research, the first two of the above mentioned steps could be completed successfully. The third step involves the modification and execution of the model by

taking care of time delays. In the final step, gate patterns are defined according to the program logic and bit files are created for FPGA. Future research may be directed in view of completing the last two steps for FPGA implementation of the models.

7.6.3 Implementation in CR communication

The simulation models developed in this research work can successfully identify the frequencies at which SOIs are present. Thus the frequency positions that are not utilised in the spectrum can be identified. These transmission holes can be used by CR communication systems. Further research in this direction may be conducted for the implementation of these simulation models in CR systems.

7.7 Publications from this Research

Through this research, the following conference papers were published. A copy of these papers are attached in Appendix A

7.7.1 SATNAC 2011

Paper Title: *Practical Support Recovery using Sub-Nyquist Sampling* [48] (Work in Progress)
Status: Accepted and Presented, Paper published in conference proceedings online
Conference Name: Southern African Telecommunication Networks and Application Conference, East London Convention Centre, South Africa
Year: September 2011

7.7.2 ICICT 2012

Paper Title: *Spectrum Sensing Technique using Modulated Wideband Converter* [49]
Status: Accepted and Presented, Paper published in conference proceedings
Conference Name: International Conference on Information, Computing and Telecommunications, New Delhi, India
Year: April 2012

7.7.3 SATNAC 2012

Paper Title: *Multiband Support Recovery in 1.2 GHz Bandwidth using the Modulated Wideband Converter* [50]
Status: Accepted and Presented , Paper published in conference proceedings online
Conference Name: Southern African Telecommunication Networks and Application Conference, Fancourt, George, Western Cape, South Africa
Year: September 2012

7.8 Achievements

"*Young Investigator Award*" for the best research paper in ICICT 2012 by Inter Science Research Network.

7.9 Summary

The thesis was concluded in this chapter by giving a brief walk through of the major steps involved in the research work that dealt with the ModelSim implementation of the WCRR and the mixed analog digital system. Through this research work, by developing simulation models for spectrum sensing, one of the major steps in the FPGA

implementation of WCRR and mixed analog digital system could be completed. These models can play a vital role in the widespread deployment of CRs due to the efficient spectrum sensing techniques involved.

Bibliography

[1] M. Mishali and Y. Eldar, "Sub-nyquist sampling," *IEEE Signal Processing Magazine*, vol. 28(6), pp. 98–124, November 2011.

[2] E. Candes and M. Wakin, "An introduction to compressive sampling," *Signal Processing Magazine*, vol. 25, no. 2, pp. 21–30, 2008.

[3] Y. Mishali. M, Eldar, "Wideband spectrum sensing at sub-nyquist rates," *Signal Processing Magazine, IEEE*, vol. 4 : 28, pp. 102 – 135, July 2011.

[4] D. W. H. L. Dr. John M. Chapin, "The path to market success for dynamic spectrum access technology," *Accepted for publication in IEEE Communications Magazine*, May 2007.

[5] T. Yucek and H. Arslan, "A survey of spectrum sensing algorithms for cognitive radio applications," *Communications Surveys & Tutorials, IEEE*, vol. 11, no. 1, pp. 116–130, 2009.

[6] D. Ariananda, M. Lakshmanan, and H. Nikoo, "A survey on spectrum sensing techniques for cognitive radio," in *Cognitive Radio and Advanced Spectrum Management, CogART 2009. Second International Workshop on*, May 2009, pp. 74–79.

[7] C. Shannon, "Communication in the presence of noise," *Proceedings of the IRE*, vol. 37, no. 1, pp. 10–21, January 1949.

[8] M. Davenport, S. Schnelle, J. Slavinsky, R. Baraniuk, M. Wakin, and P. Boufounos, "A wideband compressive radio receiver," in *MILITARY COMMUNICATIONS CONFERENCE, MILCOM*, 2010, pp. 1193–1198.

[9] M. Mishali and Y. Eldar, "From theory to practice: Sub-nyquist sampling of sparse wideband analog signals," *IEEE Journal of Selected Topics in Signal Processing,*, vol. 4, no. 2, pp. 375–391, 2010.

[10] M. D. Michael Lexa and J. Thompson, "Sampling sparse multitone signals with a random demodulator," *University of Edinburgh Institute of Digital Communications Technical Report*, January 2011.

[11] M. Mishali and Y. Eldar, "Blind multiband signal reconstruction: Compressed sensing for analog signals," *IEEE Transactions on Signal Processing*, vol. 57, no. 3, pp. 993–1009, 2009.

[12] G. G. Vining, *Statistical methods for engineers*. Pacific Grove, CA. : Duxbury Press, 1998.

[13] G. S. Robert, "Verification and validation of simulation models," *Proceedings of the Winter Simulation Conference*, pp. 166–183, 2010.

[14] ——, "Verifying and validating simulation models," *Proceedings of the Winter Simulation Conference*, pp. 55–64, 1996.

[15] A. Jerri, "The shannon sampling theorem;its various extensions and applications: A tutorial review," *Proceedings of the IEEE*, vol. 65, no. 11, pp. 1565–1596, 1977.

[16] B. Le, T. Rondeau, J. Reed, and C. Bostian, "Analog-to-digital converters," *IEEE Signal Processing Magazine*, vol. 22, no. 6, pp. 69–77, November 2005.

[17] H. Miranda, "Receiver design," EE144/EE245, Stanford University, Stanford, CA., Tech. Rep., Tech. Rep., 2007.

[18] J. Crols and M. S. J. Steyaert, "Low-if topologies for high-performance analog front ends of fully integrated receivers," *IEEE Trans. Circuits Syst. II*, vol. 45, no. 3, pp. 269–282, March 1998.

[19] W. Kester, Ed., *Mixed-signal and DSP Design Techniques (Analog Devices)*. Newnes, 2003.

[20] N. L. W. Vaughan, R. G. Scott and D. Rod, "the theory of bandpass sampling,," *IEEE Trans. Signal Processing*, vol. 39, pp. 1973–1984, 1991.

[21] A. Kohlenberg, "Exact interpolation of band-limited functions," *J. Appl. Phys*, vol. 24, pp. 1432–1435, December 1953.

[22] Y. P. Li n and P. Vaidyanathan, "Periodically nonuniform sampling of bandpass signals," *IEEE Trans. Circuits Syst. II*, vol. 45, no. 3, pp. 340–351, March 1998.

[23] H. Landau, "Sampling, data transmission, and the nyquist rate," *Proceedings of the IEEE*, vol. 55, no. 10, pp. 1701–1706, October 1967.

[24] Y. M. Lu and M. N. Do, "A theory for sampling signals from a union of subspaces," *IEEE Trans. Signal Processing*, vol. 56, no. 6, pp. 2334–2345, June 2008.

[25] J. Haupt and R. Nowak, "Compressive sampling for signal detection," in *IEEE International Conference on Acoustics, Speech and Signal Processing, ICASSP*, vol. 3, 2007, pp. III–1509–III–1512.

[26] B. S. Kashin and V. N. Temlyakoc, "A remark on compressed sensing," *Mathematical Notes*, vol. 82, no. 6, pp. 748–755, November 2007.

[27] R. Gribonval and M. Nielsen, "Sparse representations in unions of bases," *IEEE Transactions on Information Theory,*, vol. 49, no. 12, pp. 3320–3325, 2003.

[28] D. Donoho and X. Huo, "Uncertainty principles and ideal atomic decomposition," *IEEE Transactions on Information Theory,*, vol. 47, no. 7, pp. 2845–2862, 2001.

[29] M. Elad and A. Bruckstein, "A generalized uncertainty principle and sparse representation in pairs of bases," *IEEE Transactions on Information Theory,*, vol. 48, no. 9, pp. 2558–2567, 2002.

[30] J. Tropp, "Greed is good: algorithmic results for sparse approximation," *IEEE Transactions on Information Theory,*, vol. 50, no. 10, pp. 2231–2242, 2004.

[31] D. Donoho, "Compressed sensing," *IEEE Transactions on Information Theory,*, vol. 52, no. 4, pp. 1289–1306, 2006.

[32] E. Candes and T. Tao, "Near-optimal signal recovery from random projections: Universal encoding strategies?" *IEEE Transactions on Information Theory,*, vol. 52, no. 12, pp. 5406–5425, 2006.

[33] ——, "Decoding by linear programming," *IEEE Transactions on Information Theory,*, vol. 51, no. 12, pp. 4203–4215, 2005.

[34] W. Y. E. T. Hale and Y. Zhang, "A fixed-point continuation method for l1-regularized minimization with applications to compressed sensing," *Rice University, CAAM Tech. Report*, vol. TR07-07, Jul 2007.

[35] D. L. D. S. S. Chen and M. A. Saunders, "Atomic decomposition by basis pursuit," *SIAM Journal on Scientific Computing*, vol. 20, no. 1, pp. 33–61, 1998.

[36] M. S. Asif and J. Romberg, "Streaming measurements in compressive sensing: L1 filtering," *Asilomar Conference on Signals, Systems and Computers*, October 2008.

[37] M. E. D. L. Donoho and V. N. Temlyakov, "Stable recovery of sparse over complete representations in the presence of noise," *IEEE Trans. Information Theory,*, vol. 52, pp. 6 – 18, 2006.

[38] R. G. B. P. Boufounos, "1-bit compressive sensing," *Proc. of Conference on Information Sciences and Systems*, Mar 2008.

[39] P. Boufounos and R. Baraniuk, "Reconstructing sparse signals from their zero crossings," in *IEEE International Conference on Acoustics, Speech and Signal Processing, ICASSP*, 2008, pp. 3361–3364.

[40] G. Rath and C. Guillemot, "Sparse approximation with an orthogonal complementary matching pursuit algorithm," in *IEEE International Conference on Acoustics, Speech and Signal Processing, ICASSP*, 2009, pp. 3325–3328.

[41] Modelsim tutorial, software version 6.5b. online. Mentor Graphics Corporation. 8005 S.W. Boeckman Road, Wilsonville, Oregon 97070-7777. [Online]. Available: http://cseweb.ucsd.edu/classes/sp10/cse141L/lab1/modelsim_tut.pdf

[42] J. Tropp, J. Laska, M. Duarte, J. Romberg, and R. Baraniuk, "Beyond nyquist: Efficient sampling of sparse bandlimited signals," *IEEE Transactions on Information Theory,*, vol. 56, no. 1, pp. 520–544, 2010.

[43] S. J. D. Wet and A. S. J. Helberg, "Carrier detection of fm signals using the wideband compressive radio receiver," *SATNAC*, 2011.

[44] A. C. . J. Johnson. (2010) Multitone generator. 2010 comp.dsp Conference. Danville Signal Processing. [Online]. Available: http://www.compdsp.com/presentations/Clark/Multitone_Generator.pdf

[45] M. Mishali, Y. Eldar, O. Dounaevsky, and E. Shoshan, "Xampling: Analog to digital at sub-nyquist rates," *IET Circuits, Devices & Systems,*, vol. 5, no. 1, pp. 8–20, 2011.

[46] M. Mishali and Y. Eldar, "Reduce and boost: Recovering arbitrary sets of jointly sparse vectors," *IEEE Trans. Signal Process.*, vol. 56, no. 10, pp. 4692–4702, Oct 2008.

[47] M. E. Lexa, M. A.; Davies and J. S. Thompson, "Reconciling compressive sampling systems for spectrally-sparse continuous-time signals," *IEEE Transactions on Signal Processing*, vol. 60, pp. 155–171, January 2011.

[48] S.Aziz and A.S.J.Helberg, "Practical support recovery using sub-nyquist sampling," in *SATNAC*, 2011.

[49] ——, "Spectrum sensing technique using modulated wideband converter," in *ICICT*, April 2012.

[50] ——, "Multiband support recovery in 1.2ghz bandwidth using the modulated wideband converter," in *SATNAC2012*, 2012.

Appendix A

Conference Contributions from Dissertation

Practical Support Recovery using Sub-Nyquist Sampling

S Aziz and A. S. J. Helberg
School of Electrical, Electronic and Computer Engineering
North-West University, Pothcefstroom Campus
Tel: +27 18 299 1961, Fax: +27 18 299 1977
Email: {23185600, albert.helberg}@nwu.ac.za

***Abstract*—This paper presents a work in progress on the support recovery in wideband analog signals. The paper discusses an approach towards the spectrum sensing and carrier recovery of the frequency bands for cognitive radio (CR) operation. The purpose of this research is to design a simulation model and FPGA implementation of a method that detects the unused frequency regions using sub-Nyquist sampling and blind support recovery in sparse wideband analog signals for use in CR.**

***Index Terms*—Spectrum sensing, cognitive radio, sub-Nyquist sampling.**

I. Introduction

In communication, "wideband" is a relative term used to describe a wide range of frequencies in a spectrum. Spectrum sensing refers to the task of identifying the frequency support of a given input signal. The frequency support consists of those spectrum intervals in which the signal power exceeds the noise floor. Traditional methods of spectrum sensing assumes that the input is sampled at the Nyquist rate that is obtained from the Shannon sampling theorem [1] which is equal to twice the maximum frequency present in the signal. In practice this needs to be even higher. A fully spectrum blind system is a system requiring neither the knowledge of carrier frequency or the sampling method for identifying the unknown spectral support.

Recently, there has been a growing interest in spectrum sensing for CR receivers [2], which aim at utilizing unused frequency regions on an opportunistic basis. Commercialisation of CR technology necessitates a spectrum sensing mechanism that reacts in real time to cognitive decisions. There are a number of spectrum sensing methods for CR given in [3] and [4]. The analog to digital conversion (ADC) technologies which support the high bandwidth (in the GHz range) of the spectrum used by radio communications are expensive. An approach that reduces the bandwidth requirement of the ADC is compressive sampling (CS). The goal of this research is to identify the frequency support in sparse wideband analog signals using sub-Nyquist sampling for use in CR.

II. Background

A. Compressive sampling

Compressive sampling or compressed sensing, a technique for sub-Nyquist sampling, refers to the problem of recovering signals by much fewer samples than suggested by the Nyquist rate [5]. To make this possible, CS relies on two principles: sparsity, which pertains to the signals of interest (SOI), and incoherence, which pertains to the sensing modality.

Sparsity is important in compressive sensing as it determines how efficient one can acquire signals non-adaptively. It expresses the idea that the "information rate" of a continuous time signal may be much smaller than suggested by its bandwidth. CS exploits the fact that many signals are sparse or compressible in the sense that they have concise representations when expressed in the proper basis Ψ [5]. Incoherence extends the duality between time and frequency and expresses the idea that objects having a sparse representation in Ψ must be spread out in the domain in which they are acquired. CS is mainly concerned with low coherence pairs. The sampling waveforms have an extremely dense representation in Ψ and hence incoherence is as important as sparsity [5].

CS starts with compressive measurements in a basis, Φ, different from the basis, Ψ, in which the signal is known to be sparse. These compressive measurements are small and contain all the useful information [6]. Therefore, recovery of the SOI involves solving an undetermined matrix equation since the number of measurements taken is smaller than the dimensionality (order) of the original signal. This undetermined system of linear equations can be solved if the original signal is limited to be sparse, and the sparsest solution of the CS problem given in [6] is as follows

$$\min_{v \in R^m} \|v\|_0 \text{ subject to } \Phi v = y, \tag{1}$$

where $\|v\|_0$ is the size of the support of v, Φ is the sampling matrices with rows $\phi_j \in R^m$ and y is the sampled vector. However, this minimization problem is NP-hard (non-deterministic polynomial-time hard). This problem of sparse representation can be solved using $l1$-norm minimization by converting it into a linear problem. The problem of $l1$-norm minimization as given in [5], [6] is

$$\min_{v \in R^m} \|v\|_1 \text{ subject to } \Phi v = y \tag{2}$$

where $\|v\|_1 = \sum_j |v_j|$. Technically it is proved that for many problems $l1$-norm minimization is equivalent and easier than (1) and also solving using the $l1$-norm minimization leads to unique solution of (1).

B. Wideband Compressive Radio Receiver

The Wideband Compressive Radio Receiver (WCRR) is a receiver that can efficiently acquire signals within a wide frequency bandwidth [7]. The WCRR uses the random demodulator architecture [8] for compressive sampling. Random demodulator consists of an analog mixer to modulate the input signal. The modulated output is then integrated over time windows, and digitized using a low-rate ADC.

The support detection in WCRR is done by correlating the random demodulator output against a series of vectors. These vectors are obtained by feeding the random demodulator with unmixed sinusoidal waves. The correlation output gives a vector having an approximated power in the measurements at a sequence of frequencies. The demerit of WCRR is that the support recovery scheme used is very simple and not optimal [7].

III. Our Approach

In carrying out this research, CS techniques will be used during sampling and a digital algorithm will be used for identifying the support of the narrowband FM signals. The digital algorithm helps to have a simpler detection system than traditional recovery methods such as $l1$ minimization. As part of our research, the first phase that we have done is the simulation of WCRR using ModelSim. The WCRR uses a total bandwidth of 200MHz and an effective sampling rate of 4MHz whereas 400MHz is the actual Nyquist frequency of the assumed SOI. If we select the frequencies for correlating the sampled vector in the range which includes the carrier frequency used by the input signal, we could find out the support.

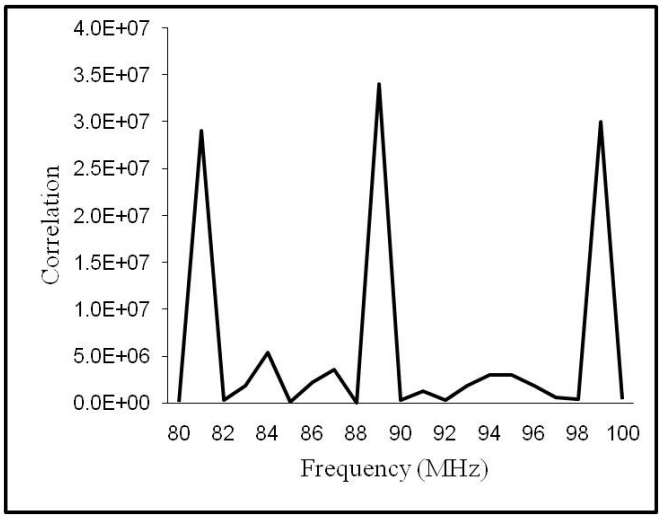

Fig. 1. Frequency Correlation Graph

The frequency correlation graph given in Fig.1 is obtained by selecting carrier frequencies 81MHz, 89MHz and 99MHz for the frequency range 80-100MHz. It illustrates that the selected carrier frequencies have the highest correlation. The noise introduced in the system is due to sampling effects.

IV. Conclusion And Future Work

It is expected that this research will help in sub-Nyquist sampling and support recovery in the CR environment. The accurate recovery of support also helps to reduce interference in CR environment. Future work includes the ModelSim simulation of mixed analog-digital spectrum sensing method [9], [10]. It uses the Modulated Wideband Converter (MWC) for CS and Continuous To Finite (CTF) block for support recovery that is especially suited to the typical wideband setting of CRs.The simulation is followed by the FPGA implementation of the overall system. The advantages of this system with respect to current architectures are threefold. First, the analog front-end is fixed. Second, both the ADC and the Digital Signal Processing (DSP) rates are substantially below Nyquist. Finally, the sensing resources are shared with the reception path of the CR, so that the low rate streaming samples can be used for communication purposes of the device, besides the sensing functionality they provide.

References

[1] C. Shannon, "Communication in the presence of noise," *Proceedings of the IRE DOI - 10.1109/JRPROC.1949.232969*, vol. 37, no. 1, pp. 10–21, 1949.

[2] I. Mitola, J., "Cognitive radio for flexible mobile multimedia communications," in *Mobile Multimedia Communications, 1999. (MoMuC '99) 1999 IEEE International Workshop on DOI - 10.1109/MOMUC.1999.819467*, 1999, pp. 3–10.

[3] T. Yucek and H. Arslan, "A survey of spectrum sensing algorithms for cognitive radio applications," *Communications Surveys & Tutorials, IEEE DOI - 10.1109/SURV.2009.090109*, vol. 11, no. 1, pp. 116–130, 2009.

[4] D. Ariananda, M. Lakshmanan, and H. Nikoo, "A survey on spectrum sensing techniques for cognitive radio," in *Cognitive Radio and Advanced Spectrum Management, 2009. CogART 2009. Second International Workshop on DOI - 10.1109/COGART.2009.5167237*, 2009, pp. 74–79.

[5] E. Candes and M. Wakin, "An introduction to compressive sampling," *Signal Processing Magazine, IEEE DOI - 10.1109/MSP.2007.914731*, vol. 25, no. 2, pp. 21–30, 2008.

[6] D. Donoho, "Compressed sensing," *Information Theory, IEEE Transactions on DOI - 10.1109/TIT.2006.871582*, vol. 52, no. 4, pp. 1289–1306, 2006.

[7] M. Davenport, S. Schnelle, J. Slavinsky, R. Baraniuk, M. Wakin, and P. Boufounos, "A wideband compressive radio receiver," in *MILITARY COMMUNICATIONS CONFERENCE, 2010 - MILCOM 2010 DOI - 10.1109/MILCOM.2010.5680108*, 2010, pp. 1193–1198.

[8] J. Tropp, J. Laska, M. Duarte, J. Romberg, and R. Baraniuk, "Beyond nyquist: Efficient sampling of sparse bandlimited signals," *Information Theory, IEEE Transactions on DOI - 10.1109/TIT.2009.2034811*, vol. 56, no. 1, pp. 520–544, 2010.

[9] M. Mishali and Y. Eldar, "Blind multiband signal reconstruction: Compressed sensing for analog signals," *Signal Processing, IEEE Transactions on DOI - 10.1109/TSP.2009.2012791*, vol. 57, no. 3, pp. 993–1009, 2009.

[10] ——, "From theory to practice: Sub-nyquist sampling of sparse wideband analog signals," *Selected Topics in Signal Processing, IEEE Journal of DOI - 10.1109/JSTSP.2010.2042414*, vol. 4, no. 2, pp. 375–391, 2010.

Shanu Aziz is currently studying towards a M.Eng in Computer and Electronics Engineering at the North-West University. She received her B. Tech degree in Electronics and Communication Engineering from Mahatma Gandhi University, Kerala, India in 2010. Her current research interests are signal processing, compressive sensing and carrier sensing for cognitive radio.

Multiband Support Recovery in 1.2GHz Bandwidth using the Modulated Wideband Converter

S. Aziz and A. S. J. Helberg
School of Electrical, Electronic and Computer Engineering
North-West University, Potchefstroom
Tel: +27 18 299 1961, Fax: +27 18 299 1977
email: {23185600, albert.helberg}@nwu.ac.za

Abstract- This paper deals with a sub-Nyquist sampling method, the Modulated Wideband Converter (MWC) that can efficiently recover the support for sparse wideband analog signals. This approach can be used in spectrum sensing and blind sub-Nyquist support recovery of the frequency bands for cognitive radio (CR) operation. The simulation results obtained for MWC of 1.2GHz bandwidth using ModelSim which is a hardware description language is presented.

Index Terms— Spectrum Sensing, Support Recovery, Cognitive Radio

I. Introduction

A wide range of frequencies in a spectrum is collectively described by a relative term in communication called ”wideband” while the task of identifying the frequency support of a specific input signal is addressed by the term “spectrum sensing”. This essentially includes those spectrum intervals where the noise floor is exceeded by the signal power. Shannon sampling theorem [1] is used to obtain the Nyquist rate for input sampling as assumed by traditional spectrum sensing methods. Even though this theorem suggests a rate equal to twice the maximum frequency present in the signal, it could be noted that a practically viable rate may be even higher than this. If it is possible for a system to identify the unknown spectral support without the knowledge of carrier frequency or the sampling method, then that type of system can be called as a spectrum blind system.

Cognitive Radio receivers [2] use spectrum sensing in opportunity based utilization of unused frequency regions. In a commercial point of view, a spectrum sensing mechanism that can react on a real time basis to the cognitive decisions is greatly demanded by the CR technology. [3] and [4] refers to a range of spectrum sensing methods that primarily require the presence of transmitted signals. On the other hand, analog to digital conversion (ADC) [5] technologies that support bandwidths in the range of gigahertz make Cognitive Rradio communications expensive. Compressive Sampling (CS) is applied to reduce the bandwidth requirements thereby making it less expensive. The recovery process turns out to be non-deterministic in nature.

In this paper we mainly focus on the identification of frequency support in sparse analog signals using sub-Nyquist sampling for use in CR. In section 2, we give a background on Compressive Sensing (CS) and CR. In section 3 we will introduce the MWC system. In section 4, the simulation results obtained for 1.2GHz frequency band is depicted along with the parameters chosen. We conclude with a discussion on the data we collected in section 5 and summarize the rate at which the Nyquist rate is reduced using MWC in section 6.

II. Background

A. Compressive Sampling

Compressive Sampling, also known as Compressed Sensing refers to the technique of recovering signals by much fewer samples than that suggested by Nyquist rate [6]. There are two major principles on which CS is based; one is sparsity pertaining to the Signals of Interest (SOI) and the other one is incoherence pertaining to the sensing modality [7].

Sparsity determines the efficiency by which signals can be acquired non-adaptively as it expresses an idea regarding required information rate of a continuous time signal and that may be much less than that suggested by its bandwidth. Many signals are compressive in the sense that they can be concisely represented when expressed in the proper basis Ψ [5] and this fact is exploited by the CS technique to a large extend.

Incoherence extends the duality between time and frequency and the idea that objects having a sparse representation in Ψ must be spread out in the domain in which they are acquired. A major concern of CS is low coherence pairs. Extremely dense representations of sampling waveforms in Ψ makes incoherence as important as sparsity.

Comparative measurements with basis Φ used by CS is smaller and different from that with basis Ψ representing mostly sparse signals and contains all the useful

information [7]. Therefore recovery of the SOI involves solving an indeterminate system of equations since the number of measurements taken is smaller than the dimensionality (order) of the original signal. This indeterminate system of linear equations can be solved if the original signal is limited to be sparse, and the sparsest solution of the CS problem given in [8] is as follows

$$\min_{v \in R^m} \|v\|_0 \text{ subject to } \Phi v = y \quad (1)$$

where $||v||_0$ is the size of the support of v, Φ is the sampling matrix with rows $\varphi_j \in R^m$ and y is the sampled vector. However, this minimization problem is NP- hard (non-deterministic polynomial-time hard). This problem of sparse representation can be solved using *l1*-norm minimization by converting it into a linear problem. The problem of *l1*-norm minimization as given in [6, 7] is

$$\min_{v \in R^m} \|v\|_1 \text{ subject to } \Phi v = y \quad (2)$$

where $||v||_1 = \sum_j |v_j|$. Technically it is proved that for many problems *l1*-norm minimization is equivalent and easier than (1) and also that solving using the *l1*-norm minimization leads to unique solution of (1).

B. Cognitive Radio and Spectrum Sensing

Traditional Communication systems such as television, radio stations, mobile carriers, air traffic control etc, are allotted with predetermined frequency bands and over the years the government has allocated the majority of the available spectrum to legacy users, reserving a particular frequency interval for each owner. This resource allocation strategy has led to spectrum congestion and the demand for permanent transmission bands can only be rarely satisfied. A recent study on the utilisation of spectrum by the Federal Communications Commission (FCC) in the United States and by similar agencies in other countries indicates that most of the spectrum remains underutilized in a given geographical location and time duration corresponding to a very small number of concurrent transmission by legacy users.

As per the definition of FCC, Cognitive Radio refers to a system that senses its operational electromagnetic environment and can dynamically and autonomously adjust its radio operating parameters to modify system operation, such as maximize throughput, mitigate interference, facilitate interoperability, access secondary markets etc. Spectrum sensing therefore takes place whenever the CR searches for available transmission holes. After a certain frequency band is chosen, the CR continuously monitors the spectrum in order to detect any change in the activity of the primary users. Once a primary user becomes active, the CR must choose another working band, or tailor its transmission to reduce in-band power. Quick and efficient spectrum sensing is evidently an essential component of CR functionality.

Recently, there has been growing interest in spectrum sensing for mobile cognitive radio (CR) receivers, which aim at utilizing unused frequency regions on an opportunistic basis. Commercialization of CR technology necessitates a spectrum sensing mechanism that reacts in real time to cognitive decisions. Sensing in CR mobiles must be performed using minimal hardware and software resources. Therefore, enabling widespread use of CRs calls for innovative spectrum sensing techniques.

C. Wideband Spectrum Sensing by Cognitive Radio

In communications, wideband is a relative term used to describe a wide range of frequencies in a spectrum. Spectrum sensing refers to the task of identifying the frequency support of a given input signal. The frequency support then consists of those spectrum intervals in which the signal power exceeds the noise floor. Also frequency support can be defined as the indices of active bands in a spectrum. In a fully spectrum blind system, the digital algorithms developed for processing the samples identifies the unknown spectral support.

III. MODULATED WIDEBAND CONVERTER

The Mixed Analog Digital system described below operates at sub-Nyquist rate and has much lower complexity than either a traditional sampling system or CS recovery techniques. MWC differ from most standard approaches to the problem of CS recovery as it does not assume that the signals of interest (SOI) are confined to a discrete set of frequencies and do not rely on traditional recovery methods such as *l1* minimization.

Modulated Wideband Converter (MWC) presented in [9, 10, 11] is a mixed analog digital system which has an analog front end and a digital back end. The main function of the analog front end is to alias the spectrum, such that a spectrum portion from each band appears in base band. MWC uses spread spectrum techniques. The advantages of this system with respect to current architectures are threefold. First, the analog front-end is fixed. Second, both the ADC and the DSP rates are substantially below Nyquist. Finally, the sensing resources are shared with the reception path of the CR, so that the low rate streaming samples can be used for communication purposes of the device, besides the sensing functionality they provide. Combining these advantages leads to a real time map of the spectrum.

Our research is based on the MWC system, which enables baseband processing using a set of random demodulators, generating a low rate sequence corresponding to any information band of interest from multiband analog signals, without going through high Nyquist rate. These low rate digital samples enter CTF block which uses a digital algorithm for support recovery.

A. Sampling Stage

In practical cases the Fourier transform of wideband signals occupies only a small portion of a wide spectrum, with unknown frequency support. In wideband communication, the receiver sees the sum of several radio-frequency transmissions. Each signal is modulated around an unknown and different carrier frequency.

Formally, the Fourier transform of *x(t)* is given as

$$X(f) = \int_{-\infty}^{\infty} x(t)e^{-j2\pi ft}\,dt \qquad (3)$$

is zero for every f is not an element of F where $F = \left[-1/2T_{nyq}\,, +1/2T_{nyq}\right]$.

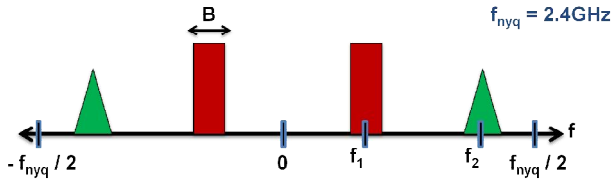

Fig 1: Spectrum of a multiband signal

The sampling stage [10, 11] consists of an RF front end which includes a bank of multiple channels in which the input signal enters simultaneously. Each channel consists of a modulator and a low pass filter. Following the RF front end is a low rate ADC on each channel which handles low analog bandwidth.

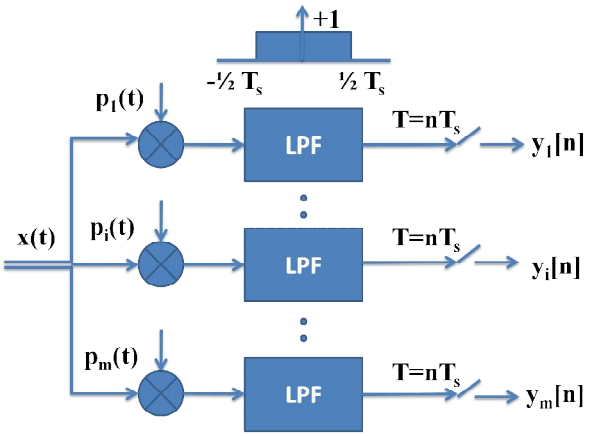

Fig 2: Modulated Wideband Converter

In each channel, the signal gets multiplied by a mixing function, $p_i(t)$ which is a periodic random bit sequence taking ±1 values that share a common period T_p seconds. The period T_p is assumed as some integer multiple of the Nyquist period $T_p = L/f_{nyq}$.

$$p_i(t) = \alpha_{ik,} \qquad (4)$$

$$where\ k\frac{T_p}{M} \le t \le (k+1)\frac{T_p}{M}\ and$$

$$0 \le k \le M-1$$

with $\alpha_{ik} \in \{+1, -1\}$ and $p_i(t + n\,T_p) = p_i(t)$ for every $n \in \mathbb{Z}$.

The Fourier expansion of $p_i(t)$ is given as

$$P_i(f) = \int_{t=-\infty}^{\infty} p_i(t)e^{-j2\pi ft}dt$$

$$= \Sigma_{l=-\infty\ to\ +\infty}\, c_{il}\,\delta(f - l/T_p) \qquad (5)$$

where δ is the Dirac delta function and

$$c_{il} = \frac{1}{T_p}\int_0^{T_p} p_i(t)e^{-j\frac{2\pi}{T_p}lt}dt$$

The purpose of this mixing is to spread the spectrum. The modulated signal is then filtered by a low pass filter with cut off $f_s/2$. Then the filtered signal is sampled uniformly at every $T_s = 1/f_s$ second. As the system consists of m channels the average sampling rate is m/T_s samples per second.

The analog multiplication of $x(t)$ with $p_i(t)$, $\tilde{x}_i(t)=x(t)p_i(t)$ will be transformed to convolution while expressed in frequency domain.

$$\widetilde{X}_i(f) = X(f)P_i(f)$$

$$= \sum_{l=-\infty}^{\infty} c_{il}X(f - lf_p) \qquad (6)$$

From (6) it is clear that $\tilde{X}_i(f)$ is a linear combination of f_p shifted copies of $X(f)$. The modulated output is then low pass filtered with $H(f)$ having an ideal rectangular function as its frequency response. The interval for the *rect* function is $[-1/2T_{s,}\ +1/2T_s\ ]$.

The DTFT of the i^{th} sequence $y_i[n]$ is given as

$$Y_i(e^{j2\pi fT_s}) = \sum_{l=-L_0}^{+L_0} c_{il}\,X(f - lf_p), \qquad f \in \mathcal{F}_s \qquad (7)$$

where L_0 is the smallest integer satisfying $2L_0 + 1 \ge f_{nyq}/f_{p.}$

The relation between unknown *X(f)* with that of $y_i[n]$ can be seen from (7). Therefore

$$y_i(f) = Y_i(e^{j2\pi f T_s}) \; ; 1 \leq i \leq m. \quad (8)$$

The output obtained from i^{th} channel is represented as $y_i[n]$. Commercial ADCs can be used for sampling purpose due to the low sampling rate appearing in each channel.

B. Recovery Stage

Support recovery in MWC is done with the help of a CTF block. The input to the CTF block is the low rate digital samples from the sampling stage.

This paper aims to recover the support of active bands from the input data *y(f)*. The support recovery algorithm is referred as the Continuous-To-Finite (CTF) [10] block given in Fig 3.

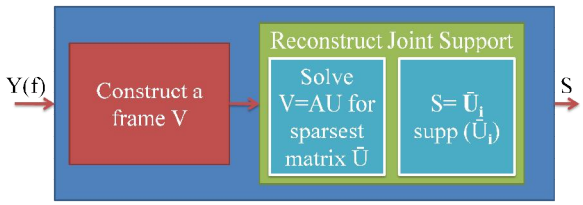

Fig 3: Continuous To Finite Block

The CTF constructs a frame from the input samples i.e. a set of y values. Such a frame can be obtained by computing [12]

$$Q = \sum_{n=-\infty}^{+\infty} y[n]\, y^T[n] \quad (9)$$

Then it solves a finite dimensional sparse representation problem, from which it identifies spectrum slices containing signal energy. Thus the digital recovery algorithm could be used for executing and detecting the correct support set and input carrier positions. The CTF block has a major role in signal reconstruction beyond the robustness in estimating spectral support. Once spectral support is known, real time processing and reconstruction is possible, that is at the (low) speed of the streaming measurements.

IV. OUR APPROACH

Mixed analog-digital spectrum sensing method uses MWC for CS and CTF block for support recovery that is especially suited for the typical wideband setting of CRs. We have implemented a mathematical model of Mixed-analog-digital system using Modelsim. Modelsim is a very powerful and versatile HDL (Hardware Description Language) simulation tool. It helps in integrating to FPGA by creating a VHDL test bench.

The flow diagram given in Fig 4 shows that the output from the signal representation block undergoes sub-Nyquist sampling using MWC and then the support recovery via CTF block. Some of the random functions like mixing function, original support are calculated using MATLAB. Then the values are written into a text file and by using ModelSim, these values are read.

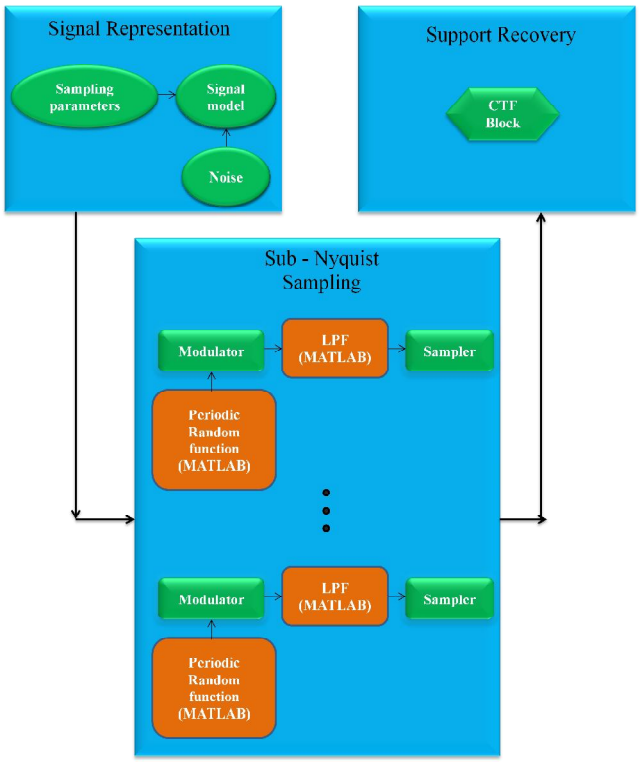

Fig 4: Flow Diagram

Our main aim is support recovery as described in section 3. Parameter choices of our MWC for 1.2GHz are given in Table 1. Also the input SNR to the input signal is considered as 10. The number of bands and the bandwidth for multiband signal under consideration is selected as 4 and 1.2GHz respectively. Therefore the Nyquist frequency will be 2.4GHz. For perfect blind reconstruction [9, 10] of a multiband signal, the bandwidth, B for each of the band in multiband must satisfy $2NB < f_{nyq}$ and the number of channels, m must be $m \geq 2N$. To avoid edge effects $f_s \geq f_p \geq B$ must be ensured.

From (7), L_0 is chosen as the smallest integer such that the sum contains all nonzero bands in the multiband signal model. L_0 can be calculated by

$$L_0 = \left[\frac{f_{nyq} + f_s}{2f_p}\right] - 1 \quad (10)$$

Decimation factor, L is therefore given as $L = 2L_0 + 1$. The number of flops in the sign alternating function, M can be calculated from [10]

$$M \geq 2\left[\frac{f_{nyq}}{2f_p} + \frac{1}{2}\right] - 1 \quad (11)$$

Table 1. Parameter Choices for 2.4GHz band MWC

Parameter Notation	Description	Choice
N	Number of bands	4
B	Maximum width of each band	25MHz
f_{nyq}	Nyquist frequency	**2.4GHz**
L	Decimation factor	51
f_p	Frequency of $p_i(t)$	f_{nyq} / L
m	Number of sampling channels	10
f_s	Sampling rate	f_p
M	Number of ±1 intervals in each period of $p_i(t)$	L

The input signal along with added noise is mixed with random periodical functions. The mixing helps in aliasing the energies to baseband and thereby the baseband operations are enabled without losing information. This mixed output from each channel is then filtered using an ideal LPF having cutoff, $1/2T_s$ = 23.5MHz. Then the high rate input sequences (Length of input signal = 1836 samples for each channel) are then down sampled to low rate ones (Length of input signal/ L = 36 samples for each channel).

The CTF block helps in support recovery by frame construction followed by replacing the infinite sum by a finite sum.

The original support is the indices of active bands. The recovered support is the result we obtained from CTF block. From Table 2, we can see that the original support set consists of 4, 5,19,33,47 and 48 where as recovered support set consists of 1, 4, 5,19,33,47, 48 and 51 as the active supports. We consider the result as success if original support set is the subset of recovered support set. Here as we can see all the original supports are identified, it is a successful recovery.

Table 2. Support Recovery using MWC

Original Support Set	Recovered Support Set
{ 4, 5, 19, 33, 47, 48 }	{ 1, **4**, **5**, **19**, **33**, **47**, **48**, 51 }

The probability for the occurrence of false positives for a successful recovery is given in the pie diagram shown in Figure 5. A false positive is that support which is present in recovered support set but not in original support. 15% of the simulation results show that the original support is equal to the recovered support, 50% shows that the recovered support set contains 2 false positives along with the original support set and 35% shows 4 false positives in recovered support set.

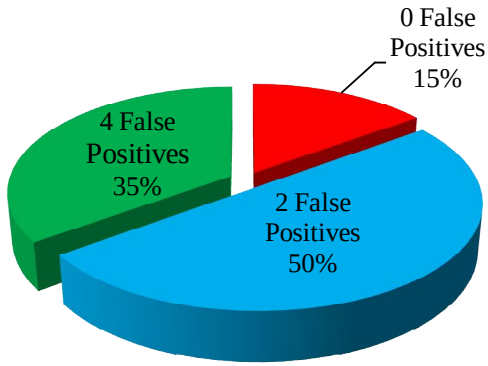

Fig 5: Probability for the occurrence of False Positives

The probability for the occurrence of false negatives for a failed recovery is given in the pie diagram shown in Figure 6. A false negative is the support which is present in original support set but not in recovered support set. 63% of the simulation results show that 2 of the original support were missing when compared with the recovered support, 32% shows that the original support set contains 4 false negatives and 5% shows 6 false negatives in original support set.

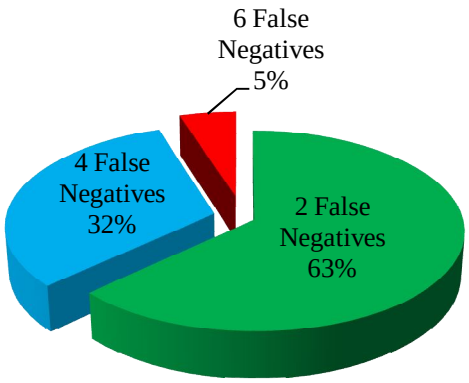

Fig 6: Probability for the occurrence of False Negatives

V. Conclusion on Data

We repeated the simulations for more than 2500 times for the above chosen parameters. The results showed successful support recovery for about 80% of the simulations and 20% showed failed recovery. As 80% showed success, the MWC is considered to be an apt technique for the support recovery of a multiband signal. We conclude that this 80% success can be raised by selecting more appropriate parameters.

VI. Summary

In this paper we showed the ModelSim simulation results for MWC, demonstrating its ability to sample and recover support at significantly below Nyquist rate. MWC is a multi-channel system which samples sparse multiband signals. Here we used 10 low-rate sampling channels to sample the 1.2GHz multiband signal. The Nyquist rate for the multiband signal is f_{nyq} = 2 * 1.2GHz = 2.4GHz. The sampling rate for each channel is fs = 2.4GHz/51 = 47.05MHz. Therefore, the actual sampling rate is 47.05MHz*10 = 470.5MHz. This shows that the sampling rate is reduced to 80% than Nyquist rate by using MWC.

VII. Acknowledgments

This research was performed at North-West University, Potchefstroom campus, South Africa. The financial assistance of the THRIP towards this research is hereby acknowledged.

VIII. References

[1] Shannon, C.E. Communication in the Presence of Noise, 1949, Proceedings of the IRE DOI - 10.1109/JRPROC.1949.232969, pp. 10--21.

[2] Mitola, J., III. Cognitive radio for flexible mobile multimedia communications. Mobile Multimedia Communications, 1999. (MoMuC '99) 1999 IEEE International Workshop on DOI - 10.1109/MOMUC.1999.819467. 1999.

[3] Yucek, T. and Arslan, H. A survey of spectrum sensing algorithms for cognitive radio applications. Communications Surveys & Tutorials, IEEE DOI - 10.1109/SURV.2009.09010. 2009, Vol. 11.

[4] Ariananda, D.D. and Lakshmanan, M.K. and Nikoo, H. A survey on spectrum sensing techniques for Cognitive Radio. Cognitive Radio and Advanced Spectrum Management, 2009. CogART 2009. Second International Workshop on DOI - 10.1109/COGART.2009.5167237. 2009.

[5] Bin Le, Thomas W. Rondeau, Jeffrey H. Reed, and Charles W. Bostian. "Analog to Digital Converters." IEEE SIGNAL PROCESSING MAGAZINE November 2005.

[6] Candes, E.J. and Wakin, M.B. An Introduction To Compressive Sampling. [book auth.] IEEE DOI - 10.1109/MSP.2007.914731 Signal Processing Magazine. 2008.

[7] S Aziz, A. S. J. Helberg, "Practical Support Recovery using Sub-Nyquist Sampling", SATNAC, September 2011.

[8] Donoho, D.L. Compressed sensing. Information Theory, IEEE Transactions on DOI - 10.1109/TIT.2006.871582. 2006.

[9] Mishali, M. and Eldar, Y.C. Blind Multiband Signal Reconstruction: Compressed Sensing for Analog Signals. [book auth.] IEEE Transactions on DOI - 10.1109/TSP.2009.2012791 Signal Processing. 2009.

[10] —. From Theory to Practice: Sub-Nyquist Sampling of Sparse Wideband Analog Signals. Selected Topics in Signal Processing, IEEE Journal of DOI - 10.1109/JSTSP.2010.2042414. 2010, Vol. 4. (Eldar)

[11] Shanu Aziz, A. S. J. Helberg, "Spectrum Sensing Technique using Modulated Wideband Converter", ICICT, April 2012.

[12] Eldar, M. Mishali and Y. C. "Reduce and boost: Recovering arbitrary." IEEE Trans. Signal Process., vol. 56, no.10 Oct 2008: 4692–4702.

Shanu Aziz is currently pursuing an M.Eng in Computer and Electronics Engineering at the North West University. She received her B.Tech in Electronics and Communication Engineering from Mahatma Gandhi University, Kerala, India in 2010. Her research interests include spectrum sensing for cognitive radio, signal processing and compressive sensing.

Spectrum Sensing Technique using Modulated Wideband Converter

Shanu Aziz
School of Electrical, Electronic and Computer Engineering
North West University
Potchefstroom, South Africa
23185600@nwu.ac.za

A. S. J. Helberg
School of Electrical, Electronic and Computer Engineering
North West University
Potchefstroom, South Africa
Albert.helberg@nwu.ac.za

***Abstract*— This paper deals with carrier detection using Modulated Wideband Converter (MWC), which is a sub-Nyquist sampling system for sparse wideband analog signals. This system samples the multiband signals at a sub-Nyquist rate. Indices of active bands are determined using this method which helps in spectrum sensing that is suited for Cognitive Radio (CR). The simulation results of MWC obtained for a bandwidth of 1GHz and 2GHz using ModelSim is presented here.**

Keywords-Cognitive Radio; sub-Nyquist rate; Spectrum Sensing

I. INTRODUCTION

Shannon sampling theorem [1], is a well known theorem in literature which states that the sampling rate of a signal being reconstructed should be twice the highest frequency and the same is applicable in the practice of image reconstruction also. In the case of discrete finite dimensional signals, the number of collected samples should be as large as its length in dimension as suggested by the fundamental linear algebra theorem, for its probable reconstruction. A peep through into the current technologies used by medical imaging systems, analog to digital converters etc may conclude that the same principle is used there also. On the other hand, the theory used by the novel compressive sensing technique is seen to be based on an entirely new approach that made it known alternatively as compressed sensing, compressive sampling and sparse recovery approach in the literature. This approach made it clear that many of the previously considered incomplete signals can be effectively approximated by expressing it in a sparse expansion in terms of a suitable basis with a small number of non zero coefficients. The compression technique as illustrated by MP3, JPEG etc achieve compression by storing only the largest basis coefficients and in the reconstruction process the non stored coefficients are set to zero. It may be observed here that the original signal has to be caught with full information and afterwards while compressing most of the information is discarded owing to the wastage of most of the signals caught by expensive measurement procedures. Compressed sensing (CS) technique can offer a method by which it can take a compressed version of the original signal for effective reconstruction based on a linear and non adaptive measurement of the original signal. The number of measurements required here is very much in agreement with the compressed size of the original signal.

Present day Cognitive Radio (CR) applications [2] can be seen to be using compressed sensing techniques [3, 4] in wide band spectrum sensing. The inherent sparsity of the wideband spectrum is sponsored by a very few number of concurrent users of largely available frequency bands and therefore our interest is primarily in detecting the vacant frequency bands. Frequency bands used by present day communication systems such as television, radio, mobile carriers etc are allocated in a predetermined manner making it necessary for every legacy user to operate in a particular range of frequencies reserved for them by the government agency. This permanent way of band allocation is leading to heavy spectrum congestion and is becoming impractical due to the limitation in available fixed frequency bands. On the contrary, many of studies conducted by agencies like Federal Communications Commission (FCC) regarding the spectrum utilization indicates that most of the time the allocated spectrums are left underutilized in a given geographical area and time given as the concurrent transmissions by legacy users are very less.

CR as defined by FCC, refers to a system that senses its operational electromagnetic environment and can dynamically and autonomously adjust its radio operating parameters to modify system operation, such as maximize throughput, mitigate interference, facilitate interoperability, access secondary markets etc. That means the CR must search for available transmission holes in a spectrum leading to the application of spectrum sensing. Once a certain frequency band is chosen, the spectrum must be continuously monitored for any change in the activity. The CR thus identifies the active status of a chosen spectrum user and should then search for a different band or in most cases may have to compress its transmission signals to reduce in-band power. This process should happen so quickly and efficiently and thus underlines the importance of spectrum sensing in CR.

The term 'wideband' refers to a wide range of frequencies in a spectrum while spectrum sensing is the identification process of frequency support of a given input signal that essentially includes the spectrum intervals in which the signal power exceeds the noise floor. A spectrum blind system, as indicated by the name is developed in view of identifying the unknown spectral support and reconstruction of the signal should happen continuously by making use of closed form expressions. Opportunity based utilization of unused frequency regions by CRs is based on the current trend of increasing interests in spectrum sensing and its capability to take real time cognitive decisions by making use of minimum hardware and software resources is becoming very crucial in a commercial environment.

This paper focuses on mixed analog digital system that operates at sub-Nyquist rate and is considered to be simpler than either a traditional sampling system or CS recovery system. This method differ from most of the standard approaches followed by the recovery part of the Compressive Sensing technology as they do not assume that the signals of interest (SOI) are confined to a discrete set of frequencies. In addition to this they do not rely on traditional recovery methods such as l1 minimization. Instead these methods develop a simple detection system that identifies the support of the narrow band FM signals.

II. Literature Review on Compressive Sensing

'Sparsity' pertaining to the Signals of Interest (SOI) and 'Incoherence' pertaining to the sensing modality are the two major principles based on which a CS technique is developed. Sparsity expresses an idea regarding required information rate of a continuous time signal that may be much lesser than that suggested by its bandwidth and determines the non adaptive acquisition efficiency of the signals. Many signals are compressive in the sense that they can be concisely represented when expressed in the proper basis Ψ [5] and this fact is being exploited by the CS technique to a larger extend. Incoherence extends the duality between time and frequency and also the idea that objects having a sparse representation in Ψ must be spread out in the domain in which they are acquired is expressed. A major concern of the CS is regarding low coherence pairs. Extremely denser representation of sampling waveforms in Ψ makes incoherence as important as sparsity.

There are several recovery algorithm approaches by CS from undersampled non adaptive measurements. The measurement matrix, ϕ can be obtained by taking m linear measurements of a signal x where $x \in C_N$ and is k-sparse is given as

$$y = \phi x. \tag{1}$$

where $\phi \in C_m \; X \; N$ and $y \in C_m$ is called the measurement vector. It is said to be vastly undersampled when $m << N$ and the recovery of x from y is impossible. Also solving (1) gives infinite solutions as the system is underdetermined. As x is k-sparse, $\ell 0$-miminization can be used for the recovery for the sparsest vector x.

$$min_{v \epsilon R^m} ||v||_0 \text{ subject to } \phi v = y \tag{2}$$

However, this combinatorial minimization problem is NP- hard (non-deterministic polynomial-time hard) in general [6, 7]. Although solving of (2) for any matrix is intractable, the alternatives for this problem is given in CS. They are convex relaxation technique leading to $\ell 1$-minimization — also called basis pursuit [8] — and greedy algorithms, such as various matching pursuits [9, 10]. Solution can be obtained only for subclass of matrices and certain y values, which clearly shows that the NP hardness cannot be relaxed.

The $\ell 1$-minimization approach [11] that is the convex relaxation of (2) considers the solution of

$$min_{v \epsilon R^m} ||v||_1 \text{ subject to } \phi v = y \tag{3}$$

which is a convex optimization problem leading to a solution using different techniques [12]. The real-valued case, (2) leads to a linear program and the complex-valued case leads to a second order cone program.

III. Modulated Wideband Converter

Modulated Wideband Converter (MWC) presented in [13, 14] is a mixed analog digital system which has an analog front end and a digital back end. MWC is a multichannel system that has got an analog front end for aliasing the spectrum which helps in sampling the sparse multiband signals. MWC uses the spread spectrum techniques as it has the ability to spread portions of the spectrum in baseband. The locations of the active bands are recovered within the assumed bandwidth. Multiband signal models are often suitable for wideband radio frequency scanning applications. MWC system enables baseband processing using a set of random demodulators [15]. This helps in generating a low rate sequence corresponding to any information band of interest from multiband analog signals, without going through high Nyquist rate. These low rate digital samples enter CTF block which uses a digital algorithm for active band recovery.

A. Sampling Stage

In MWC, the signal $x(t)$ enters m channels simultaneously. Formally, the Fourier transform of $x(t)$ is given as

$$X(f) = \int_{t=-\infty \text{ to } +\infty} x(t)\, e^{-j2\pi ft}\, dt \tag{4}$$

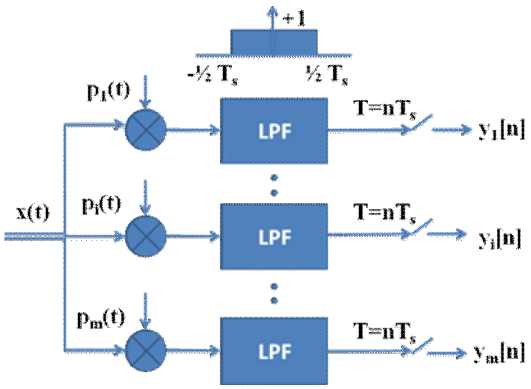

Figure 1. Modulated Wideband Converter

is zero for every f is not an element of F where $F = [-1/2T_{nyq}, +1/2T_{nyq}]$.

In the i^{th} channel, $x(t)$ is multiplied by a mixing function, $p_i(t)$ which is T_p periodic alternates between the levels ±1 for each of M equal time intervals.

$$p_i(t) = \alpha_{ik},$$

$$kT_p / M \le t \le (k+1)T_p / M,\ 0 \le k \le M-1 \qquad (5)$$

with $\alpha_{ik} \in \{+1, -1\}$ and $p_i(t + n T_p) = p_i(t)$ for every $n \in \mathbb{Z}$.

The Fourier expansion of $p_i(t)$ is given as

$$P_i(f) = \int_{t=-\infty \text{ to } +\infty} p_i(t)\, e^{-j2\pi ft}\, dt$$

$$= \sum_{n=-\infty \text{ to } +\infty} c_{il}\, \delta\,(f - n/T_{nyq}) \qquad (6)$$

where δ is the Dirac delta function and

$$c_{il} = 1/T_p \int_{t=-0 \text{ to } Tp} p_i(t)\, e^{-j2\pi lt/T_p}\, dt$$

.

In each channel, the analog output from the modulator is converted to digital by passing it through a low pass filter with cut off $1/2T_s$ and then sampled at a rate of $1/T_s$. As the system consists of m channels the average sampling rate is m/T_s samples per second. The samples produced by MWC are at a constant rate. So it doesn't require synchronizing the non uniform sequences using additional hardware.

The analog multiplication of $x(t)$ with $p_i(t)$, $\tilde{x}_i(t)=x(t)p_i(t)$ will be transformed to convolution while expressed in frequency domain.

$$\tilde{X}_i(f) = X(f)\, P_i(f)$$

$$= \sum_{l=-\infty \text{ to } +\infty} c_{il}\, X(f - lf_p) \qquad (7)$$

From (7) it is clear that $\tilde{X}_i(f)$ is a linear combination of f_p shifted copies of $X(f)$. The modulated output is then low pass filtered with $H(f)$ having an ideal rectangular function as its frequency response. The interval for the rect function is $[-1/2T_{s,} +1/2T_s]$.

The DTFT of the i^{th} sequence $y_i[n]$ is given as

$$Y_i(e^{j2\pi fT_s}) = \sum_{l=--l0 \text{ to } +l0} c_{il}\, X(f - lf_p),\ f \in F_s \qquad (8)$$

where l_0 is the smallest integer satisfying $2l_0 + 1 \ge f_{nyq} / f_p$.

The relation between unknown $X(f)$ with that of $y_i[n]$ can be seen from (8). Therefore

$$y_i(f) = Y_i(e^{j2\pi fT_s});\ 1 \le i \le m. \qquad (9)$$

B. *Recovering Stage*

Indices of active bands can be found out with the help of a CTF block in MWC. The input to the CTF block is the low rate digital samples from the sampling stage. This paper aims to recover the support of active bands from the input data $y(f)$. The support recovery algorithm is referred as the Continuous to Finite (CTF) block given in Fig 2.

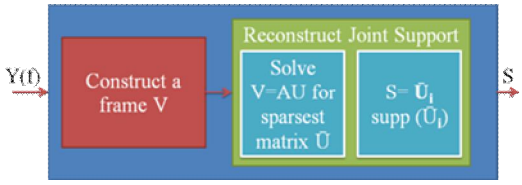

Figure 2. Continuous To Finite Block

The construction of frame in CTF is done with the samples coming out of MWC. Such a frame can be obtained by computing [16]

$$Q = \sum_{n=-\infty \text{ to } +\infty} y[n]\, y^T[n] \qquad (10)$$

This frame can be defined as $Q = VV^H$ for $y(f)$. Then it solves a finite dimensional sparse representation problem, from which helps in identifying the spectral locations of the active bands. Thus the digital recovery algorithm could be used for executing and detecting the correct support set and input carrier positions. The CTF block has a major role in signal reconstruction beyond the robustness in estimating spectral support

IV. Simulation Results

Mixed analog-digital spectrum sensing method uses MWC for CS and CTF block for support recovery that is especially suited for the typical wideband setting of CRs.

TABLE I
SUPPORT RECOVERY USING MWC

N = 4, B = 30MHz, m=15	
f_{nyq}=1GHz L=25	f_{nyq}=2GHz L=51
Original Support Set	
{3, 6, 7, 19, 20, 23}	{8, 17, 35, 44}
Recovered Support Set	
{**3**, 4, **6**, **7**, **19**, **20**, 22, **23**}	{**8**, **17**, 18, 21, 31, 34, **35**, **44**}

Modelsim simulation of MWC is done. We have considered multiband signals which are bandlimited to 1GHz and 2GHz. The number of active bands is selected as 4 and a maximum bandwidth, B of 30MHz for each of them. For both experimentations we have assumed that the number of channels as 15 with a decimation factor, L of 25 and 51 for 1GHz and 2GHz respectively.

The original support is the indices of active bands. The recovered support is the result we obtained from CTF block. From Table 1, it can be seen that the support is recovered successfully as original support set is the subset of recovered support set.

V. CONCLUSION

In this paper, we briefly described the MWC which is a sub-Nyquist sampling strategy for sparse wideband signals. Here we presented some preliminary results demonstrating the ability of MWC to sample and identify the locations of active bands at a sub-Nyquist rate. MWC uses compressed samples for the active band identification, thereby helping the cost reduction for signal recovery and perhaps aid in real time signal processing applications.

For MWC, the analog front end is fixed. The Analog to Digital Converters (ADC) [17] and the DSP rates are substantially below Nyquist. The sensing resources are shared with the reception path of the CR. These advantages make it possible for a real time map of the spectrum.

ACKNOWLEDGMENT

This research was performed at North West University, Potchefstroom Campus, South Africa. The financial assistance of the National Research Foundation (NRF) towards this research is hereby acknowledged.

REFERENCES

[1] Shannon, C.E. Communication in the Presence of Noise, 1949, Proceedings of the IRE DOI - 10.1109/JRPROC.1949.232969, pp. 10—21

[2] Joseph Mitola, *Cognitive Radio: An Integrated Agent Architecturefor Software Defined Radio*, Ph.D. thesis, Royal Institute of Technology (KTH), Stockholm, May 2000.

[3] Zhi Tian and G.B. Giannakis, "Compressed sensing for wideband cognitive radios," in *IEEE Int. Conf. Acoustics, Speech and Signal Proc., 2007. ICASSP 2007.*, 15-20 2007, vol. 4, pp. IV–1357 –IV–1360.

[4] Y.L. Polo, YingWang, A. Pandharipande, and G. Leus, "Compressive wide-band spectrum sensing," in *IEEE Int. Conf. Acoustics, Speech and Signal Proc., 2009. ICASSP 2009.*, 19- 24 2009, pp. 2337 –2340.

[5] Candes, E.J. and Wakin, M.B. An Introduction To Compressive Sampling. [book auth.] IEEE DOI - 10.1109/MSP.2007.914731 Signal Processing Magazine. 2008

[6] S. G. Mallat and Z. Zhang. Matching pursuits with time-frequency dictionaries. IEEE Trans. Signal Process., 41(12):3397–3415, 1993.

[7] B. K. Natarajan. Sparse approximate solutions to linear systems. SIAMJ. Comput., 24:227–234, 1995.

[8] S. S. Chen, D. L. Donoho, and M. A. Saunders. Atomic decomposition by Basis Pursuit. SIAM J. Sci. Comput., 20(1):33–61, 1999.

[9] J. Tropp and D. Needell. CoSaMP: Iterative signal recovery from incomplete and inaccurate samples. Appl. Comput. Harmon. Anal., page 30, 2008.

[10] J. A. Tropp. Greed is good: Algorithmic results for sparse approximation. IEEE Trans. Inform. Theory, 50(10):2231–2242, 2004.

[11] Donoho, D.L. Compressed sensing. Information Theory, IEEE Transactions on DOI - 10.1109/TIT.2006.871582. 2006.

[12] S. Boyd and L. Vandenberghe. Convex Optimization. Cambridge Univ. Press, 2004.

[13] Mishali, M. and Eldar, Y.C. Blind Multiband Signal Reconstruction: Compressed Sensing for Analog Signals. [book auth.] IEEE Transactions on DOI - 10.1109/TSP.2009.2012791 Signal Processing. 2009.

[14] —. From Theory to Practice: Sub-Nyquist Sampling of Sparse Wideband Analog Signals. Selected Topics in Signal Processing, IEEE Journal of DOI - 10.1109/JSTSP.2010.2042414. 2010, Vol. 4. (Eldar)

[15] Tropp, J.A. and Laska, J.N. and Duarte, M.F. and Romberg, J.K. and Baraniuk, R.G. Beyond Nyquist: Efficient Sampling of Sparse Bandlimited Signals. [book auth.] IEEE Transactions on DOI - 10.1109/TIT.2009.2034811 Information Theory. 2010.

[16] Eldar, M. Mishali and Y. C. "Reduce and boost: Recovering arbitrary." IEEE Trans. Signal Process., vol. 56, no.10 Oct 2008: 4692–4702.

[17] Bin Le, Thomas W. Rondeau, Jeffrey H. Reed, and Charles W. Bostian. "Analog to Digital Converters." IEEE SIGNAL PROCESSING MAGAZINE November 2005.